QUANTITATIVE INVESTIGATION OF THE BENEFITS FROM STORING RED BLOOD CELLS UNDER NORMOGLYCEMIC CONDITIONS

By

Ruipeng Mu

A DISSERTATION

Submitted to
Michigan State University
in partial fulfillment of the requirements
for the degree of

Chemistry – Doctor of Philosophy

2017

ABSTRACT

QUANTITATIVE INVESTIGATION OF THE BENEFITS FROM STORING RED BLOOD CELLS UNDER NORMOGLYCEMIC CONDITIONS

By

Ruipeng Mu

Red blood cell (RBC) transfusion has become a highly organized and life-saving component of critical healthcare. Approximately 40,000 units of RBCs are transfused every day in the US, therefore the safety and efficiency of RBC transfusions are essential to patients' health. However, post-transfusion complications still exist, therefore remaining a threat to the patients' life. It is well-known that stored RBCs experience metabolic and physical changes during the storage period, collectively known as the storage lesion, which may cause adverse effects after transfusion. The Spence group hypothesizes that the high concentration of glucose present in the blood storage solutions plays an important role in the development of the storage lesion. In order to improve the quality of stored RBCs, normoglycemic versions for the current FDA approved blood storage solutions have been proposed, where the glucose concentrations were modified to 5.5 mM. The benefits of normoglycemic storage of RBCs were quantitatively evaluated through a variety of experiments.

First, flow-induced ATP released from stored RBCs was studied using a 3D-printed fluidic device. It is well-known that the primary function of the RBC is to deliver oxygen to tissues. Besides that, the RBC acts as a blood flow regulator by releasing adenosine triphosphate (ATP) into the blood stream. RBC-derived ATP release can stimulate nitric oxide (NO), a known vasodilator, production within endothelial cells, increasing blood flow. RBC

derived-ATP release decreases approximately 50% when cells are stored in hyperglycemic environments, compared to normoglycemic storage. This result indicates that RBCs stored in normoglycemic conditions may have improved blood flow during and after transfusion. Next, the mechanism of impaired ATP release was explored by studying cell deformability. This work was done by applying a 3D-printed, multi-port membrane based device accompanied with flow cytometry for cell counting. It is shown that RBCs stored in hyperglycemia lost 15 – 20% of their deformability. One possible element causing cell deformability loss is oxidative damage triggered by the massive production of intracellular sorbitol from RBCs stored in standard storage solutions.

In order to further discover the mechanisms of concentrated glucose damage to stored RBCs, cell membrane phosphatidylethanolamine (PE) glycation was analyzed by a high resolution/accurate mass spectrometry. The results showed that the glycated product of PE, Amadori-PE, to normal PE ratio on the RBC membrane decreases as a function of time during the storage period when cells are stored in physiological levels of glucose.

In summary, the work here demonstrates that the excess glucose present in storage solutions might be the main contributor for the development of storage lesions. Alternatively, storing RBCs in normoglycemic conditions can reduce the severity of those deleterious effects, therefore having high potential benefits in the clinic.

This thesis is dedicated to Mom, Dad and my wife.
Thank you! I love you!

ACKNOWLEDGEMENTS

First, I would like to thank to my advisor, Dr. Dana M. Spence. He is a great advisor, always willing to provide help and guidance for his students. Especially in my second year, when my research didn't go well, his patience and encouragement helped me get through those dark months. Also, he is a good example of how to balance personal career and family life, since he is a father of four kids. It is difficult to grow four kids while still keeping supportive to graduate students. In addition, I would like to thank my former second reader, Dr. Merlin Bruening, who is really good at teaching classes. Please keep giving out quiz every single day. I appreciate for all the critical insights and helpful suggestions provided by my current committee members, including my second reader Dr. Liangliang Sun, as well as Dr. Marcus Dantus and Dr. William Wulff.

I feel grateful to all Spence group members, past and present. Kari and Suzanne, thank you for telling me a lot of things about PhD life in US. Yimeng, thanks for leaving a good start for the whole blood banking project, which makes my PhD career much easier. I hope you enjoy your life in Beijing with chinchillas. Sarah, Jayda and Bethany, it's great to have you guys in the group. I appreciate your help for my seminar and second year oral exam preparation. Yueli, I sincerely thank for your help in my research and job applications. I hope you can meet your Mr. Right soon. Chengpeng, we had a lot of fun in Yellowstone and many conferences. I wish you good luck in your faculty position seeking. Kristine, you are such a warm and enthusiastic person. Thanks for helping me passing my biochemistry classes. Tiffany, Cody, Andrew and Hamideh, I am going to miss all the joyful time spent

with you guys. Andre, Morgan and Rebecca, I wish you have a great time in the Spence group.

Furthermore, I would like to acknowledge National Institutes of Health for funding support and Brian Wright for his help related to 3D printing. Special thank you to Todd Lydic, who has taught me a lot about lipid study using mass spectrometer.

Finally, I would like to thank to my friends. Thanks for always being supportive to me, especially during the lunch time. And my parents, thanks for being such a great mom and dad, always believe in me. Special thank you to my wife, who has been with me for more than eight years. Thanks for your endless love and master level cooking skill.

At last, I want to say “Do you have lunch?”

TABLE OF CONTENTS

LIST OF TABLES ix

LIST OF FIGURES x

KEY TO ABBREVATIONS xviii

Chapter 1 – Introduction 1
1.1 The Development of Red Blood Cell Storage 1
1.2 Current Red Blood Cell Collection and Storage in US 5
1.3 Clinical Performance of Stored Red Blood Cells 10
1.4 Red Blood Cell Storage Lesion 14
1.4.1 Metabolic Effects 15
1.4.2 Oxidative Damages 19
1.4.3 Cell Membrane Changes 22
1.5 Flow Property of Red Blood Cells 24
1.6 Normoglycemic Storage of Red Blood Cells 26
1.7 Modern Techniques Utilized for Red Blood Cell Study 28
REFERENCES 35

Chapter 2 – Evaluating the Benefits from Normoglycemic Red Blood Cell Storage 44
2.1 Introduction 44
2.2 Experimental 58
2.2.1 RBC Collection and Storage 58
2.2.2 Monitoring the Glucose Concentration 62
2.2.3 Determining the Hemolysis Level 63
2.2.4 Quantification of Sorbitol Accumulation 64
2.2.5 Measuring Cell Osmotic Fragility 65
2.2.6 3D-Printed Fluidic Device: Design and Fabrication 66
2.2.7 Determination of Cell-Derived ATP Release 66
2.3 Results 70
2.3.1 Glucose Concentration 70
2.3.2 Hemolysis Level 74
2.3.3 Sorbitol Accumulation 74
2.3.4 Osmotic Fragility 74
2.3.5 ATP Measurement 77
2.4 Discussion 79
2.5 Conclusion 88
REFERENCES 90

Chapter 3 – Investigating the Feasibility of RBC Storage with Low Glucose Maintenance by an IV Piggyback System 96
3.1 Introduction 96
3.2 Experimental 102
3.2.1 Storing RBCs in Newly Developed Bags 102
3.2.2 The Creation of an IV-Piggyback Glucose Bag for Normoglycemic Cell Storage 105
3.2.3 Glucose Feeding Guideline 108
3.2.4 The Design and Fabrication of 3D-printed Membrane Based Device 108
3.2.5 Determination of Cell Deformability 109
3.2.6 Measuring Hemolysis, Glucose and Sorbitol Levels 110
3.3 Results 113
3.3.1 Quantification of Hemolysis, Glucose and Sorbitol Levels 113
3.3.2 Comparison of Cell Deformability 114
3.4 Discussion 120
3.5 Conclusion 125
REFERENCES 127

Chapter 4 – Studying the RBC Membrane Lipid Glycation During Storage 131
4.1 Introduction 131
4.2 Experimental 138
4.2.1 Sample Preparation 138
4.2.2 *In vitro* Synthesis of Amadori-PE 140
4.2.3 Optimizing PE and Amadori-PE Determination 140
4.2.4 PE and Amadori-PE Determination of Stored RBCs 141
4.3 Results 142
4.3.1 Optimization of PE and Amadori-PE Detection 142
4.3.2 PE Glycation in Stored RBCs 143
4.4 Discussion 150
4.5 Conclusion 154
REFERENCES 156

Chapter 5 – Conclusions and Future Directions 160
5.1 Conclusions 160
5.1.1 Storing RBCs in Physiological Levels of Glucose Can Reduce Storage Lesion 160
5.1.2 Low Glucose Storage of RBC can be Achieved by Implementing a Piggyback Bag System 164
5.1.3 3D-Printed Devices Are Useful Tools for Analytical Scientists 165
5.2 Future Directions 166
REFERENCES 171

LIST OF TABLES

Table 1.1 – Contents of different blood storage solutions……8

Table 1.2 – List of post-transfusion related complications……..13

Table 2.1 – Components of normoglycemic versions of blood storage solutions…….60

Table 3.1 – Prediction of extracellular glucose concentration increment (mM)…….107

Table 4.1 – List of PE and Amadori-PE targeted in stored RBC lipid extract……145

LIST OF FIGURES

Figure 1.1 – Standard blood collection and storage system. 450 mL of whole blood is collected from a donor's vein into a primary bag containing 63 mL of CPD. The entire bag is centrifuged, followed by the removal of plasma and buffy coat layers. Packed RBCs are exported out from the bottom port into a satellite bag that contains 110 mL of AS-1. The resulting RBC suspension in AS-1 can be further purified by leukoreduction. RBCs are stored at 4 °C for up to 42 days.....7

Figure 1.2 – RBC anaerobic glycolysis pathway. The glycolysis pathway generates 90% of the ATP as the energy source to maintain the metabolism of RBCs.....17

Figure 1.3 – The regeneration of GSH and oxidative damage. GSH is an active antioxidant in cells, which can prevent damage from ROS such as free radicals and peroxide. The regeneration of GSH is essential for cell anti-oxidation capacity. Because of the acidic environment of RBC storage, the activity of the enzyme, glucose 6-phosphate dehydrogenase, is inhibited. As the consequence, the production of NADPH will be decreased, causing obstacles in GSH regeneration process.....18

Figure 1.4 – The formation of lipid peroxide. Free radicals generated through Fenton reactions can further react with lipids or proteins to form peroxide products, causing RBCs to undergo progressive oxidative insult. The reaction above describes a typical lipid peroxidation process. A similar reaction may also occur in proteins.....21

Figure 1.5 – PDMS device for NO measurement. The microfluidic device contains two slabs of PDMS, where the bottom one has channels with inside diameters closing to arterioles in vivo, while the top one equipped with a 1/8" hole for optical detection of NO. A polycarbonate membrane was fixed between the two layers of PDMS and sealed. Endothelial cells were cultured on one side of the membrane. A 7% RBC suspension was pumped through the channel, and the NO production by endothelial cells was quantitated by DAF-FM. (Copyright by Yimeng Wang. Reprinted from Wang, Y.; Giebink, A.; Spence, D. M. Integr Biol (Camb) 2014, 6, 65-75.).....29

Figure 1.6 – 3D-printed device for NO measurement. The size of the printed device is the same as a standard 96-well plate, allowing placing the device directly into a commercial plate reader for chemiluminescence detection. The device contains six channels with three detection wells on each channel, enabling high-throughput analytical measurement. Trans-well membrane inserts were plugged into detection wells for ATP separation and quantification. The circulation loop was closed by connecting both ends using Tygon tubes via male leur lock adapters. RBC suspension was circulating in the channels, and the ATP release from RBCs can diffuse through the membrane into wells and further be detected. (Copyright by Chengpeng Chen. Reprinted from Chen, C.; Wang, Y.; Lockwood, S. Y.;

Spence, D. M. Analyst 2014, 139, 3219-3226.)……33

Figure 1.7 – 3D-printed filtration device for cell deformability measurement. The concept behind the design is only cells with sufficient deformability would be able to pass through the membrane, since the pore size of the membrane is smaller than the diameter of RBCs. The deformability of RBCs from different storage solutions could be compared by measuring the volume of RBC suspension collected in the cuvette and counting the number of cells presented in suspension. The device has two slabs printed with clear material and O rings printed with black rubbery material. Polycarbonate membrane (5 μm pore size) was fixed between the two O rings. A suspension of 5% RBC was pumped through the membrane and collected using a cuvette. (Copyright by Chengpeng Chen. Reprinted from Chen, C. 3D-PRINTED IN VITRO ANALYTICAL DEVICES FOR DIABETES THERAPEUTICS AND BLOOD BANKING STUDIES. Michigan State University2015……34

Figure 2.1 – Reaction of the enzymatic fluorescence method for glucose measurement. Glucose is converted to glucose-6-phosphate by the enzyme, hexokinase, at the presence of ATP. Then, the glucose-6-phosphate is catalyzed by glucose-6-phosphate dehydrogenase to form 6-phosphote-D-glucono-1,5-lactone. In that process, NADP+ is reduced to NADPH that has a fluorescence emission at 460 nm……49

Figure 2.2 – RBC polyol pathway and sorbitol. More glucose in RBC will enter polyol pathway instead of the glycolysis pathway if the intracellular pH is lowered down. Sorbitol, the production in polyol pathway, may cause osmotic pressure because it's not membrane permeable. Also, due to NADPH being consumed in the reaction, the cells might suffer from oxidative damage……51

Figure 2.3 – Reaction of the enzymatic fluorescence method for sorbitol measurement. The sorbitol assay is based on the addition of sorbitol dehydrogenase to samples, oxidizing sorbitol to fructose. NAD+ is reduced to NADH during the reaction. NADH has an emission of fluorescence at 460 nm after excitation of 340 nm. The fluorescence intensity is proportional to the amount of NADH generated, as well as the sorbitol reacted……52

Figure 2.4 – The mechanism of RBCs regulation of blood flow through ATP release. There is millmolar levels of intracellular ATP in RBCs. RBCs can release hundreds of nanomoles of ATP to endothelial cells lining along with the blood vessel, which stimulates the production of endothelium-derived NO. The produced NO can diffuse to the smooth muscle cell layer, causing smooth muscle cell relaxation. This process enables vasodilation and a reduction in blood flow resistance……56

Figure 2.5 – Reaction of the chemiluminescence assay for ATP quantification. Luciferin can be oxidized by oxygen, in the presence of ATP. Firefly luciferase, a monomeric 61k Da protein, catalyzes luciferin oxidation using Mg^{2+} as a co-substrate. Chemiluminescence is produced by converting the chemical energy of luciferin oxidation through an electron transition, forming the product molecule oxyluciferin.……57

Figure 2.6 – Miniaturized blood collection and storage protocol. a) 1 mL of anti-coagulant solution (CPD, CP2D or CPDN) was injected into a non-heparinized vacuum tube; b) whole blood was drawn into each tube; c) after centrifugation, plasma and buffy coat were removed from the RBCs; d) AS was added to packed RBCs at a volume ratio 1:2. The combination of anticoagulant solution and AS followed FDA regulations (CPD/AS-1, CP2D/AS-3, CPD/AS-5) and their normoglycemic version (CPDN/AS-1N, CPDN/AS-3N, CPDN/AS-5N), respectively; e) an RBC suspension was aliquoted into sterilized PVC bags; f) for RBCs stored in normoglycemic solutions, the bags were opened weekly and a small amount of glucose saline (200 mM) solution was added to maintain the glucose concentration……61

Figure 2.7 – The design of the 3D-printed device. a) Engineering sketch of the fluidic device with dimensions (mm); b) 3D-printed fluidic device in VeroClear material, with membrane inserts in detection wells; c) 3D-printed fluidic device is designed to fit into a commercial plate reader like a standard 96-well plate……68

Figure 2.8 – The measurement of flow-induced ATP release from stored RBCs. a) A schematic cross section of RBCs circulated in a channel with membrane insert. The loop was closed by connecting Tygon tubing at both ends of a channel with a fingertight adapter. ATP released from RBCs will diffuse through the polyester membrane into the loading solution in the membrane insert; b) Stored RBC samples were diluted and loaded into 6 channels of the device. The flow was maintained by a peristaltic pump at a flow rate of 200 μL/min……69

Figure 2.9 – Glucose concentrations in stored RBCs. Glucose levels in solution (blank) and on RBC (black), for RBCs stored in standard storage solutions (circle) and our normoglycemic storage solutions (triangle). a) RBCs stored in CPD/AS-1 and CPDN/AS-1N; b) RBCs stored in CP2D/AS-3 and CPDN/AS-3N; c) RBCs stored in CPD/AS-5 and CPDN/AS-5N. Glucose concentrations, both in solution and on the RBC, are higher for those stored in FDA approved solutions, in which CPD/AS-1 provides the highest level. However, in normoglycemic storage conditions, glucose concentration can be maintained between 4 ~ 6 mM, the blood glucose level in healthy humans, throughout a 35-day storage. Data represent mean ± s.e.m. (n = 4 humans for all)……71

Figure 2.10 – Hemolysis level of stored RBCs. The percentage of hemolysis in the blood storage bags, including RBCs stored in high glucose environments (black circle) and low glucose environments (blank circle). a) RBCs stored in CPD/AS-1 and CPDN/AS-1N; b) RBCs stored in CP2D/AS-3 and CPDN/AS-3N; c) RBCs stored in CPD/AS-5 and CPDN/AS-5N. FDA requires the percent cell lysis less than 1% during RBC storage period. Stored RBCs meet the criteria until day 21, but exceed the threshold on day 35. The high percentage of hemolysis is partially due to the samples didn't pass through a leukofiltration membrane. Data represent mean ± s.e.m. (n = 4 humans for all)……72

Figure 2.11 – Sorbitol accumulation in stored RBCs. Intracellular sorbitol produced when

RBCs are stored in standard storage solutions (black bar) and normoglycemic storage solutions (grey bar). The dashed line represents the sorbitol level of fresh blood. a) RBCs stored in CPD/AS-1 and CPDN/AS-1N; b) RBCs stored in CP2D/AS-3 and CPDN/AS-3N; c) RBCs stored in CPD/AS-5 and CPDN/AS-5N. RBCs stored in standard solutions result in a significantly higher concentration of sorbitol accumulation in cells from day 1 through day 35. Notably, there is a significant increase of sorbitol concentration from day 7 to day 14 for RBCs stored in hyperglycemic conditions. This trend indicates permanent damage occurred during the first 2 weeks storage. Data represent mean ± s.e.m. (*p < 0.01, n = 5 humans for all)……..73

Figure 2.12 – Osmotic fragility of RBCs stored in hyperglycemic conditions (black bar) and normoglycemic conditions (grey bar). Dash line represents the ability of fresh RBCs to resist osmotic pressure. a) RBCs stored in CPD/AS-1 and CPDN/AS-1N; b) RBCs stored in CP2D/AS-3 and CPDN/AS-3N; c) RBCs stored in CPD/AS-5 and CPDN/AS-5N. RBCs stored in normoglycemic condition tend to be more rigid in the first week. However, after 2 weeks of storage, both hyperglycemic and normoglycemic storage show no difference, which further suggests that stored RBCs suffer from some permanent damage after 2 weeks in storage. Data represent mean ± s.e.m. (*p < 0.05, n = 5 humans)……..76

Figure 2.13 – Flow-induced ATP released from RBCs stored in standard storage solutions (black bar) and our modified storage solutions (grey bar). a) RBCs stored in CPD/AS-1 and CPDN/AS-1N; b) RBCs stored in CP2D/AS-3 and CPDN/AS-3N; c) RBCs stored in CPD/AS-5 and CPDN/AS-5N. During 35 days of storage, RBCs stored in our modified storage solutions keep their ability to release ATP, performing similar to fresh RBCs from healthy people (190 ± 10 nM). However, RBCs stored in standard storage solutions are only able to release about 50% of the ATP as typically measured from controls, thus resembling RBCs from people with diabetes. Data represent mean ± s.e.m. (*p < 0.05, n = 4 humans)……..78

Figure 3.1 – The mechanism of deformation-induced stimulation of ATP release. The process is started by mechanical deformation of a G-protein coupled receptor (GPCR) on the cell membrane, which binds to and activates heterotrimeric G proteins, Gi/Gs. Then, G proteins will activate adenylate cyclase (AC) to produce cyclic adenosine monophosphate (cAMP) through activation of protein kinase A (PKA). This will result in the cystic fibrosis transmembrane conductance regulator protein (CFTR) to become phosphorylated and regulate ATP release through one or more undetermined channels. Two candidates of ATP release avenue are CFTR and Pannexin 1 hemichannel……..100

Figure 3.2 – New blood storage bags. a) A new blood storage bags with 5 mL RBC sample stored in CPD/AS-5. The bag contains two parts, a 3D-printed part and a PVC plastic part. Three sides of the bag were sealed by impulse sealer. The top part of the bag, where the two parts were attached, was sealed by double-side tape and Teflon tape; b) A picture of 5 mL RBC sample stored in CPDN/AS-5N with a needle punched through the 3D-printed part. Two different materials were used in the 3D printing process. One is a white solid material. The other one is a black rubbery material. The PVC plastic part was adhered to

the white material. A needle can be inserted through the rubbery material, allowing concentrated glucose saline solution to be added to stored RBCs without opening bags; c) A schematic diagram of adding RBC sample into a blood bag. Utilizing the new blood storage bags, RBC samples were moved in or out from the bags using syringes. In this way, the process of opening, closing and reopening blood storage bags can be avoided……104

Figure 3.3 – Piggyback bag system for normoglycemic RBC storage. a) Engineering sketch of the glucose saline reservoir and switch with dimensions (mm); b) Storing RBCs under normal glucose levels using the piggyback bag system. The blood bag is connected to the 3D-printed piggyback bag by a Tygon tube and needle. The flow of glucose saline solution is controlled by the switch; c) A closer view of the 3D-printed glucose reservoir and switch. There is 2 mL of concentrated glucose saline solution in the container; d) Four sets of piggyback bag system fixed on the wall of a refrigerator. The blood samples were from four different donors……106

Figure 3.4 – The design of the membrane based deformability analysis device. a) Engineering sketch of the upper part of the device with dimensions (mm); b) Engineering sketch of the lower part of the device with dimensions. The printed device is composed of two different materials, a semi-transparent clear material and a black rubbery material. Polycarbonate membranes were placed on the black material areas. The two parts can be assembled together before deformability measurements. There are 6 ports on the device, enabling a high throughput deformability analysis. The diameter of the channels is 2.5 mm, which means the area of filtering RBCs is approximately 19.6 mm^2……111

Figure 3.5 – The determination of cell deformability applying 3D-printed device. a) A schematic illustration of measuring RBC deformability by filtration method. Diluted RBC suspension is pumped through a polycarbonate membrane with a pore size smaller than the diameter of RBCs. More deformable cells will be able to pass the membrane, while less deformable cells will be blocked; b) and c) Pictures of the printed membrane based device using clear material and black material; d) High throughput RBC deformability analysis using a syringe pump and printed device; e) A close view of RBC suspensions passing through membranes and being collected in tubes……112

Figure 3.6 – Hemolysis level of RBC stored in new blood bags. Black dots represent RBCs collected and stored in CPDN/AS-5N, which has physiological level of glucose. White dots represent RBCs processed using CPD/AS-5, which is the standard high glucose storage solution. RBCs were stored for 4 weeks in this study. The percent cell lysis is less than 0.8% throughout the storage period, which meets the FDA criteria for blood products. There is no difference between the hyperglycemia and normoglycemia cell storage. Data represents mean ± s.e.m. (n = 4 humans for all)……116

Figure 3.7 – Extracellular glucose concentration of storing RBCs using piggyback bag system. The glucose concentration in the solution supernatants was detected by a commercial glucose meter. It was well maintained at 4 – 6 mM, which is the healthy

glucose level in bloodstream, during a 28-day storage. A successful controlling of the extracellular glucose level can be achieved by using the piggyback bag system. Data represents mean ± s.e.m. (n = 4 humans for all)……117

Figure 3.8 – Sorbitol accumulation in stored RBCs. Black bars represent RBCs stored in the modified CPDN/AS-5N collection and storage solutions. White bars represent RBCs stored in FDA approved CPD/AS-5. Sorbitol production in RBCs stored in the high glucose environment is significantly higher than RBCs stored in the normal glucose condition, from the first day of storage. There is a slow increment of sorbitol concentration as a function of time, when cells were stored in CPDN/AS-5N. Data represents mean ± s.e.m. (*p < 0.05, n = 5 humans for all)……118

Figure 3.9 – Deformability measurements of stored RBCs. Black bars represent RBCs stored in normoglycemic conditions, and suspended in normal PSS. Lighter grey bars represent RBCs stored in hyperglycemic conditions, and suspended in high glucose PSS. Darker grey bar represent RBCs stored in hyperglycemic conditions, but suspended in normal glucose level PSS. This process is trying to mimic a real blood transfusion situation, where the high concentration of glucose is diluted in patients' bloodstream. All results from deformability measurements were normalized to the result from cells stored in normoglycemia on day 1. RBCs stored in hyperglycemic environments lost 10 – 20% of their deformability from the first day of storage. However, cell deformability can be maintained close to 100% when the modified storage solutions were utilized. Moreover, RBCs stored in standard storage solutions lost their reversibility of deformability after two weeks of storage. Data represents mean ± s.e.m. (*p < 0.05 when compared to the lighter grey bar, n = 4 humans for all)……119

Figure 4.1 – Diagram of RBC membrane structure. The RBC membrane is composed of three layers: a glycocalyx layer, which is rich in carbohydrates, on the exterior; a lipid bilayer, which is composed of cholesterol and phospholipids; and cytoskeleton proteins, a structural network of proteins located on the inner surface of the lipid bilayer. There are two kinds of membrane proteins. Integral proteins, which are embedded in the membrane via hydrophobic interactions with lipids. Such as, glycophorin and band 3. The other kind of membrane proteins are peripheral proteins, which are located on the inner side of lipid bilayer. Those proteins, including spectrin, ankyrin, actin and band 4.1, are responsible for cell deformation……134

Figure 4.2 – Chemical structures of RBC membrane lipids. There are five major phospholipids on RBC membranes, including phosphatidylcholine (PC) and sphingomyelin (SM), which are located on the outer monolayer of cell membrane; and phosphatidylethanolamine (PE), phosphatidylserine (PS) and phosphatidylinositol (PI), which are distributed in the inner layer. Notably, PE and PS, both containing an amino group, can react with glucose to form glycation products……135

Figure 4.3 – Non-enzymatic glycation reactions of PE. Glucose chemically reacts with

primary amine groups on PE, forming a reversible Schiff base within minutes. After that, the Schiff base product undergoes an Amadori rearrangement to form Amadori-PE, a more stable ketoamine compound. Once Amadori-PE is formed, it can further undergo complex reactions to form PE-linked advanced glycation end products (AGE-PE), such as carboxymethyl-PE (CM-PE) and carboxyethyl-PE (CE-PE)……..136

Figure 4.4 – MS and MS/MS scan of standard PE (14:0/14:0) and synthesized Amadori-PE (14:0/14:0). a) MS scan of synthesized Amadori-PE sample. Standard PE (14:0/14:0) shows a peak at m/z = 636.44. Synthesized Amadori-PE peak is located at m/z = 798.51; b) A zoomed-in spectrum of synthesized Amadori-PE sample at range m/z = 790 to m/z = 800; c) MS/MS detection of standard PE (14:0/14:0). A di-glyceride product ion peak at m/z = 495.44 was acquired. The fragmentation of PE, as well as the structure of XDG is presented; d) MS/MS detection of synthesized Amadori-PE (14:0/14:0). The same XDG peak at m/z = 495.44 was obtained……144

Figure 4.5 – MS results of Amadori-PE to PE ratio in stored RBC lipid extract. The black bars represent fresh blood control. The light grey bars represent RBCs collected and stored in CPD/AS-1, which is a high glucose environment. The dark grey bars represent RBCs collected and stored in CPDN/AS-1N, which is a normal glucose environment. Data is displayed as the ratio of Amadori-PE to PE in percentage at different storage length. On day 1, the ratio of Amadori-PE/PE is higher in stored RBC than fresh blood. The ratio decreases as a function of time. When RBCs were stored in physiological level of glucose, the ratio decreases faster. There is a significant difference between the two bars on day 14. In addition, the ratio of Amadori-PE/PE is significantly higher than the fresh blood level, when RBCs were stored in CPD/AS-1 on day 1 and day 14. Data represents mean ± s.e.m. (*$p < 0.05$, n = 4 ~ 6 humans)……..146

Figure 4.6 – Normalized Amadori-PE to PE ratios in stored RBCs. The black bars represent RBCs collected and stored in CPD/AS-1, which is a hyperglycemic condition. The grey bars represent RBCs collected and stored in CPDN/AS-1N, which is a normoglycemic condition. The ratios of Amadori-PE to PE at different storage lengths were normalized to the ratio on day 1, in order to have an improved visualization of trend and eliminate some human variations. The normalized ratios of Amadori-PE/PE, on day 14 and day 35, are significantly lower than day 1, from both normoglycemia and hyperglycemia cell storage. There was a significant difference observed on day 14 between the samples from CPD/AS-1 and CPDN/AS-1N. The trend of decreasing Amadori-PE/PE ratio, which was found in Figure 4.5, is also demonstrated in this bar graph. Data represents mean ± s.e.m. (*$p < 0.05$, n = 4 humans)……..148

Figure 4.7 – Normalized Amadori-PE to PE ratios from the second set of RBC samples. The black bars represent RBCs collected and stored in CPD/AS-1. The grey bars represent RBCs collected and stored in CPDN/AS-1N. The ratio of Amadori-PE to PE at different storage length was normalized to the ratio on day 1. Compared to Figure 4.6, the same trend was observed here when RBCs were collected and stored in normal glucose condition. The

normalized ratio decreases as the function of time. The results from day 1 were significantly higher than results from day 14 and day 35. However, the results are not reproducible to that from the first set of RBC samples when cells were stored in high glucose condition. Here, the normalized ratio does not change with the storage length. Additionally, there was a significant difference between the results on day 35. Data represents mean ± s.e.m. (*p < 0.05, n = 4 humans)……149

KEY TO ABBREVATIONS

RBC: Red blood cell

CPD: Citrate phosphate dextrose

AS: Additive solution

ATP: Adenosine triphosphate

NO: Nitric oxide

INOBA: Insufficient nitric oxide bioavailability

Hb: Hemoglobin

TRAIL: Transfusion-related acute lung injury

NADPH: Nicotinamide adenine dinucleotide phosphate

NAD: Nicotinamide adenine dinucleotide

GSH: Glutathione

PSS: Physiological saline solution

PBS: Phosphate buffer saline

AGE: Advanced glycation end product

PE: Phosphatidylethanolamine

MS: Mass spectrometry

ESI: Electrospray ionization

Chapter 1 – Introduction

In this chapter, the history of transfusion medicine and red blood cell (RBC) storage will be introduced, followed by a brief description of the current RBC collection and storage procedures in the United States. Post-transfusion related complications and prior clinical studies of stored RBCs will be discussed followed by a review of the *in vitro* changes to RBCs that occur during storage and effects on flow properties of these cells. An evaluation of hyperglycemia, which may significantly contribute to the genesis of the RBC storage lesion will be explored, followed by a discussion of technologies that may help investigate stored cells.

1.1 The Development of Red Blood Cell Storage

After over a century of improvements, the transfusion of RBCs has become a life-saving intervention for millions of chronically or massively transfused recipients worldwide every year. Historically, the first blood transfusions were performed by directly connecting the blood vessels from donor to recipient, and thereby their circulations, before clotting intervened. The separation of donor and recipient in time and space was achieved by blood collection and storage.[1] This separation has permitted the organization of donor services, and improvements in the quality and availability of blood products.

The first RBC storage solution was developed by Rous and Turner in 1915, using a mixture of citrate and glucose for storing rabbit RBCs.[2] This discovery helped the establishment of the world's first blood bank in France during World War Ⅰ by Robertson, which significantly increased the survival rate in the battlefield.[3] Two essential components to modern RBC storage were introduced by this remarkable work: citrate, as an

anticoagulant, allows the donor and recipient to be separated in space, while the use of glucose as a preservative, enables donors and recipients to be separated in time.[4] Later, because of the risk of bacterial contamination, as well as caramelization that occurs when heating a solution with glucose, a 3.8% sodium citrate solution was used for the collection of whole blood and a 5-day storage on ice, thus representing the first blood banking standard protocol.[5]

In the 1940s, at the beginning of World War II, Loutit and Mollison discovered that a mixed solution of glucose and citrate could be sterilized by autoclave if the pH was below 5.8. Therefore, citric acid was used as the citrate source, thus extending the storage of whole blood to 21 days.[6] The solution, acid citrate dextrose (ACD), enabled whole blood to be shipped around the world, and was the basis for building national blood systems in the US.[7]

In the 1950s, the US Food and Drug Administration (FDA) licensed a new solution, citrate phosphate dextrose (CPD). The addition of phosphate to ACD helped maintain the production of adenosine triphosphate (ATP) in RBCs, which increased the percentage of *in vivo* recovery in the first 3 weeks of storage.[8] During this same timeframe, isotope labelled Chromium-51 became available, which improved the accuracy of measurements for the fraction of RBCs that survived in the circulation in the first 24 h after transfusion (*in vivo* recovery).[9]

In the 1960s, plastic bags replaced glass bottles for storage, creating lighter weight storage that was resistant to breakage. Furthermore, plastic bags showed advantages for military bases. Finally, a sterilized closed collection system comprised of interconnected

bags also decreased the rate of bacterial contamination.[10] In addition to the advances, the most important contribution from using plastic bags was the introduction of diethylhexyl phthalate (DEHP), a plasticizer used with polyvinyl chloride (PVC). The leaching out DEHP from plastic bags can enter the RBC membrane and prevent the releasing of microvesicles. As a consequence, the hemolysis during storage was reduced four fold.[11]

In addition to the introduction of plastic bags in the 1960s, Simon and colleagues proposed that the addition of adenine could extend storage and improve RBC recovery and osmotic fragility; this work was inspired by Nakao who demonstrated the relationship of the loss of ATP in RBCs and cell lysis during storage. [12,13] A new solution, citrate phosphate dextrose adenine (CPDA-1), was developed in 1968, enabling whole blood storage for up to 5 weeks. However, it was not licensed in the US until 1979.[14]

In the 1970s, blood banks started to manufacture components to prepare RBCs for storage, as opposed to storing whole blood. CPDA-1 was first tested for both packed RBCs and whole blood. The recovery of RBCs stored as packed cells tends to be lower than whole blood storage.[15] This is mainly due to the hematocrit of packed cells being unfavorably high, causing the nutrients to be used up quickly.[16] Another two modified CPDA-1 solutions, CPDA-2 and CPDA-3, where the glucose and adenine concentration were elevated, were proposed by researchers.[17] However, adding more glucose would result in unnecessary amounts of glucose present for other components.

In the 1980s, additive solutions (AS) were developed to provide additional volume and nutrients for longer storage and better flow of stored RBCs.[18] The first AS was created by

Hogman *et al.*, named saline adenine glucose (SAG). The addition of AS successfully decreased the hematocrit from ~ 80% to ~ 55%.[19] Subsequently, mannitol was added as it demonstrated it could serve as a free radical scavenger, thereby stabilizing the cell membrane.[20] Adding 30 mM mannitol resulted in a reduction in hemolysis by 50%, thereby lengthening storage duration.[21] The solution, saline adenine glucose mannitol (SAGM), is the prototype of all current AS storage mixtures, and the standard AS used in Europe. Three variants from SAGM, AS-1, AS-3 and AS-5, are currently widely used in US. None of these AS appears to have significant advantages over the others.

Leukoreduction was brought into the RBC storage field in the 1990s. White blood cells (WBCs) that remain in blood bags can release proteases and lipases that damage RBC membranes. Therefore, the removal of WBCs, by aspiration of the buffy coat layer, also known as leukoreduction, can improve RBC recovery and reduce hemolysis. Heaton *et al*. demonstrated that leukoreduced RBCs have an increased recovery by 4%, and decreased hemolysis by 40% at 6 weeks, compared to non-leukoreduced cells.[22] Leukoreduction has become widely applied in the US, and has dramatically contributed to blood storage efficacy.

The most recent improvement in RBC storage solutions was the development of AS-7, which was approved by the FDA in 2013[23] and is the first commercialized alkaline RBC AS. AS-7, proposed by the group of Hess and Greewalt, ameliorates the long term storage lesion resulting in significantly increased viability *in vitro* and *in vivo*.[24,25] Until now, only a limited number of studies related to AS-7 have been performed, thus the benefits and limitations of AS-7 need to be further explored. Since AS-7 is not involved in this thesis,

the concept behind alkaline storage will be discussed in Chapter 5. The main part of this dissertation will be focused on the three AS extensively used in the US; AS-1, AS-3 and AS-5.

1.2 Current Red Blood Cell Collection and Storage in US

According to the 2011 National Blood Collection and Utilization Survey Report (NBCUS), approximately 16 million units of RBCs were prepared by blood centers and hospitals in the US.[26] The blood collection and storage is regulated by the US FDA. A typical procedure of blood collection and storage is shown in Figure 1.1. Briefly, 450 mL of whole blood is drawn from a donor's vein into a primary collection bag containing 63 mL of an anticoagulant solution such as citrate-phosphate-dextrose (CPD). After centrifugation of the entire bag, the plasma and buffy coat (containing platelets and WBCs, respectively) in the layers at the upper part of the bag are removed. Then, the RBCs sedimented at the bottom of the bag are transferred into a satellite bag containing 110 mL of an AS (such as AS-1).[27] The resulting ~ 300 mL RBC suspension in AS, of which the hematocrit is about 50 – 60%, can be stored at 4 °C for up to 42 days. In recent years, RBCs are usually further modified by leukoreduction prior to storage by passing through a filter membrane. Although there might be minor differences between blood collection and storage systems provided from different companies, a similar procedure and amount of solutions are used during the process. All bags used in blood collection and storage are polyvinyl chloride (PVC) bags.

There are four sets of blood storage solutions (anticoagulant solution + AS) approved by the FDA in the US, including CPD/AS-1 (Adsol, produced by Baxter), citrate phosphate

double dextrose (CP2D)/AS-3 (Nutricel, produced by Pall Medical), CPD/AS-5 (Optisol, produced by Terumo) and CPD/AS-7 (SOLX, produced by Hemerus). Except for CPD/AS-7, which was licensed in 2013, the products have been commercially available for almost three decades.[1,24] It is worth noting the differences between CPD/AS-7 and the other three blood collection and storage systems. AS-7, also called "SOLX@ Additive Solution" or "SOLX@ Additive System", utilizes two satellite containers with different solutions. Container A has 80 mL of SOLX@ Additive Solution A, while there is 30 mL of SOLX@ Additive Solution B in container B. The contents in container B are completely drained into container A and well mixed prior to adding the combined solutions to the RBCs.[23] The logic behind this procedure is that AS-7 is a basic (pH) solution, which means that glucose will be caramelized during autoclave sterilization. The separation into two solutions, where solution B is an acidic glucose solution and solution A containing other components, allows the solutions to be sterilized.[23]

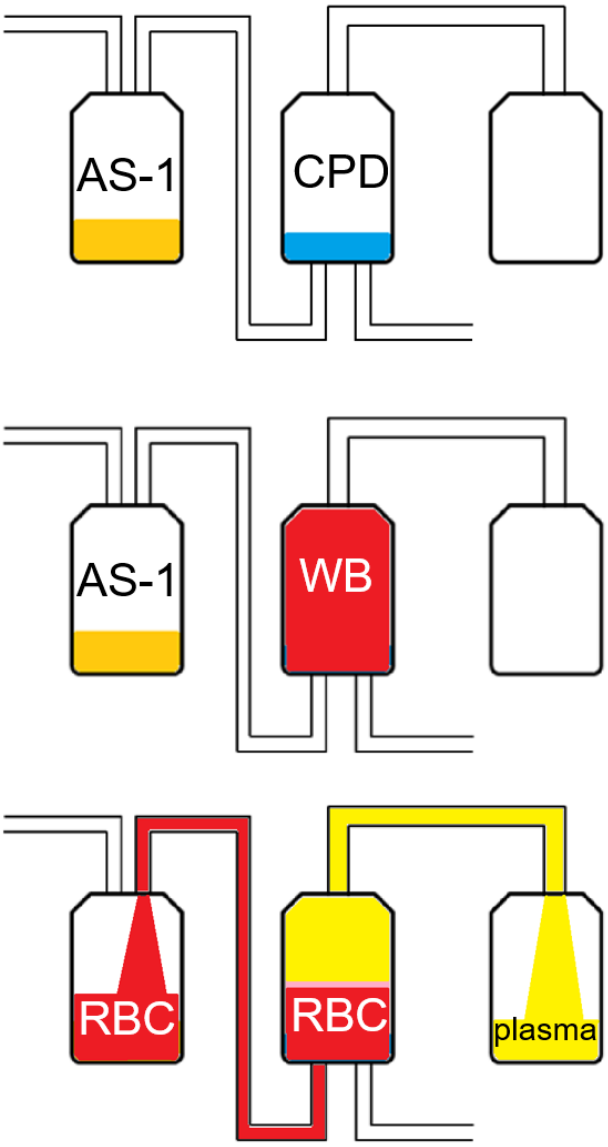

Figure 1.1 – Standard blood collection and storage system. 450 mL of whole blood is collected from a donor's vein into a primary bag containing 63 mL of CPD. The entire bag is centrifuged, followed by the removal of plasma and buffy coat layers. Packed RBCs are exported out from the bottom port into a satellite bag that contains 110 mL of AS-1. The resulting RBC suspension in AS-1 can be further purified by leukoreduction. RBCs are stored at 4 °C for up to 42 days.

Table 1.1 – Contents of different blood storage solutions

Constituents (mM)	CPD	CP2D	AS-1	AS-3	AS-5	AS-7
Sodium citrate	89.4	89.4	/	20	/	/
Citric acid	15.6	15.6	/	2.0	/	/
NaH_2PO_4	16.1	16.1	/	20	/	/
Na_2HPO_4	/	/	/	/	/	12
$NaHCO_3$	/	/	/	/	/	26
Glucose	129	258	111	55	45	80
NaCl	/	/	154	70	150	/
Adenine	/	/	2.0	2.2	2.2	2.0
Mannitol	/	/	41	/	29	55
pH	5.6	5.6	5.8	5.8	5.8	8.5

The components of different blood storage solutions are listed in Table 1.1. All additives listed in the table hold specific purposes. For example, citrate is added to chelate calcium ions in the plasma to prevent coagulation of blood.[2] The addition of phosphate reduces the internal and external RBC phosphate concentration gradient, resulting in an increase of ATP synthesis.[8] Citric acid is added as a buffered component to control the pH below 5.8.[6] Studies have shown that the addition of adenine can improve RBC recovery after a transfusion.[12,13] The purpose of adding mannitol is to protect the RBC membrane and reduce hemolysis.[20] Glucose serves as the energy source of RBCs, since these cells rely on the breakdown of glucose to ATP to maintain cellular metabolism. The contribution from the PVC bag is DEHP, a plasticizer, which leaches out from the bag to stabilize the membrane of RBCs.[11]

The FDA has proposed acceptance criteria for RBC storage product to be licensed. The most vital two standards are the hemolysis level of stored RBCs should be less than 1% at the end of storage; and the recovery of RBCs at 24 h after transfusion should be higher than 75%.[28] However, an evaluation of a total of 941 RBC recoveries obtained from 11 laboratories and 34 studies shows that the probability of passing these criteria for currently FDA approved products was poor.[29] The conclusion highly suggests that the quality of RBC products are still not 100% safe, even though products have continually been improved over a century. In the next section, the current transfusion status in clinical institutes in the US will be discussed, where the necessity of further investigating and improving stored RBCs will be highlighted.

1.3 Clinical Performance of Stored Red Blood Cells

RBC transfusion is one of the most frequently manipulated healthcare strategies in clinical institutes in the US. It has been a standard of care for the management of anemia for more than 100 years, which affects almost 90% of critically ill patients.[30] The definition of anemia includes a blood hemoglobin (Hb) concentration of less than 12 g/dL in females and 13 g/dL in males.[31] Anemia can cause fatal consequences in multiple scenarios, including cardiac surgery, trauma, critical care and cancer.[32] Approximately 40% of critical patients will receive 2 – 5 units of RBCs via transfusion during their hospitalization.[33,34] RBC transfusion can potentially resolve anemic symptoms by increasing oxygen delivery and cell mass. The standard threshold for a transfusion was set to be a blood Hb level of < 10 g/dL or a hematocrit < 30%.[35-37] A restrictive threshold of Hb < 7 g/dL is recommended in the new American Association of Blood Banks (AABB) guidelines.

Blood transfusion practices have been continually developed for more than a hundred years. Due to advances in donor screening, improved testing, automated data systems, and changes in transfusion medicine practices, the blood supply is safer today than any other time in history. Accompanying this improved safety was the 2011 NBCUS report indicating that, in recent years, the available supply of RBC units was sufficient to meet the overall transfusion demand.[26] However, the transfusion process remains a balance between the risk of anemia and the risk of post-transfusion related complications. Although RBC transfusion is a life-saving treatment of hemorrhagic shock, it can be associated with numerous and significant complications, especially when massive transfusion is performed. The three most common definitions of massive transfusion in

adult patients are (1) transfusion of ≥ 10 RBC units within 24 h (2) transfusion of > 4 RBC units in 1 h with the anticipation of continuous blood product support or (3) the replacement of > 50 % of the total blood volume within 3 h.[38] The identified complications associated with blood transfusions are listed in Table 1.2.[39] Transfusion-related acute lung injury (TRALI) is the No.1 cause of major morbidity and death. It presents itself as an acute respiratory distress syndrome either during or within 6 h of transfusion.[40] From 2011 to 2015, 40% of reported transfusion mortality was caused by TRALI, followed by transfusion associated circulatory overload (TACO) (24%). Totally, about 60 fatalities directly associated to transfusion were reported in each year over the past five years.[41]

People may argue that this number is low, though it is not negligible. However, this does not mean complications associated with blood transfusion is not a serious issue. The number of reported deaths is not decreasing, reflecting that the quality of blood products might be a barrier of blood transfusion safety. Also, the federal reports include mortality, but not morbidity. There is no annual summary of all transfusion-related complications that occurred in hospitals. More importantly, due to the difficulties in post-transfusion related complications diagnosis, the number of fatalities might be underestimated. For example, there is no diagnostic tests available for TRALI. Although the US National Heart, Lung and Blood Institute Working Group formulated a case definition of TRALI based on clinical and radiological parameters in 2004, the characteristics of TRALI are still indistinguishable from acute lung injury due to other causes, such as sepsis or lung contusion.[42-44] The absence of absolute definition of TRALI leads to other risk factors that must be ruled out in the diagnosis process, resulting in underdiagnosis.

Many clinical studies have been conducted in the past three decades to discover the relationship between RBC storage and clinical practice. Unfortunately, the clinical significance of storing RBCs is controversial. In 1989, a publication of a small, randomized, single center trial that compared the effects of fresh whole blood (< 12 h) with stored blood (2 – 5 days) aroused the interest in the relationship between the duration of RBC storage and transfusion outcomes.[45] Twenty years later, a highly debated retrospective study by Koch *et al.* showed that patients who underwent cardiac surgery and received "older" blood (> 14 days) had worse outcomes than those who received fresher blood (≤ 14 days), suggesting the potential negative association between the age of RBCs and transfusion outcomes.[46] One systematic review published in 2013 summarized relevant papers in RBC storage and clinical effects during the last three decades. The authors reviewed a total of 55 studies, mostly retrospective, among which 47% indicated that long-term stored RBCs caused adverse effects in transfusion, whereas the remaining 53% revealed no difference.[47] Another project conducted by Wang *et al.* analyzed 21 observational studies published between 2001 and 2011, including 409,966 patients in total. They performed quantitative meta-analysis, which lead to the conclusion that RBC storage was associated with an increased risk of mortality.[48]

Table 1.2 – List of post-transfusion related complications

Acute	Delayed
Acute hemolytic transfusion reactions	Delayed hemolytic transfusion reactions
Transfusion-related acute lung injury	Transfusion related immunomodulation
Allergic reactions	Microchimerism
Bacterial sepsis	Post-transfusion graft-vs-host disease
Hypocalcemia	Post transfusion purpura
Hypokalemia, hyperkalemia	Transfusion-transmitted diseases
Acidosis	
Hypothermia	
Dilutional coagulopathy	
Dilutional thrombocytopenia	
Transfusion-associated circulatory overload	
Febrile non-hemolytic transfusion reactions	

Although dozens of clinical research studies have been conducted in different fields, including cardiac surgery, trauma, critical care, and cancer, the clinical effects of RBC storage have not been confirmed. There are several limitations in clinical trials. Ethical and operational issues have prevented careful study of the oldest stored RBCs. The definition of "fresher" and "older" RBCs are varied from institute to institute. For example, some used 7 days as a marker, while 14 days and 21 days are also widely used. This issue is particularly problematic in massive transfusions where multiple units of different storage duration RBCs were transfused. Moreover, a retrospective study omits several important clinical factors, such as baseline patient characteristics, underlying diseases, and volume transfused. An observational study can't determine whether the mortality of morbidity is due to the transfusion itself or other causes. There is no strict standard regulating the study of RBC storage and clinical performance. In addition, well organized control experiments to evaluate the consequences of transfusion cannot be performed due to ethical issues.

Since there are several barriers that cannot be overcome in *in vivo* studies, a comprehensive and deep understanding of *in vitro* changes to stored RBCs might be an alternative way of leading people to build the link between RBC storage and transfusion outcomes.

1.4 Red Blood Cell Storage Lesion

After removal from a donor's circulation and entering standard blood banking conditions, the environment of RBCs is changed from *in vivo* to *in vitro.* The decline in RBC quality and function occurring during the storage is called the storage lesion. Compared to clinical

studies, the storage lesion has been well documented and demonstrated *in vitro.* There are three separate, yet interrelated, categories of the storage lesion: metabolic effects, oxidative damages and cell membrane changes.

1.4.1 Metabolic Effects

Unlike other mammalian cells, RBCs lack such organelles as mitochondria; therefore, the generation of ATP in the RBC solely depends on the anaerobic glycolysis pathway.[49] The glycolysis pathway of glucose in the RBC is shown in Figure 1.2. Protons are produced when glucose is phosphorylated by hexokinase, the first step of the glycolysis pathway, and an ATP hydrolysis reaction. Because of the current blood storage solutions lack of buffering capacity, intracellular pH continually decreases over time, reaching 6.5 – 6.8 by the end of storage.[50] The acidic environment slows down glycolysis by inhibiting such key enzymes as phosphofructokinase and hexokinase. As a result, ATP production is reduced.

In addition to glycolysis pathway, Luebering-Rapoport shunt that involves the formation of 2,3-diphosphoglycerate (2,3-DPG), is affected. 2,3-DPG that can bind and stabilize deoxyhemoglobin is essential for RBC oxygen unloading ability. However, diphosphoglyceromutase phosphatase (DPGP) is activated when the pH falls below 7.2, leading to a decrease in 2,3-DPG to an undetectable level with 2 weeks of storage.[51] A low level of 2,3-DPG will increase the binding affinity of hemoglobin to oxygen, causing difficulties in releasing oxygen to nearby tissues. Normally, the concentration of 2,3-DPG recovers back to physiological levels within 48 h after entering the circulation.[52]

In addition to glycolysis pathway, Luebering-Rapoport shunt that involves the formation of 2,3-diphosphoglycerate (2,3-DPG), is affected. 2,3-DPG that can bind and stabilize deoxyhemoglobin is essential for RBC oxygen unloading ability. However, diphosphoglyceromutase phosphatase (DPGP) is activated when the pH falls below 7.2, leading to a decrease in 2,3-DPG to an undetectable level with 2 weeks of storage.[51] A low level of 2,3-DPG will increase the binding affinity of hemoglobin to oxygen, causing difficulties in releasing oxygen to nearby tissues. Normally, the concentration of 2,3-DPG recovers back to physiological levels within 48 h after entering the circulation.[52]

Furthermore, the glucose molecule favors the polyol pathway instead of the glycolysis pathway at low pH. In the polyol pathway, sorbitol is derived from glucose instead of fructose, catalyzed by aldose reductase. The optimal pH for hexokinase is 7.5 – 9.0, while its 6.2 – 6.8 for aldose reductase.[53,54] Thereby, polyol pathway is activated at lower pH values. Sorbitol is a well-known biomarker for diabetes mellitus, a disease having hyperglycemia as a hallmark feature.[55] The production of sorbitol, a major product of the aldose reductase (polyol) pathway, may cause the cells to suffer from oxidative stress, which will be discussed next.

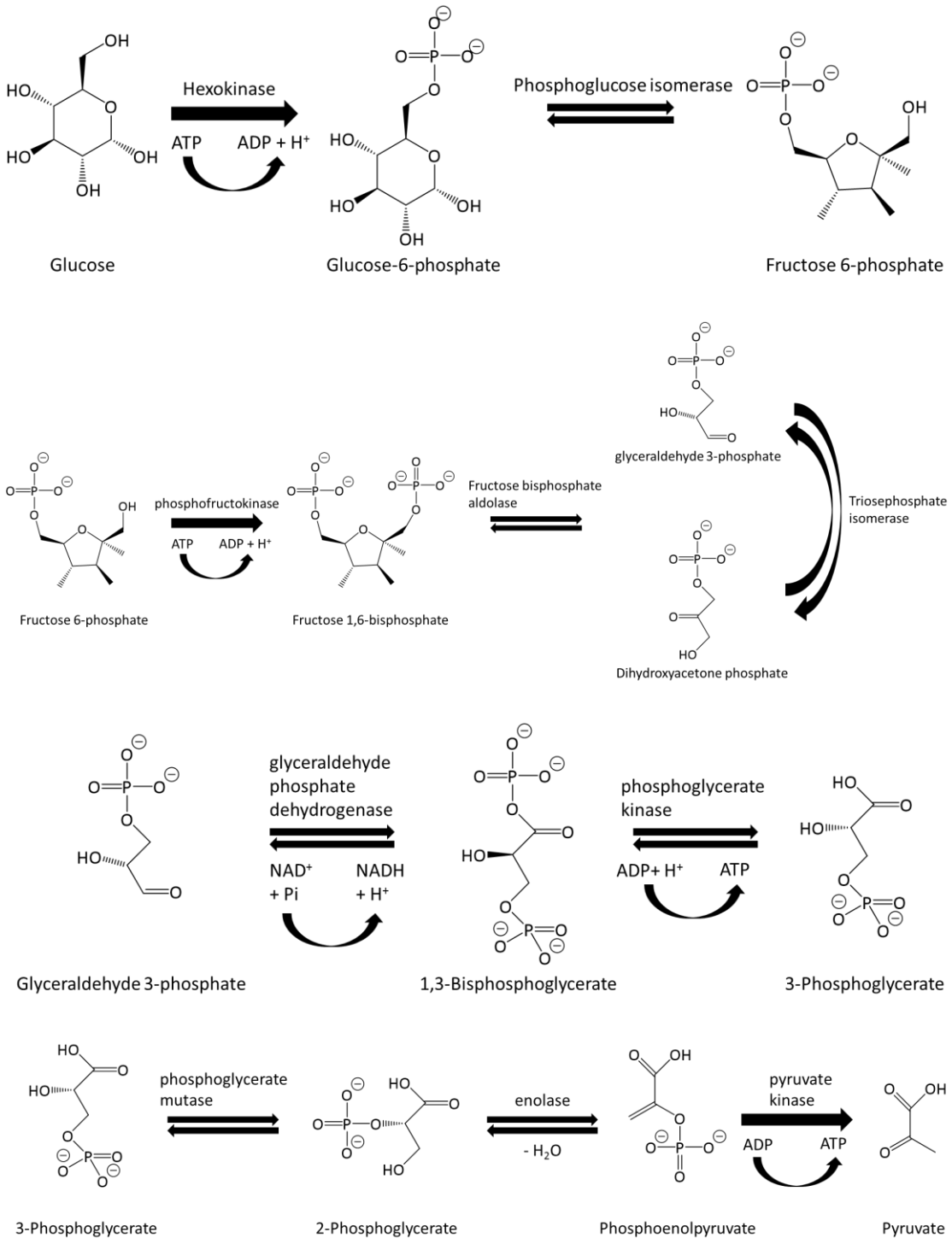

Figure 1.2 – RBC anaerobic glycolysis pathway. The glycolysis pathway generates 90% of the ATP as the energy source to maintain the metabolism of RBCs.

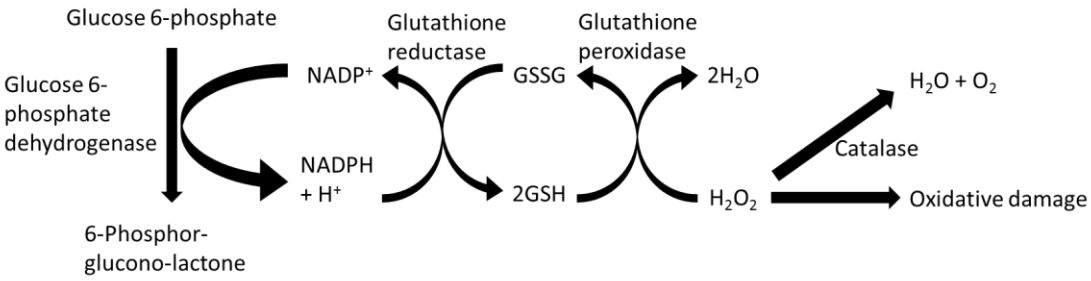

Figure 1.3 – The regeneration of GSH and oxidative damage. GSH is an active antioxidant in cells, which can prevent damage from ROS such as free radicals and peroxide. The regeneration of GSH is essential for cell anti-oxidation capacity. Because of the acidic environment of RBC storage, the activity of the enzyme, glucose 6-phosphate dehydrogenase, is inhibited. As the consequence, the production of NADPH will be decreased, causing obstacles in GSH regeneration process.

1.4.2 Oxidative Damages

RBCs are typically 75% saturated with oxygen when collected from the donors and stored under aerobic condition.[56] Normally, RBCs are well equipped with superoxide dismutase and methemoglobin reductase, as well as nicotinamide adenine dinucleotide phosphate (NADPH) and glutathione (GSH), to prevent and repair any oxidative damage. GSH is an important antioxidant, capable of preventing damage from reactive oxygen species (ROS) such as free radicals. GSH can be oxidized to GSSG, by donating a reducing equivalent ($H^+ + e^-$) to other molecules from the thiol group of cysteine. The anti-oxidation capacity of cells will be impaired if the concentration of GSH is decreased. The regeneration of GSH highly depends on the production of NADPH, when glucose 6-phosphate is converted to 6-phosphor-glucono-lactone, catalyzed by glucose 6-phosphate dehydrogenase (G6PD). This pathway is called hexose-monophosphate shunt. While the optimal pH for G6PD is 8.5, this process will be hindered if cells are stored in acidic environments.[57] Also, NADPH is consumed during the conversion of sorbitol from glucose. Therefore, the ability of stored RBCs to maintain NADPH and GSH levels through the hexose-monophosphate pathway will be impaired, which is illustrated in Figure 1.3.[49,58]

The likelihood of hydroxyl radical formation via the Fenton reaction increases in stored RBCs because the cell antioxidant defense system is damaged.[58] The Fenton reaction is shown below:

$$Fe^{2+} + H_2O_2 \rightarrow Fe^{3+} + HO\bullet + OH^-$$

$$Fe^{3+} + H_2O_2 \rightarrow Fe^{2+} + HOO\bullet + H^+$$

RBCs contain high concentrations of intracellular iron, and the Fenton reaction is the most common way of generating free radicals *in vivo.*

The generated free radicals, including but not limited to peroxides, superoxide and hydroxyl radical, can further oxidize cell lipids or proteins, resulting in progressive oxidative damage to stored RBCs. For example, it is hypothesized that Band 3 clustering due to oxidation is a mechanism for senescent RBC removal.[59] Moreover, oxidative stress can cause the formation of lysophospholipids, especially lysophosphatidylcholine (lysoPC), which has been suggested to be the main contributor to non-antibody mediated TRALI.[51,60] Importantly, oxidative stress to spectrin, an important cell membrane skeleton protein, is correlated to microvesicles formation as well as RBC mechanical feature changes during the storage.[61] Peroxidation reaction, which is shown in Figure 1.4, happening to cell membrane unsaturated lipids may affect RBC shape and deformability.

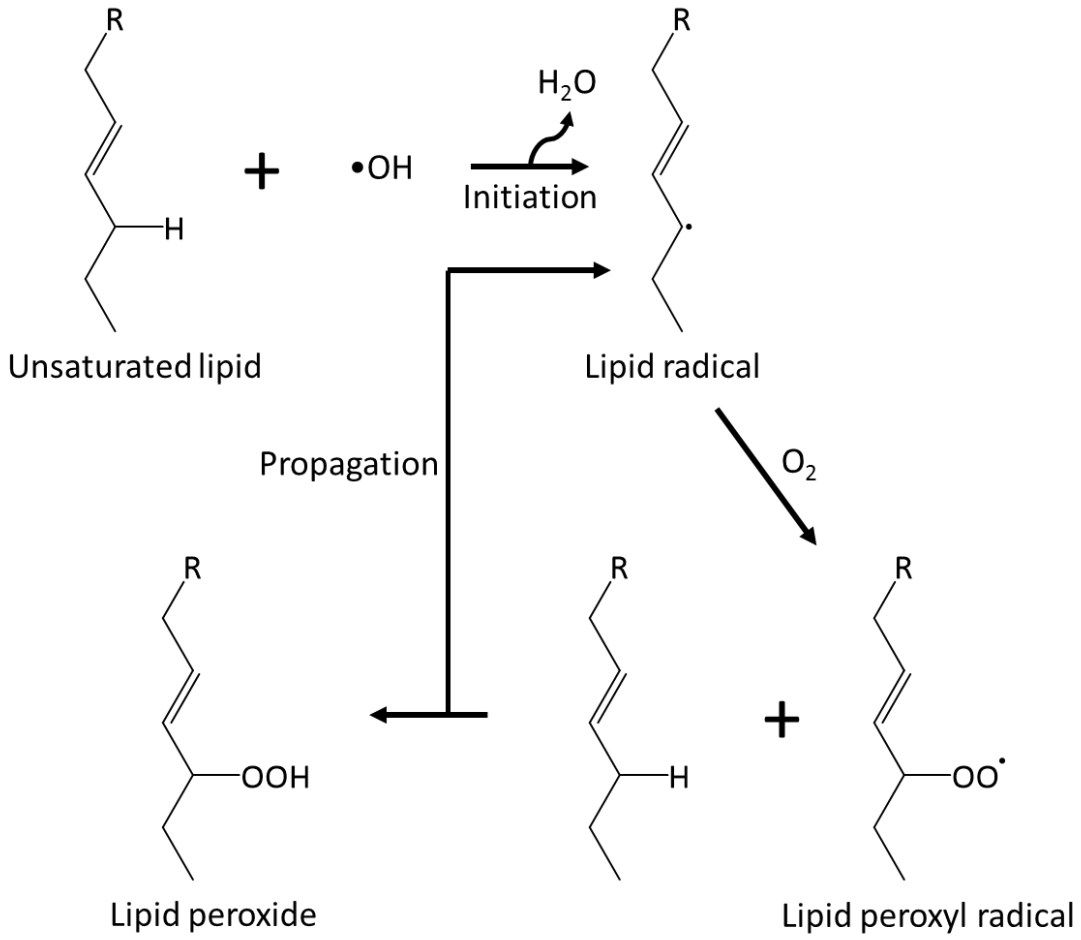

Figure 1.4 – The formation of lipid peroxide. Free radicals generated through Fenton reactions can further react with lipids or proteins to form peroxide products, causing RBCs to undergo progressive oxidative insult. The reaction above describes a typical lipid peroxidation process. A similar reaction may also occur in proteins.

1.4.3 Cell Membrane Changes

The oxidative stress discussed above may influence some cell membrane properties, resulting in RBC shape change as well as loss of deformability. The healthy RBC has a 6 – 8 μm diameter biconcave disc shape with a volume of ~ 90 fL. This shape provides the RBC with a maximum surface area to facilitate gas exchange and necessary deformability to pass through narrow capillaries. During storage, RBCs slowly change from smooth biconcave discs to subtly bumpy discs to grossly bumpy spheres called spheroechinocytes.[62] The shape changes are thought to reduce RBC post-transfusion survival due to decreased surface to volume ratio and deformability.[63,64] The shape alternation is partially due to the metabolic changes that occur in RBCs during storage. ATP has been shown to play an important role in maintaining RBC shape. Nakao *et al.* reported that RBC shape change can be induced by depleting ATP, and reverted back to the original shape by the supplementation of adenine.[65]

Some morphological changes are reversible after transfusion or by rejuvenation prior to transfusion, if the duration of cell storage is less than two weeks.[62] However, modifications to cell shape or cell surface membrane via exporting microvesicles is irreversible. Microvesicles have a diameter ranging from 100 to 1000 nm, consisting of phospholipids, transmembrane proteins and cytoskeletal proteins.[66] The release of microvesicles is partially caused by oxidative damage, as previously discussed.[67] The formation of microvesicles has been proposed as a mechanism of cells to remove damaged cellular components.[68] The decreased cell surface to volume ratio and deformability caused by microvesiculation is a permanent damage to the stored RBC,

which can't be reversed. The clinical effects of microvesicles in blood products are still under debate.

In addition to oxidative damages, glycation is another common cell alteration that occurs to stored RBCs membrane components. Lipids and proteins with an amino group are able to react with glucose molecules non-enzymatically to form glycation products. The most common protein glycation is forming glycated hemoglobin, as 96% of the RBC (by mass) is hemoglobin. One type of hemoglobin glycation product, HbA1c, is a well-known indicator of average blood glucose levels during a three-month period. It has been implicated that the non-enzymatic glycation of hemoglobin adversely affects the function and structural properties of the protein, leading to oxidative stress and pathological complications of diabetes mellitus.[69] In addition to HbA1c, advanced glycation end products (AGEs), a heterogeneous group of chemically active compounds, are also found in stored RBCs. A study reported by Mangalmurti demonstrated that AGEs can increase endothelial cell ROS generation through interaction with an AGE receptor and thereby damage endothelial cells.[70] Moreover, Lysenko and colleagues reported that AGEs may contribute to post-transfusion related complications.[71]

Another cell membrane structure change happened during RBC storage is the exposure of phosphatidylserine (PS). PS is one of the primary RBC membrane lipids existing in the inner leaflet. The exposure of PS in the outer layer of the cell membrane has been proven to be correlated with cell apoptosis.[72] It has been shown that PS translocation to the cell surface increases during storage, resulting in progressive adherence of RBCs to endothelial cells.[73] The increases in adhesion to endothelial cells, accompanied with

decreased cell deformability, could potentially cause problematic blood flow after transfusion, which will be discussed in the next section.

1.5 Flow Property of Red Blood Cells

RBCs are a special type of human cells, because they constantly move in the blood stream as opposed to being sessile, like adherent cells. The primary function of the RBC *in vivo* is to deliver oxygen to tissues and carry away metabolic waste, such as carbon dioxide. Therefore, a consistent blood flow is crucial for RBCs to function. Many detrimental diseases, such as shock, are due to a high resistance in blood flow. Despite a large amount of studies involving the storage lesion, investigations of the stored RBC under flow properties is insufficient, especially for new types of AS being discovered.

Although flow is not often a part of most studies involving the effect of the storage lesion, flow itself is a very important aspect of the downstream effects of the storage lesion on the RBC. It has been reported that sialic acid content of stored RBCs decreases as a function of time, leading to reduction of the electrostatic repulsive forces that protect RBCs from aggregation.[73,74] As a consequence, the blood viscosity will increase and potentially block flow in small vessels. Also, a study of stored RBCs under standard blood banking conditions showed significantly enhanced aggregability and decreased deformability at 2 weeks of storage.[75]

Clinical trials have shown that increased morbidity and mortality is associated with transfusing aged RBCs.[45,46] To explain the observations, Roback *et al.* proposed a concept about insufficient nitric oxide bioavailability (INOBA).[76] Nitric oxide (NO), a Nobel Prize winning molecule, participates in vasodilation by stimulating cyclic guanine

monophosphate (cGMP) production inside the smooth muscle cells.[77,78] cGMP is a regulator of ion channel conductance, which can cause smooth muscle cell relaxation, resulting in an increase in blood flow.[79]

Because of INOBA, the function of RBCs is no longer limited to gas exchange; rather it's a potential blood flow determinant by regulating local NO concentration. There are three proposed mechanisms to describe how RBCs provide NO to smooth muscle cells. First, NO originally secreted from endothelial cells can bind to sulfur atoms on cysteine β-93 of hemoglobin (SNO-Hb).[80,81] Because the SNO-Hb bond is unstable, NO can be released from RBCs when oxygen tension is low.[82] Second, plasma nitrite can be reduced to NO by deoxygenated hemoglobin, and SNO-Hb is produced in this case as well.[83] In both mechanisms, NO is derived from RBCs via the SNO-Hb bond, though the origin of NO molecules is different. However, NO is a free radical with a half-life less than a few seconds and may not be able to diffuse from hemoglobin, through the RBC membrane, through plasma, through the endothelium and to smooth muscle cells without being oxidized, scavenged, or depleted.[84] Moreover, NO can be quenched by AGEs, microvesicles and free hemoglobin molecules present in the blood stream and cell surface. Hence, RBC-derived NO mechanisms are facing great challenges.[85,86]

The third mechanism, in which our group is particularly interested, describes that NO production in endothelial cells is stimulated by RBC-derived ATP. RBCs are able to release hundreds of nanomoles of ATP under several stimuli, including shear stress, hypoxia, C-peptide, and hydroxyurea.[87-92] ATP can diffuse to endothelial cells, binding to the purinergic receptor (P2Y), further resulting in activation of endothelial nitric oxide

synthase (eNOS), which catalyzes production of NO from L-arginine.[93] In this case, the diffusion of NO from endothelial cells to smooth muscle cells is more practical and efficient, since it does not have to pass through the RBC membrane and blood stream.

1.6 Normoglycemic Storage of Red Blood Cells

Although the storage lesion and RBC rheology has been well studied for several decades, the origin of the storage lesion remains undetermined. Interestingly, there are similarities between stored and diabetic RBCs, including their exposure to elevated concentrations of glucose. It is well-acknowledged that the blood glucose concentration is within 4 – 6 mM for a healthy human, while its 7 – 9 mM for people with well controlled diabetes mellitus.[94] Many *in vitro* changes occur to stored RBCs, which was described in the last section, can also be found in diabetic RBC studies. For example, the Spence group showed that RBC-derived ATP release from type II diabetic cells was less than half of that measured from healthy controls.[95] McMillan reported that diabetic RBCs lost 50% of their deformability.[96] Additionally, Dincer and coworkers demonstrated that RBCs from people with diabetes suffered from oxidative stress due to the insufficient antioxidant defense by the GSH pathway, which may be one of the factors responsible for the development of diabetes complications.[97] *A*n augmentation of blood lipid glycation and lipid oxidation in diabetic patients was discovered by Miyazawa *et al*.[98] Also, AGEs were found accumulating on the surface of diabetic RBCs.[99] It would be rational to hypothesize that the RBC storage lesion and diabetic complications may have the same origin. In other words, hyperglycemia may significantly contribute to the development of the RBC storage lesion.

The best clinical practice for diabetes mellitus treatment is controlling blood glucose levels, by insulin injection, exercise, and diet.[100] It would be premature to assume that it's beneficial for stored RBCs if the glucose concentration is well maintained within healthy levels. Previous results suggested a normoglycemic environment for RBC storage, and highlighted some advantages of removing the excess glucose. For instance, Wang reported a modified CPD/AS-1, labelled CPDN/AS-1N, where N represents normoglycemic. The glucose level in CPDN/AS-1N was kept within 4 – 6 mM during a 35-day storage of RBCs. Results showed that RBCs stored in normoglycemic conditions release significantly higher amounts of ATP, further increasing the NO production in endothelial cells by 25%.[101] In addition, using the same storage solutions, Liu demonstrated that the ability of stored RBCs to bind C-peptide was adversely affected by the high concentration of glucose, while normoglycemic storage solutions had no adverse effects on C-peptide binding.[102] Chen explored the relationship between high glucose RBC storage with cell deformability and reversibility. He concluded that cell deformability was lost as soon as the first day of storage when RBCs were stored in CPD/AS-1. However, the cell deformability remained unchanged if the modified low glucose storage solution was utilized.[103]

In addition to CPD/AS-1, there are two other standard processing and storage solutions widely used in the US, CP2D/AS-3 and CPD/AS-5. In order to further demonstrate the benefits of normoglycemic RBC storage, all three blood collection and storage solutions, along with their normoglycemic versions, were investigated and will be described in this dissertation.

1.7 Modern Techniques Utilized for Red Blood Cell Study

Scientists have been studying RBCs for more than 100 years. Multiple analytical methods have been developed and utilized. For example, to investigate metabolic changes, Popp and Snijders used a capillary gas chromatography to determine the concentration of sorbitol produced in RBCs from both diabetic and healthy subjects.[104] Umeda developed an enzymatic fluorometric method with an improved deproteinization procedure for sorbitol determination in human RBCs. In addition, to studying cell membrane properties, individual cell deformability measurement can be accomplished by micropipette aspiration, atomic force microscopy (AFM), optical tweezers, magnetic twisting cytometry, quantitative phase imaging and dynamic light scattering.[105-109] While filtration methods, microfluidic filtration, and erythrocyte shape recovery are available approaches for multiple cells deformability measurement.[110-112] Moreover, to determine storage biomedical effects, Miyazawa applied an LC-MS/MS method to quantify cell membrane carboxymethylated (CML) and carboxyethylated (CEL) phosphatidylethanolamines (PE), two well-known AGEs of cell membrane lipids.[113]

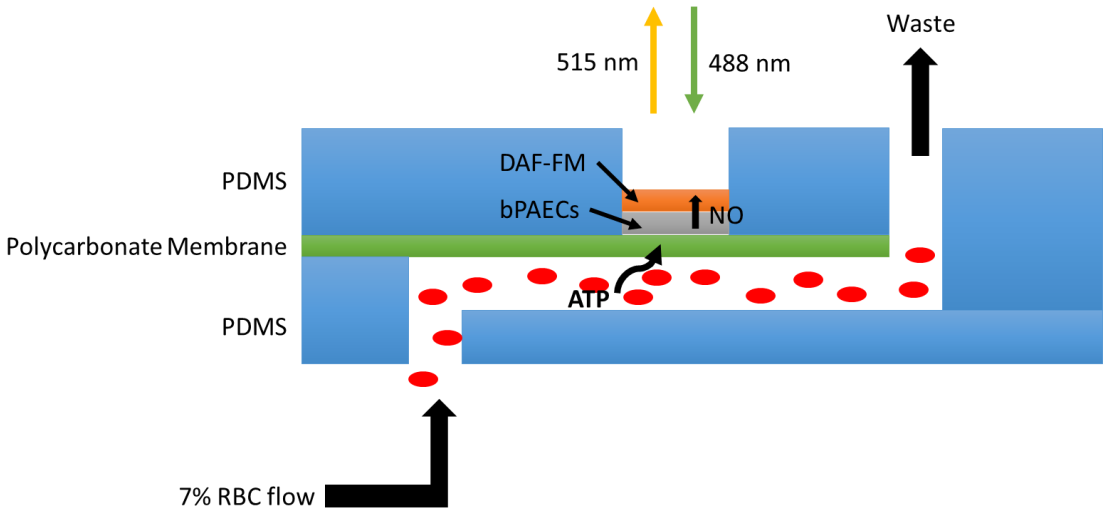

bPAECs: Bovine Pulmonary Artery Endothelial Cells
DAF-FM: 4-amino-5-methylamino-20,70-difluorescein

Figure 1.5 – PDMS device for NO measurement. The microfluidic device contains two slabs of PDMS, where the bottom one has channels with inside diameters closing to arterioles *in vivo*, while the top one equipped with a 1/8" hole for optical detection of NO. A polycarbonate membrane was fixed between the two layers of PDMS and sealed. Endothelial cells were cultured on one side of the membrane. A 7% RBC suspension was pumped through the channel, and the NO production by endothelial cells was quantitated by DAF-FM. (Copyright by Yimeng Wang. Reprinted from Wang, Y.; Giebink, A.; Spence, D. M. Integr Biol (Camb) 2014, 6, 65-75.)

Investigating RBC flow properties is an essential part of RBC studies and a popular way to perform cell flow studies is by using microfluidic devices. A functional microfluidic device contains several components, including channels, mixers and valves. Not only can it be applied during a flow study, but it also enables cell-cell communication investigations under flow conditions. Wang fabricated the microfluidic device by a soft photolithographic method using poly(dimethylsiloxane) (PDMS), shown in Figure 1.5. The microfluidic device utilized two slabs of PDMS, where the bottom slab contained channels with inside diameters that approximate arterioles *in vivo*, while the top was equipped with a 1/8" hole for optical detection of NO. A track-etch polycarbonate membrane was placed between the two layers of PDMS and sealed. The polycarbonate membrane was coated with fibronectin solution prior to culture endothelial cells on one side of the membrane. A 7% RBC suspension was pumped through the channel, and the NO production by endothelial cells was quantitated by a fluorescence probe.[101]

Applying PDMS platforms for cellular studies is of great interest.[101,114-117] However, there are some shortcomings of PDMS based devices. PDMS devices are usually not rugged enough, which might leak during experiments. Because most PDMS devices are only single-use, the reproducibility of the measurement is not ideal, even in the same lab. The complexity, difficulty, and lack of standardization in the PDMS manufacturing process leads to a limited number of PDMS products being commercialized. In order to improve the reproducibility and reusability of a microfluidic device, a novel prototyping technology, 3D printing, has emerged into this field and attracted great attention.[89,90,118-124] 3D printing is an additive fabrication process, where the three-dimensional object is built

layer by layer. The creation of printed parts is accomplished by using a computer aided design (CAD) program, such as AutoCAD and Autodesk. The design can be exported as a universal .STL format, which can be interpreted by a 3D printer.

Chen created a 3D-printed device using a semitransparent material for flow-induced ATP release from RBCs. The design and printed device is shown in Figure 1.6. The device has six channels with three detection wells on each channel, enabling high-throughput analytical measurements. The dimensions of the device are identical to a standard 96-well plate, resulting in direct optical detection using plate reader. Trans-well membrane inserts were plugged into detection wells for ATP separation and quantification. ATP release from RBCs stored in CPD/AS-1 and CPDN/AS-1N was successfully determined in this work.[125] The designed device also allows NO detection when culturing endothelial cells in membrane inserts and cell-cell communication studies.[103]

Another work done by the Spence group using the 3D printing technique is the building of a filtration device for cell deformability measurement. The design and pictures of the device are shown in Figure 1.7. The device includes two slabs printed with clear material. O rings were printed using black rubbery material and fixed on the slabs. A piece of polycarbonate membrane with 5 μm pore size was placed between the two O rings. A suspension of 5% RBC was pumped through the membrane and collected using a cuvette. After a certain time of filtration, the volume of RBC suspension collected in the cuvette was measured. And, the number of cells presented in the cuvette was counted using hemocytometer. Because the pore size of the membrane is smaller than the diameter of RBCs, only cells with sufficient deformability would be able to pass through the

membrane. The printed device has been used for deformability study of RBCs stored in CPD/AS-1 and CPDN/AS-1N. The results reveal that RBCs stored in low glucose condition are able to hold their deformability, while cells stored in standard blood banking solutions lost 20% of their deformability from the first day of storage.[103] The printed device was also utilized in the study of effects of C-peptide and Zinc to RBC deformability.[102]

The usage of the 3D printing technique significantly increases the reproducibility and reusability of fluidic devices in research laboratories. It has a great potential to become a gold standard of manufacturing fluidic devices. 3D-printed devices are frequently discussed in this thesis.

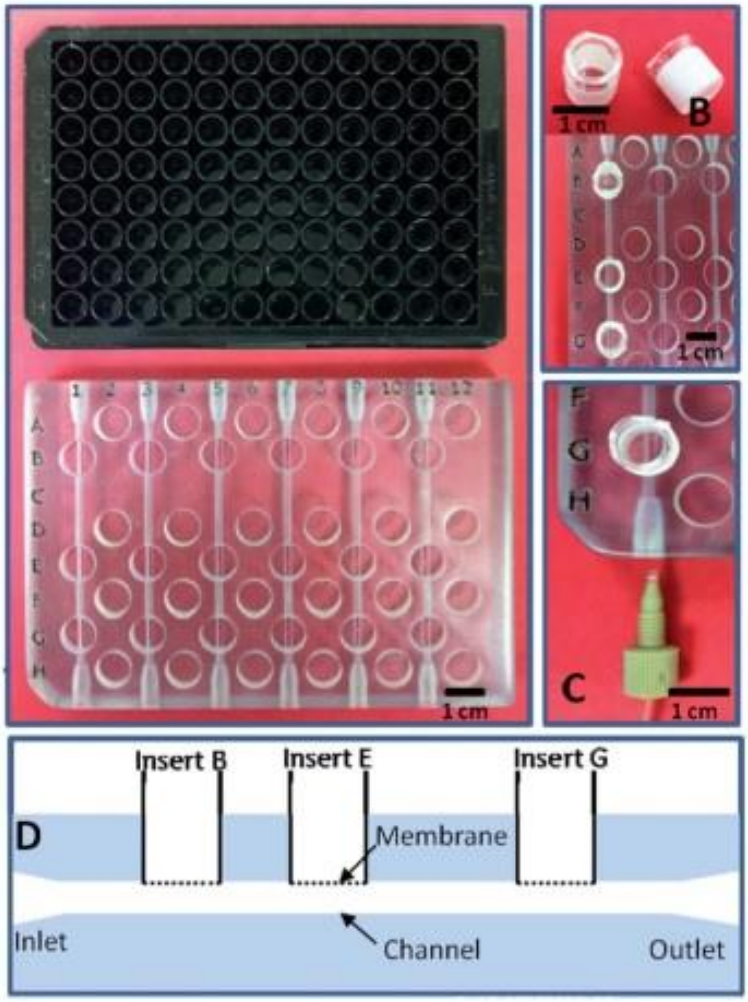

Figure 1.6 – 3D-printed device for NO measurement. The size of the printed device is the same as a standard 96-well plate, allowing placing the device directly into a commercial plate reader for chemiluminescence detection. The device contains six channels with three detection wells on each channel, enabling high-throughput analytical measurement. Trans-well membrane inserts were plugged into detection wells for ATP separation and quantification. The circulation loop was closed by connecting both ends using Tygon tubes via male leur lock adapters. RBC suspension was circulating in the channels, and the ATP release from RBCs can diffuse through the membrane into wells and further be detected. (Copyright by Chengpeng Chen. Reprinted from Chen, C.; Wang, Y.; Lockwood, S. Y.; Spence, D. M. Analyst 2014, 139, 3219-3226.)

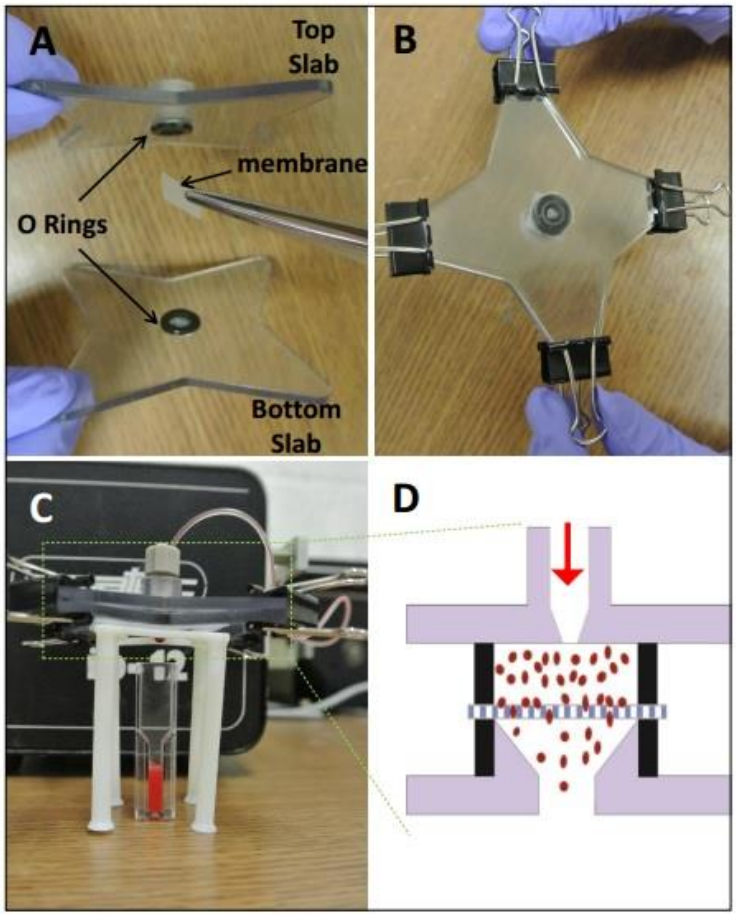

Figure 1.7 – 3D-printed filtration device for cell deformability measurement. The concept behind the design is only cells with sufficient deformability would be able to pass through the membrane, since the pore size of the membrane is smaller than the diameter of RBCs. The deformability of RBCs from different storage solutions could be compared by measuring the volume of RBC suspension collected in the cuvette and counting the number of cells presented in suspension. The device has two slabs printed with clear material and O rings printed with black rubbery material. Polycarbonate membrane (5 μm pore size) was fixed between the two O rings. A suspension of 5% RBC was pumped through the membrane and collected using a cuvette. (Copyright by Chengpeng Chen. Reprinted from Chen, C. 3D-PRINTED IN VITRO ANALYTICAL DEVICES FOR DIABETES THERAPEUTICS AND BLOOD BANKING STUDIES. Michigan State University2015.)

REFERENCES

REFERENCES

(1) Hess, J. R. *Vox Sang* **2006**, *91*, 13-19.

(2) Rous, P.; Turner, J. R. *J Exp Med* **1916**, *23*, 219-237.

(3) Robertson, O. H. *Br Med J* **1918**, *1*, 691-695.

(4) Mollison, P. L. *Br J Haematol* **2000**, *108*, 13-18.

(5) GW, C.; TR, B.; WB, C.; WL, M.; B, V.; RG, H.; BJ, L., A Report Upon Transfusion of Blood for the Recently Injured in the United States Army; American Red Cross: Paris, 1918.

(6) Loutit, J. F.; Mollison, P. L. *Br Med J* **1943**, *2*, 744-745.

(7) DB, K., Army, D. o. t., Ed.: Washington DC, Office of the Surgeon General, 1964, pp 217-232.

(8) Orlina, A. R.; Josephson, A. M. *Transfusion* **1969**, *9*, 62-69.

(9) Ebaugh, F. G., Jr.; Ross, J. F. *Vox Sang* **1985**, *49*, 304-307.

(10) Carmen, R. *Transfus Med Rev* **1993**, *7*, 1-10.

(11) Hill, H. R.; Oliver, C. K.; Lippert, L. E.; Greenwalt, T. J.; Hess, J. R. *Vox Sang* **2001**, *81*, 161-166.

(12) Nakao, K.; Wada, T.; Kamiyama, T.; Nakao, M.; Nagano, K. *Nature* **1962**, *194*, 877-878.

(13) Simon, E. R.; Chapman, R. G.; Finch, C. A. *J Clin Invest* **1962**, *41*, 351-359.

(14) Shields, C. E. *Transfusion* **1969**, *9*, 115-119.

(15) Zuck, T. F.; Bensinger, T. A.; Peck, C. C.; Chillar, R. K.; Beutler, E.; Button, L. N.; McCurdy, P. R.; Josephson, A. M.; Greenwalt, T. J. *Transfusion* **1977**, *17*, 374-382.

(16) Beutler, E.; West, C. *Blood* **1979**, *54*, 280-284.

(17) Moore, G. L.; Ledford, M. E.; Peck, C. C. *Transfusion* **1980**, *20*, 419-426.

(18) Moore, G. L. *Crit Rev Clin Lab Sci* **1987**, *25*, 211-229.

(19) Hogman, C. F.; Hedlund, K.; Zetterstrom, H. *N Engl J Med* **1978**, *299*, 1377-1382.

(20) Beutler, E.; Kuhl, W. *Transfusion* **1988**, *28*, 353-357.

(21) Hogman, C. F.; Hedlund, K.; Sahlestrom, Y. *Vox Sang* **1981**, *41*, 274-281.

(22) Heaton, W. A.; Holme, S.; Smith, K.; Brecher, M. E.; Pineda, A.; AuBuchon, J. P.; Nelson, E. *Br J Haematol* **1994**, *87*, 363-368.

(23) Administration, U. F. a. D., Ed., 2013.

(24) Cancelas, J. A.; Dumont, L. J.; Maes, L. A.; Rugg, N.; Herschel, L.; Whitley, P. H.; Szczepiokowski, Z. M.; Siegel, A. H.; Hess, J. R.; Zia, M. *Transfusion* **2015**, *55*, 491-498.

(25) Dumont, L. J.; Cancelas, J. A.; Maes, L. A.; Rugg, N.; Whitley, P.; Herschel, L.; Siegal, A. H.; Szczepiorkowski, Z. M.; Hess, J. R.; Zia, M. *Transfusion* **2015**, *55*, 485-490.

(26) Whitaker, B. I., National Blood Collection and Utilization Survey Report; US Department of Health and Human Services2011.

(27) Hogman, C. F.; Eriksson, L.; Hedlund, K.; Wallvik, J. *Vox Sang* **1988**, *55*, 211-217.

(28) Hogman, C. F.; Meryman, H. T. *Transfusion* **2006**, *46*, 137-142.

(29) Dumont, L. J.; AuBuchon, J. P. *Transfusion* **2008**, *48*, 1053-1060.

(30) Long, B.; Koyfman, A. *J Emerg Med* **2016**, *51*, 120-130.

(31) JE, E.; B, M.; R, P., Organization, W. H., Ed.: Geneva, Switzerland, 1997.

(32) Qu, L.; Triulzi, D. J. *Cancer Control* **2015**, *22*, 26-37.

(33) Vincent, J. L.; Baron, J. F.; Reinhart, K.; Gattinoni, L.; Thijs, L.; Webb, A.; Meier-Hellmann, A.; Nollet, G.; Peres-Bota, D.; Investigators, A. B. C. *JAMA* **2002**, *288*, 1499-1507.

(34) Blood Observational Study Investigators of, A.-C. T. G.; Westbrook, A.; Pettila, V.; Nichol, A.; Bailey, M. J.; Syres, G.; Murray, L.; Bellomo, R.; Wood, E.; Phillips, L. E.; Street, A.; French, C.; Orford, N.; Santamaria, J.; Cooper, D. J. *Intensive Care Med* **2010**, *36*, 1138-1146.

(35) Hebert, P. C.; Wells, G.; Blajchman, M. A.; Marshall, J.; Martin, C.; Pagliarello, G.; Tweeddale, M.; Schweitzer, I.; Yetisir, E. *N Engl J Med* **1999**, *340*, 409-417.

(36) Blair, S. D.; Janvrin, S. B.; McCollum, C. N.; Greenhalgh, R. M. *Br J Surg* **1986**, *73*, 783-785.

(37) Bracey, A. W.; Radovancevic, R.; Riggs, S. A.; Houston, S.; Cozart, H.; Vaughn, W. K.; Radovancevic, B.; McAllister, H. A., Jr.; Cooley, D. A. *Transfusion* **1999**, *39*, 1070-1077.

(38) Pham, H. P.; Shaz, B. H. *Br J Anaesth* **2013**, *111 Suppl 1*, i71-82.

(39) Sihler, K. C.; Napolitano, L. M. *Chest* **2010**, *137*, 209-220.

(40) Bux, J. *Vox Sang* **2005**, *89*, 1-10.

(41) Fatalities Reported to FDA Following Blood Collection and Transfusion; US Food and Drug Administration2015.

(42) Kleinman, S. *Transfusion* **2006**, *46*, 1465-1468.

(43) Toy, P.; Popovsky, M. A.; Abraham, E.; Ambruso, D. R.; Holness, L. G.; Kopko, P. M.; McFarland, J. G.; Nathens, A. B.; Silliman, C. C.; Stroncek, D.; National Heart, L.; Blood Institute Working Group on, T. *Crit Care Med* **2005**, *33*, 721-726.

(44) Goldman, M.; Webert, K. E.; Arnold, D. M.; Freedman, J.; Hannon, J.; Blajchman, M. A.; Panel, T. C. *Transfus Med Rev* **2005**, *19*, 2-31.

(45) Wasser, M. N.; Houbiers, J. G.; D'Amaro, J.; Hermans, J.; Huysmans, H. A.; van Konijnenburg, G. C.; Brand, A. *Br J Haematol* **1989**, *72*, 81-84.

(46) Koch, C. G.; Li, L.; Sessler, D. I.; Figueroa, P.; Hoeltge, G. A.; Mihaljevic, T.; Blackstone, E. H. *N Engl J Med* **2008**, *358*, 1229-1239.

(47) Lelubre, C.; Vincent, J. L. *Crit Care* **2013**, *17*, R66.

(48) Wang, D.; Sun, J.; Solomon, S. B.; Klein, H. G.; Natanson, C. *Transfusion* **2012**, *52*, 1184-1195.

(49) van Wijk, R.; van Solinge, W. W. *Blood* **2005**, *106*, 4034-4042.

(50) Bicalho, B.; Serrano, K.; Dos Santos Pereira, A.; Devine, D. V.; Acker, J. P. *Transfus Med Hemother* **2016**, *43*, 19-26.

(51) Zimrin, A. B.; Hess, J. R. *Vox Sang* **2009**, *96*, 93-103.

(52) Matthes, G.; Strunk, S.; Siems, W.; Grune, T. *Infusionsther Transfusionsmed* **1993**, *20*, 89-92.

(53) Sols, A.; De La Fuente, G.; Villarpalasi, C.; Asensio, C. *Biochim Biophys Acta* **1958**, *30*, 92-101.

(54) Sands, J. M.; Schrader, D. C. *J Am Soc Nephrol* **1991**, *2*, 212-218.

(55) Malone, J. I.; Knox, G.; Benford, S.; Tedesco, T. A. *Diabetes* **1980**, *29*, 861-864.

(56) Meshalkin, E. N.; Vlasov Iu, A.; Shishkina, T. N.; Okuneva, G. N.; Pinegin, S. L. *Kardiologiia* **1982**, *22*, 45-49.

(57) Kanji, M. I.; Toews, M. L.; Carper, W. R. *J Biol Chem* **1976**, *251*, 2255-2257.

(58) Hess, J. R. *J Proteomics* **2010**, *73*, 368-373.

(59) Kay, M. M. *Cell Mol Biol (Noisy-le-grand)* **1993**, *39*, 131-153.

(60) Peters, A. L.; van Hezel, M. E.; Juffermans, N. P.; Vlaar, A. P. *Blood Rev* **2015**, *29*, 51-61.

(61) Wagner, G. M.; Chiu, D. T.; Qju, J. H.; Heath, R. H.; Lubin, B. H. *Blood* **1987**, *69*, 1777-1781.

(62) Lockwood, W. B.; Hudgens, R. W.; Szymanski, I. O.; Teno, R. A.; Gray, A. D. *Transfusion* **2003**, *43*, 1527-1532.

(63) Tinmouth, A.; Chin-Yee, I. *Transfus Med Rev* **2001**, *15*, 91-107.

(64) Card, R. T.; Mohandas, N.; Mollison, P. L. *Br J Haematol* **1983**, *53*, 237-240.

(65) Nakao, M.; Nakao, T.; Yamazoe, S. *Nature* **1960**, *187*, 945-946.

(66) Greenwalt, T. J. *Transfusion* **2006**, *46*, 143-152.

(67) Rubin, O.; Canellini, G.; Delobel, J.; Lion, N.; Tissot, J. D. *Transfus Med Hemother* **2012**, *39*, 342-347.

(68) Bosman, G. J.; Werre, J. M.; Willekens, F. L.; Novotny, V. M. *Transfus Med* **2008**, *18*, 335-347.

(69) Sen, S.; Kar, M.; Roy, A.; Chakraborti, A. S. *Biophys Chem* **2005**, *113*, 289-298.

(70) Mangalmurti, N. S.; Chatterjee, S.; Cheng, G.; Andersen, E.; Mohammed, A.; Siegel, D. L.; Schmidt, A. M.; Albelda, S. M.; Lee, J. S. *Transfusion* **2010**, *50*, 2353-2361.

(71) Lysenko, L.; Mierzchala, M.; Gamian, A.; Durek, G.; Kubler, A.; Kozlowski, R.; Sliwinski, M. *Arch Immunol Ther Exp (Warsz)* **2006**, *54*, 357-362.

(72) Connor, J.; Pak, C. C.; Schroit, A. J. *J Biol Chem* **1994**, *269*, 2399-2404.

(73) Koshkaryev, A.; Zelig, O.; Manny, N.; Yedgar, S.; Barshtein, G. *Transfusion* **2009**, *49*, 2136-2143.

(74) Izumida, Y.; Seiyama, A.; Maeda, N. *Biochim Biophys Acta* **1991**, *1067*, 221-226.

(75) Relevy, H.; Koshkaryev, A.; Manny, N.; Yedgar, S.; Barshtein, G. *Transfusion* **2008**, *48*, 136-146.

(76) Roback, J. D.; Neuman, R. B.; Quyyumi, A.; Sutliff, R. *Transfusion* **2011**, *51*, 859-866.

(77) Ignarro, L. J.; Buga, G. M.; Wood, K. S.; Byrns, R. E.; Chaudhuri, G. *Proc Natl Acad Sci U S A* **1987**, *84*, 9265-9269.

(78) Ignarro, L. J.; Byrns, R. E.; Buga, G. M.; Wood, K. S. *Circ Res* **1987**, *61*, 866-879.

(79) Carvajal, J. A.; Germain, A. M.; Huidobro-Toro, J. P.; Weiner, C. P. *J Cell Physiol* **2000**, *184*, 409-420.

(80) Bohlen, H. G.; Zhou, X.; Unthank, J. L.; Miller, S. J.; Bills, R. *Am J Physiol Heart Circ Physiol* **2009**, *297*, H1337-1346.

(81) Stamler, J. S.; Simon, D. I.; Osborne, J. A.; Mullins, M. E.; Jaraki, O.; Michel, T.; Singel, D. J.; Loscalzo, J. *Proc Natl Acad Sci U S A* **1992**, *89*, 444-448.

(82) Bhatia, S. N.; Balis, U. J.; Yarmush, M. L.; Toner, M. *FASEB J* **1999**, *13*, 1883-1900.

(83) Lundberg, J. O.; Weitzberg, E.; Gladwin, M. T. *Nat Rev Drug Discov* **2008**, *7*, 156-167.

(84) Hakim, T. S.; Sugimori, K.; Camporesi, E. M.; Anderson, G. *Physiol Meas* **1996**, *17*, 267-277.

(85) Azarov, I.; Liu, C.; Reynolds, H.; Tsekouras, Z.; Lee, J. S.; Gladwin, M. T.; Kim-Shapiro, D. B. *J Biol Chem* **2011**, *286*, 33567-33579.

(86) Bucala, R.; Tracey, K. J.; Cerami, A. *J Clin Invest* **1991**, *87*, 432-438.

(87) Price, A. K.; Fischer, D. J.; Martin, R. S.; Spence, D. M. *Anal Chem* **2004**, *76*, 4849-4855.

(88) Edwards, J.; Sprung, R.; Sprague, R.; Spence, D. *Analyst* **2001**, *126*, 1257-1260.

(89) Erkal, J. L.; Selimovic, A.; Gross, B. C.; Lockwood, S. Y.; Walton, E. L.; McNamara, S.; Martin, R. S.; Spence, D. M. *Lab Chip* **2014**, *14*, 2023-2032.

(90) Liu, Y.; Chen, C.; Summers, S.; Medawala, W.; Spence, D. M. *Integr Biol (Camb)* **2015**, *7*, 534-543.

(91) Raththagala, M.; Karunarathne, W.; Kryziniak, M.; McCracken, J.; Spence, D. M. *Eur J Pharmacol* **2010**, *645*, 32-38.

(92) Lockwood, S. Y.; Erkal, J. L.; Spence, D. M. *Nitric Oxide* **2014**, *38*, 1-7.

(93) Communi, D.; Raspe, E.; Pirotton, S.; Boeynaems, J. M. *Circ Res* **1995**, *76*, 191-198.

(94) American Diabetes, A. *Diabetes Care* **2004**, *27 Suppl 1*, S11-14.

(95) Carroll, J.; Raththagala, M.; Subasinghe, W.; Baguzis, S.; D'Amico Oblak, T.; Root, P.; Spence, D. *Mol Biosyst* **2006**, *2*, 305-311.

(96) McMillan, D. E.; Utterback, N. G.; La Puma, J. *Diabetes* **1978**, *27*, 895-901.

(97) Dincer, Y.; Akcay, T.; Alademir, Z.; Ilkova, H. *Metabolism* **2002**, *51*, 1360-1362.

(98) Suzuki, K.; Nakagawa, K.; Miyazawa, T. *Clin Chem Lab Med* **2014**, *52*, 47-52.

(99) Wautier, J. L.; Wautier, M. P.; Schmidt, A. M.; Anderson, G. M.; Hori, O.; Zoukourian, C.; Capron, L.; Chappey, O.; Yan, S. D.; Brett, J.; et al. *Proc Natl Acad Sci U S A* **1994**, *91*, 7742-7746.

(100) R.D., H. S. W.; RN, J. P. *Real-Life Guide to Diabetes: Practical Answers to Your Diabetes Problems*; American Diabetes Association, 2009.

(101) Wang, Y.; Giebink, A.; Spence, D. M. *Integr Biol (Camb)* **2014**, *6*, 65-75.

(102) Liu, Y. *DELIVERY OF A PANCREATIC BETA CELL-DERIVED HORMONE TO ERYTHROCYTES BY ALBUMIN AND DOWNSTREAM CELLULAR EFFECTS*. Michigan State University2015.

(103) Chen, C. *3D-PRINTED IN VITRO ANALYTICAL DEVICES FOR DIABETES THERAPEUTICS AND BLOOD BANKING STUDIES*. Michigan State University2015.

(104) Popp-Snijders, C.; Lomecky, M. Z.; de Jong, A. P. *Clin Chim Acta* **1983**, *132*, 83-89.

(105) Evans, E. A.; La Celle, P. L. *Blood* **1975**, *45*, 29-43.

(106) Kamruzzahan, A. S.; Kienberger, F.; Stroh, C. M.; Berg, J.; Huss, R.; Ebner, A.; Zhu, R.; Rankl, C.; Gruber, H. J.; Hinterdorfer, P. *Biol Chem* **2004**, *385*, 955-960.

(107) Svoboda, K.; Block, S. M. *Annu Rev Biophys Biomol Struct* **1994**, *23*, 247-285.

(108) Puig-de-Morales-Marinkovic, M.; Turner, K. T.; Butler, J. P.; Fredberg, J. J.; Suresh, S. *Am J Physiol Cell Physiol* **2007**, *293*, C597-605.

(109) Park, Y.; Best-Popescu, C. A.; Dasari, R. R.; Popescu, G. *J Biomed Opt* **2011**, *16*, 011013.

(110) Reid, H. L.; Barnes, A. J.; Lock, P. J.; Dormandy, J. A.; Dormandy, T. L. *J Clin Pathol* **1976**, *29*, 855-858.

(111) Wang, R.; Ding, H.; Mir, M.; Tangella, K.; Popescu, G. *Biomed Opt Express* **2011**, *2*, 485-490.

(112) Dobbe, J. G.; Streekstra, G. J.; Strackee, J.; Rutten, M. C.; Stijnen, J. M.; Grimbergen, C. A. *IEEE Trans Biomed Eng* **2003**, *50*, 97-106.

(113) Shoji, N.; Nakagawa, K.; Asai, A.; Fujita, I.; Hashiura, A.; Nakajima, Y.; Oikawa, S.; Miyazawa, T. *J Lipid Res* **2010**, *51*, 2445-2453.

(114) Anderson, K. B.; Halpin, S. T.; Johnson, A. S.; Martin, R. S.; Spence, D. M. *Analyst* **2013**, *138*, 137-143.

(115) Johnson, A. S.; Anderson, K. B.; Halpin, S. T.; Kirkpatrick, D. C.; Spence, D. M.; Martin, R. S. *Analyst* **2013**, *138*, 129-136.

(116) Vogel, P. A.; Halpin, S. T.; Martin, R. S.; Spence, D. M. *Anal Chem* **2011**, *83*, 4296-4301.

(117) Halpin, S. T.; Spence, D. M. *Anal Chem* **2010**, *82*, 7492-7497.

(118) Chen, C.; Mehl, B. T.; Munshi, A. S.; Townsend, A. D.; Spence, D. M.; Martin, R. S. *Anal Methods* **2016**, *8*, 6005-6012.

(119) Gross, B. C.; Erkal, J. L.; Lockwood, S. Y.; Chen, C.; Spence, D. M. *Anal Chem* **2014**, *86*, 3240-3253.

(120) Gross, B.; Lockwood, S. Y.; Spence, D. M. *Anal Chem* **2017**, *89*, 57-70.

(121) LaBonia, G. J.; Lockwood, S. Y.; Heller, A. A.; Spence, D. M.; Hummon, A. B. *Proteomics* **2016**, *16*, 1814-1821.

(122) Lockwood, S. Y.; Meisel, J. E.; Frederick J. Monsma, J.; Spence, D. M. *Anal Chem* **2016**, *88*, 1864-1870.

(123) Gross, B. C.; Anderson, K. B.; Meisel, J. E.; McNitt, M. I.; Spence, D. M. *Anal Chem* **2015**, *87*, 6335-6341.

(124) Selimovic, A.; Erkal, J. L.; Spence, D. M.; Martin, R. S. *Analyst* **2014**, *139*, 5686-5694.

(125) Chen, C.; Wang, Y.; Lockwood, S. Y.; Spence, D. M. *Analyst* **2014**, *139*, 3219-3226.

Chapter 2 – Evaluating the Benefits from Normoglycemic Red Blood Cell Storage

Mu, R.; Chen, C.; Wang, Y.; Spence, D. M. analytical Methods 2016, 8, 6856 - 6864

2.1 Introduction

RBC transfusion has been used as one of the most common medical procedures in clinical practice for decades. Based on the statistics from the most recent NBCUS, the market is satisfied with the supply of blood products.[1] However, all medical interventions have side effects. Post-transfusion related complications still exist as the major barrier preventing transfusion from becoming safer. It is expected that the transfused RBC has good cell flow and gas exchange properties, so they can increase cell mass and deliver oxygen effectively. Ethical and operational issues have prevented careful *in vivo* study of stored RBCs for transfusion. Therefore, an overall analysis of cells *in vitro* is needed. Scientists have been dedicated to studying the RBC storage lesion for decades, evident by an abundance of reviews.[2-6] However, only three new storage methods have been proposed by researchers to minimize the detrimental effects to RBCs during storage.

First, anaerobic storage of RBCs, where O_2 and CO_2 is depleted with inert gas, was explored by Yoshida *et al.*, to prevent damage due to oxidative stress. They reported that anaerobic storage improves both *in vitro* quality and 24 h post-transfusion recovery of stored RBCs, enhancing the uniformity and overall quality of RBCs.[7-11] The drawback of depleting O_2 is the resultant negative effects on glutathione homeostasis due to a depressed pentose phosphate pathway and nicotinamide adenine dinucleotide phosphate (NADPH) generating potential.[12] While anaerobic storage may not translate

into clinical practice because deoxygenation processes complicates manufacturing, it provides some new insights for further RBC storage advancements.

A second storage innovation alkaline AS, AS-7, where the pH of the solution is basic instead of acidic, was licensed by the FDA in 2013.[13] The reason for applying acidic solutions in current blood banking was discussed in Chapter 1 and is mainly performed to reduce the caramelization that occurs during autoclave sterilizing. Notably, there is no buffer components in AS-1 and AS-5, while AS-3 has limiting buffer capacity. As a result, the internal pH of stored RBCs drops down rapidly below 7.0. The acidic environment leads to the impairment of the glycolysis pathway, causing decreased adenosine triphosphate (ATP) synthesis. AS-7 was developed by the group of Hess and Greenwalt using the 'chloride shift' principle,[14,15] which is a method that keeps 2,3-DPG levels high during storage. Meryman and Hornblower showed that if extracellular chloride is replaced by citrate, chloride will leave the RBCs. Then, hydroxyl ions will enter the cells, causing a higher intracellular pH, because they are the only permeable anions available for charge compensation.[16,17] It has been shown that AS-7 reduces the RBC storage lesion.[15]

The third new storage method, which is the basis of this dissertation, is normoglycemic storage of RBCs. The idea was pioneered by the Spence group in 2008. The similarity between stored RBCs and diabetic RBCs led to the hypothesis that the high concentration of glucose presented in blood storage solutions might be a major contributor to the RBC storage lesion. In order to improve RBC storage by minimizing adverse effects to stored cells, a normoglycemic version of blood storage solutions was proposed. The glucose level

in blood storage solutions, CPD/AS-1, was lowered down to 5.5 mM, which is within the range of blood glucose levels in healthy, non-diabetic humans. The glucose concentration was maintained at 4 – 6 mM during a 35-day storage by adding concentrated glucose saline in volumes that were negligible to the total original volume. The normoglycemic storage method significantly increased the flow-induced ATP release from RBCs, resulting in elevated NO production in cultured endothelial cells. This work strongly implied that RBCs stored in normoglycemic conditions may have better flow properties after transfusion into a patient's bloodstream.[18]

Other work reported by the Spence group further illustrates the benefits of normoglycemic storage of RBCs. For example, RBCs stored in standard CPD/AS-1 have an impaired ability to bind C-peptide, while binding is not affected for those cells stored in a normoglycemic environment. C-peptide is a 31 amino acid peptide co-secreted with insulin from pancreatic β-cells. It was reported that the uptake of C-peptide by RBCs can enhance ATP release and cell deformability.[19,20] Additionally, when RBCs are stored in CPDN/AS-1N, they tend to have improved cell deformability and reversibility compared to cells stored under high-glucose levels.[21]

The Spence group has proposed that the excess amount of glucose might contribute to the development of storage lesion. Therefore, glucose concentrations, both intracellular and extracellular, were monitored in hyperglycemic and normoglycemic RBC storage. The analytical methodologies of measuring glucose have been commercialized for decades. For example, a typical way to conduct glucose measurements is by using an amperometric method with an enzyme such as glucose oxidase.[22] Here, in order to achieve high-

throughput measurements, an enzymatic fluorescence method was utilized accompanied with a plate reader for optical detection. Glucose, catalyzed by hexokinase, reacts with ATP and gets converted into glucose-6-phosphate (G6P). Subsequently, G6P, catalyzed by glucose-6-phosphate dehydrogenase, reacts with NADP+ gets converted into 6-phosphote-D-glucono-1, 5-lactone. The fluorescence emission at 460 nm from NADPH was measured. The reaction is shown in Figure 2.1. The glucose concentrations were being monitored to determine if low glucose levels during storage improved various storage parameters, such as hemolysis.

One of the essential criteria to evaluate the quality of the RBC product is the percentage of cells lysed during the cold storage period. Hemolysis levels higher than 1% are not acceptable under FDA regulations.[23] A study of a total of 14,087 measures of hemolysis during and at the end of storage, obtained under seven different storage solutions, were conducted in 2009. Results reveal that the distributions of percent hemolysis are skewed normal and outliers are random. There is no statistical advantage of using one specific AS over others. The hemolysis level can be decreased by 53% if RBCs are leukoreduced.[24]

Here, the percentage of cell lysis was determined weekly to ensure the modified normoglycemic RBC storage product can meet the federal requirement. Percent hemolysis was calculated as the ratio of free Hb in the environment to the total Hb including extra- and intercellular levels of Hb. Quantitative determination of Hb was achieved by absorbance spectroscopy using Drabkin's solution. The solution is able to lyse RBCs and release Hb. Following that, Hb and its derivatives will be oxidized to methemoglobin in the presence of alkaline potassium ferricyanide. Methemoglobin will

further react with potassium cyanide to form cyanmethemoglobin, a colored compound with a maximum absorption at 540 nm.

In addition to glycolysis, glucose can also be metabolized to sorbitol through the polyol pathway. The structure of the sorbitol molecule and the effects of the polyol pathway are shown in Figure 2.2. In a hyperglycemic environment, more glucose will participate in the conversion to sorbitol. This reaction is catalyzed by aldose reductase, which consumes NADPH. The consumption of NADPH, the reducing agent in glutathione (GSH) regeneration, may cause an increase in oxidative stress. In addition, sorbitol will accumulate in RBCs because it cannot pass through cell membranes. The osmotic balance will be shifted, resulting in cells becoming more fragile. Previously, it was reported that sorbitol has an elevated value in RBCs obtained from the whole blood of people with diabetes, and correlates with plasma glucose concentration.[25] Onaya *et al.* showed the increased RBC sorbitol concentration is related to the development of diabetic complications, indicating that the polyol pathway is involved in the pathogenesis of long term complications.[26] Moreover, McMillan demonstrated that RBC deformability is diminished in diabetes.[27] Since stored RBCs are similar to diabetic RBCs in several manners, it is rational to hypothesize that there is a higher amount of sorbitol produced in those RBCs stored in hyperglycemic conditions.

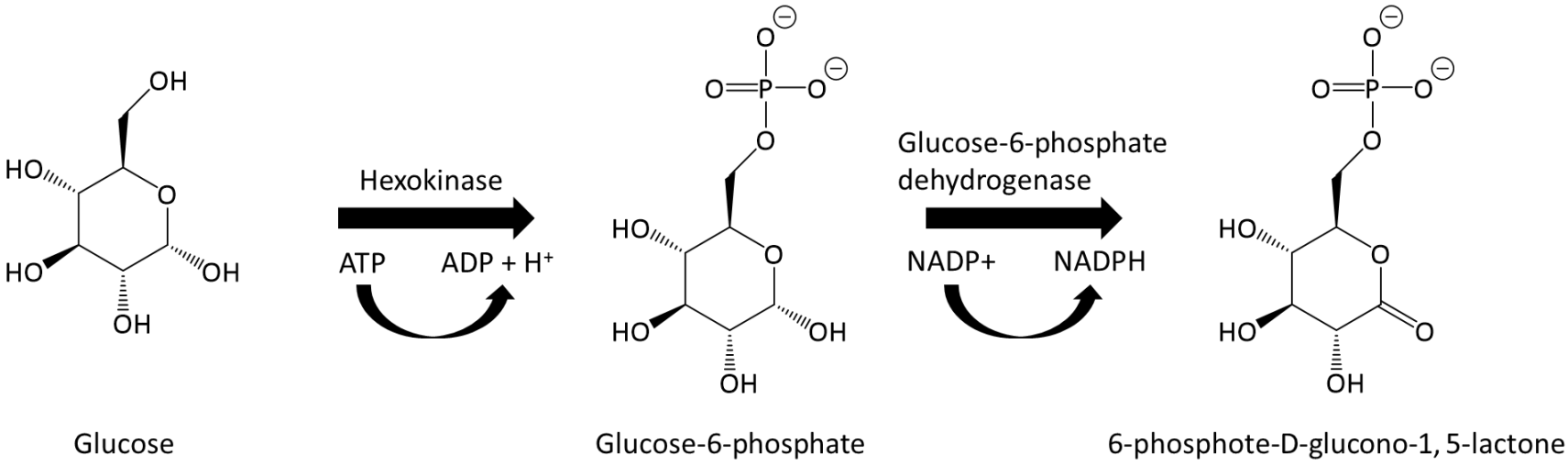

Figure 2.1 – Reaction of the enzymatic fluorescence method for glucose measurement. Glucose is converted to glucose-6-phosphate by the enzyme, hexokinase, at the presence of ATP. Then, the glucose-6-phosphate is catalyzed by glucose-6-phosphate dehydrogenase to form 6-phosphote-D-glucono-1,5-lactone. In that process, NADP+ is reduced to NADPH that has a fluorescence emission at 460 nm.

The intracellular sorbitol accumulation was measured weekly, using an enzymatic fluorescence technique discovered by Umeda.[28] The measurement is based on the reaction of oxidizing sorbitol to fructose, catalyzed by sorbitol dehydrogenase. Nicotinamide adenine dinucleotide (NAD+) will reduce back to NADH and the fluorescence emitted from NADH will be measured. The reaction is shown in Figure 2.3.

In addition to sorbitol determinations, osmotic fragility was also detected weekly to further explore the effects of the polyol pathway on stored RBCs. Osmotic fragility tests are commonly performed in hematology, especially for the diagnosis of spherocytosis where RBCs are abnormally sphere-shaped instead of biconcave discs.[29] Interestingly, stored RBCs undergo shape change from biconcave discs to grossly abnormally-shaped spheres. This shape change results in the loss of cell-membrane associated deformability, making RBCs more prone to rupture. Considering sorbitol accumulation, plus the shape change, it is reasonable to hypothesize that standard storage solutions may induce severe osmotic imbalance to stored RBCs, in comparison to normal glucose storage.

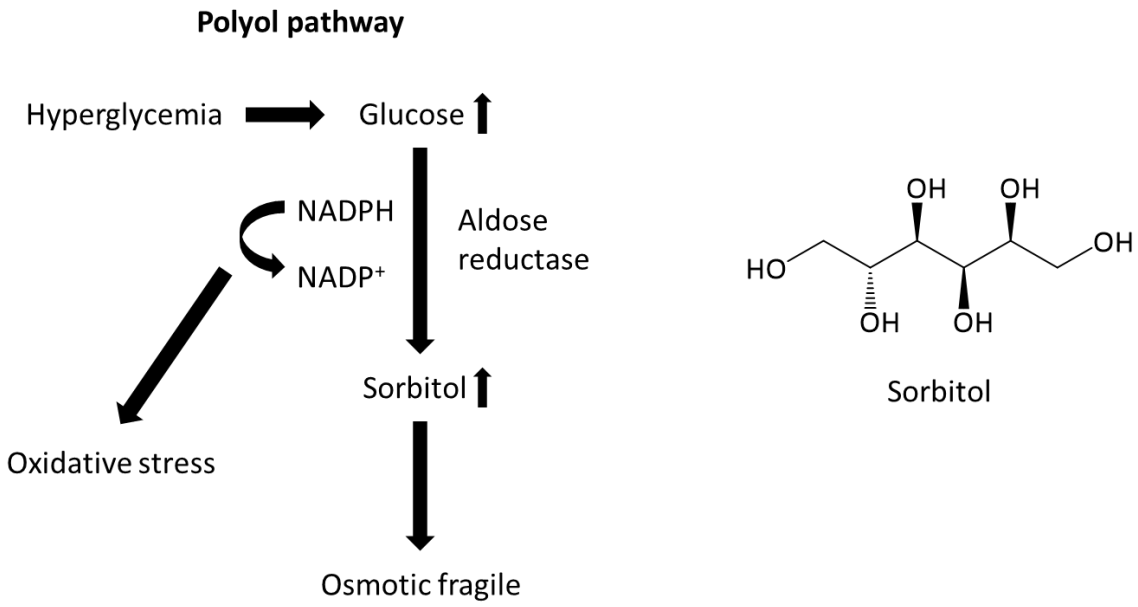

Figure 2.2 – RBC polyol pathway and sorbitol. More glucose in RBC will enter polyol pathway instead of the glycolysis pathway if the intracellular pH is lowered down. Sorbitol, the production in polyol pathway, may cause osmotic pressure because it's not membrane permeable. Also, due to NADPH being consumed in the reaction, the cells might suffer from oxidative damage.

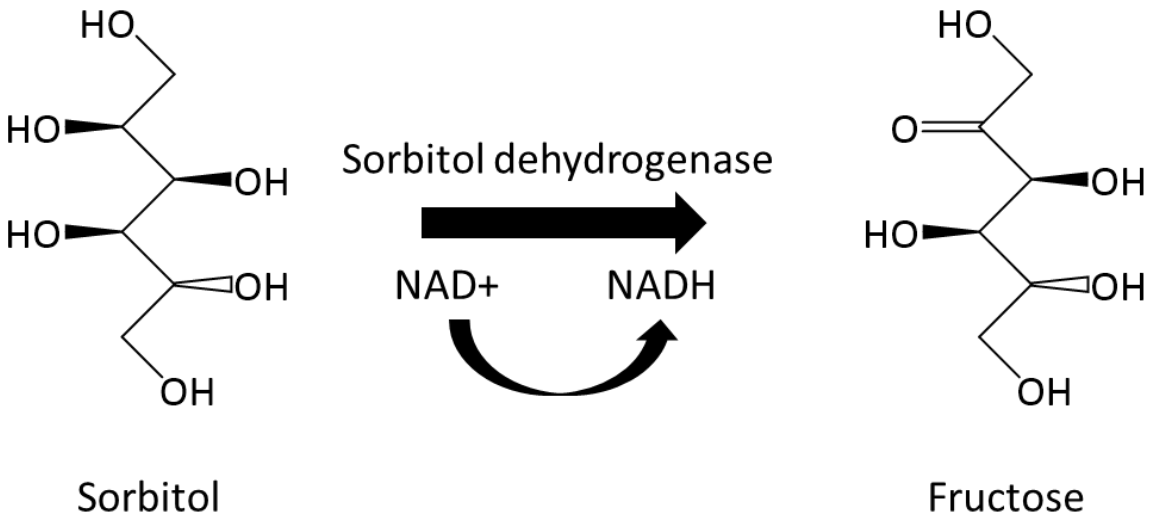

Figure 2.3 – Reaction of the enzymatic fluorescence method for sorbitol measurement. The sorbitol assay is based on the addition of sorbitol dehydrogenase to samples, oxidizing sorbitol to fructose. NAD+ is reduced to NADH during the reaction. NADH has an emission of fluorescence at 460 nm after excitation of 340 nm. The fluorescence intensity is proportional to the amount of NADH generated, as well as the sorbitol reacted.

The standard osmotic fragility test is performed by achieving the median corpuscular fragility, which is the concentration of NaCl solution causing 50% of the RBCs to lyse. A curve representing the lysis of the RBCs under different concentrations of NaCl is usually created in the test. A simplified method was applied here to quantify osmotic fragility of the stored RBCs by measuring the percentage of lysis when placing the RBC samples into a hypotonic solution that has a lower osmotic pressure.[30] The rupture of the RBC membrane occurs under hypotonic conditions, causing release of Hb from cells. By measuring the free Hb concentration in the media, the percentage of hemolysis at different concentrations of NaCl can be calculated.

The flow properties of stored RBCs, such as ensuring that they do not lyse, are an essential factor for consideration when evaluating blood product quality. The RBC primarily serves as a carrier that delivers oxygen to tissues, and then takes away carbon dioxide. However, in addition to carrying oxygen, the RBC is also indirectly a determinant in regulating blood flow.

There are three proposed mechanisms to explain how RBCs affect blood flow, and all share the common feature that the RBC controls blood flow by regulating local nitric oxide (NO) concentration, improving the insufficient nitric oxide bioavailability (INOBA) problem. The divergence is the origin of NO. Bohlen believes that NO originally secreted from endothelial cells can bind to sulfur atoms on cysteine β-93 of Hb (SNO-Hb).[31,32] Gladwin *et al.* proposed that plasma nitrite is reduced to NO by deoxygenated Hb, and produces SNO-Hb.[33] Both mechanisms involve the formation of SNO-Hb.

However, our group is strongly interested in the mechanism that has been well-described by Sprague and shown in Figure 2.4. The function of gas exchange, as well as regulating blood flow, requires the expenditure of metabolic energy.[34] Because mature RBCs lack nuclei and mitochondria, the production of ATP is through anaerobic glycolysis. Glucose molecules are broken down to generate new ATP molecules as the energy source to support the cells in an active form, resulting in millmolar levels of intracellular ATP.[35] A 7% RBC suspension can release hundreds of nanomoles of ATP to the environment under several stimuli, such as shear stress, hypoxia, C-peptide, and hydroxyurea.[19,36-40] The ATP released from RBCs can diffuse to the endothelium layer, stimulating the production of NO in endothelial cells.[41] The produced NO can further diffuse to the adjacent smooth muscle cell layer, resulting in smooth muscle cell relaxation.[42,43] Multiple reports from Sprague studying pulmonary vascular resistance (PVR) in an *ex vivo* rabbit lung model provide evidence to support the proposed mechanism.[44-46] It has been shown that NO is the determinant of PVR in the presence of blood.[44] It is our hypothesis that ATP, released from RBCs as they traverse the pulmonary circulation, evokes endogenous NO synthesis.[45,46]

The detection of ATP can be accomplished by applying an amperometric method with dual enzymes, glucose-oxidase and hexokinase.[47] In this work, the luciferin-luciferase chemiluminescence ,method was selected, as shown in Figure 2.5.[48] Luciferin, reacts with oxygen and ATP, catalyzed by luciferase and Mg^{2+}, to form oxyluciferin. The electron in the product molecule, oxyluciferin, is in the excitated state. Light is emitted when the electron transfers to the ground state, converting chemical energy to light. Because there

is no background interference from an excitation source (as is the case with most luminescent assays), chemiluminescence provides better sensitivity and lower detection limits for ATP quantitation. In this study, ATP was measured weekly, using a novel 3D-printed device that enabled blood flow to stimulate ATP release from RBCs.

Here, in order to further explore the benefits of low glucose RBC storage, CP2D/AS-3 and CPD/AS-5 were included in the study, along with CPD/AS-1 that has been studied previously.[18] The three standard processing and storage solutions, as well as their normoglycemic versions (CPDN/AS-1N, CPDN/AS-3N and CPDN/AS-5N) were quantitatively appraised in this chapter. Multiple *in vitro* cellular analyses, including glucose levels (both intracellular and extracellular), hemolysis, sorbitol production, osmotic fragility and flow-induced ATP release, were accurately determined by modern analytical techniques.

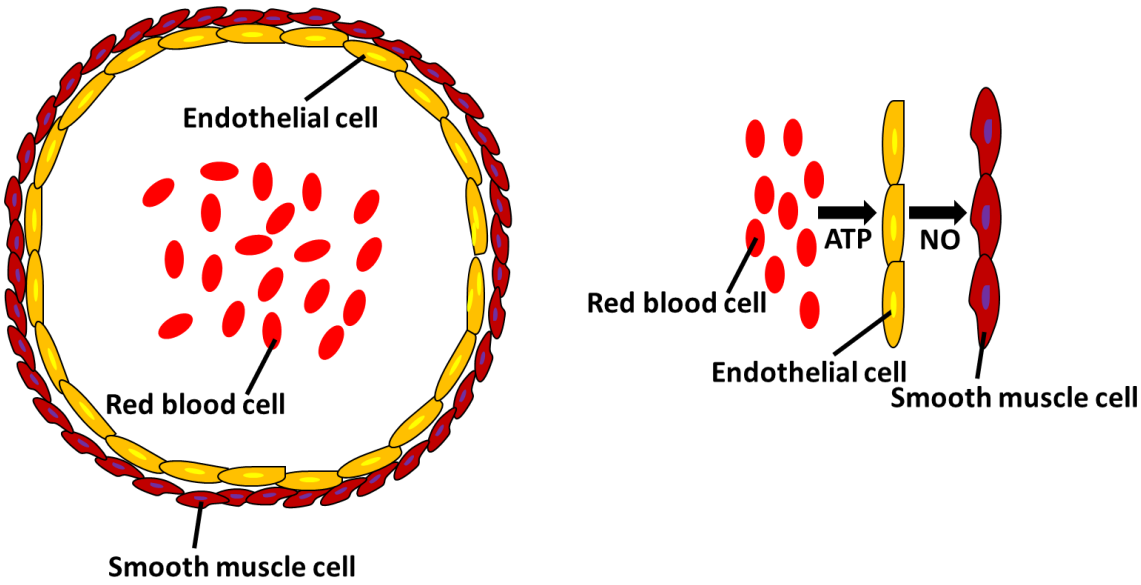

Figure 2.4 – The mechanism of RBCs regulation of blood flow through ATP release. There is millmolar levels of intracellular ATP in RBCs. RBCs can release hundreds of nanomoles of ATP to endothelial cells lining along with the blood vessel, which stimulates the production of endothelium-derived NO. The produced NO can diffuse to the smooth muscle cell layer, causing smooth muscle cell relaxation. This process enables vasodilation and a reduction in blood flow resistance.

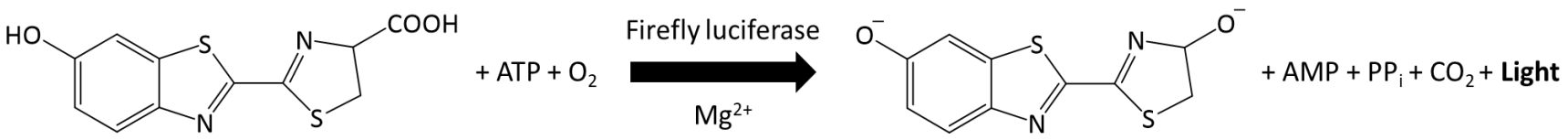

Figure 2.5 – Reaction of the chemiluminescence assay for ATP quantification. Luciferin can be oxidized by oxygen, in the presence of ATP. Firefly luciferase, a monomeric 61k Da protein, catalyzes luciferin oxidation using Mg^{2+} as a co-substrate. Chemiluminescence is produced by converting the chemical energy of luciferin oxidation through an electron transition, forming the product molecule oxyluciferin.

2.2 Experimental

2.2.1 RBC Collection and Storage

All reagents were purchased from Sigma-Aldrich (St. Louis, MO, USA) unless otherwise indicated. Blood was collected via venipuncture from informed and consented donors. Collection procedures were approved by the Biomedical and Health Institutional Review Board at Michigan State University. All processes described here were performed under sterile conditions, and all materials were sterilized. RBCs were collected and stored in both FDA-approved standard storage solutions and modified storage solutions. The components of modified storage solutions, CPDN/AS-1N, CPDN/AS-3N and CPDN/AS-5N, are listed in Table 2.1. Prior to use, all storage solutions were autoclaved at 120°C, 1.5 bar (2340M manual autoclave, Tuttnauer, Hauppauge, NY, USA).

To reduce the amount of blood needed from each donor, a miniaturized blood storage protocol was applied in this study, as shown in Figure 2.6.[18] Briefly, 1 mL of anticoagulant solutions were injected by syringe into 6 non-heparinized 10 mL glass Vacutainer tubes (BD, Franklin Lakes, NJ, USA); 2 tubes contained CPD, 1 tube contained CP2D, while the remaining tubes contained CPDN. Whole blood was drawn from donors (approximately 7 mL into each tube) and mixed with the appropriate anticoagulant solution by inverting the tube a few times. The blood samples were allowed to rest for 30 minutes at room temperature prior to centrifugation at 2,000 *g* for 10 minutes. Plasma and white blood cells were removed by aspiration. The volume of remaining packed RBC was estimated in graduated plastic tubes. AS was added to the packed RBCs at a 1:2 ratio (v/v). Leukofiltration was not performed due to the minimal amount of blood being collected

from each donor; such small amounts make it difficult to remove the buffy layer by filtration.

Storage PVC bags were prepared by using a PVC roll (ULINE, Pleasant Prairie, WI, USA) and a tabletop impulse sealer (ULINE). RBCs were stored in sealed PVC bags at 4°C for 35 days. The hematocrit of RBC suspensions in this miniaturized blood storage is around 50% – 60%, which falls into the same range used in standard RBC storage. There is approximately 1 mL of RBC suspension in each bag, and 6 bags for each sample. When experiments are being performed, one bag of sample was opened for testing and discarded after usage. In order to maintain the glucose level at 4 – 6 mM for RBCs stored in normoglycemic conditions throughout the 35-day storage, 10 μL of a 200 mM glucose saline solution were added every 5 days and bags resealed by a tabletop impulse sealer. In summary, RBCs were collected and stored in 6 different conditions, CPD/AS-1, CP2D/AS-3, CPD/AS-5, CPDN/AS-1N, CPDN/AS-3N and CPDN/AS-5N. Because of the minimal amount of blood being collected each time, RBC samples were collected and stored separately for the following experiments.

Table 2.1 – Components of normoglycemic versions of blood storage solutions

Constituents (mM)	CPDN	AS-1N	AS-3N	AS-5N
Sodium citrate	89.4	/	20.0	/
Citric acid	15.6	/	2.0	/
NaH_2PO_4	16.1	/	20.0	/
Na_2HPO_4	/	/	/	/
$NaHCO_3$	/	/	/	/
Glucose	**5.5**	**5.5**	**5.5**	**5.5**
NaCl	/	154.0	70.0	150.0
Adenine	/	2.0	2.2	2.2
Mannitol	/	41.0	/	29.0
pH	5.6	5.8	5.8	5.8

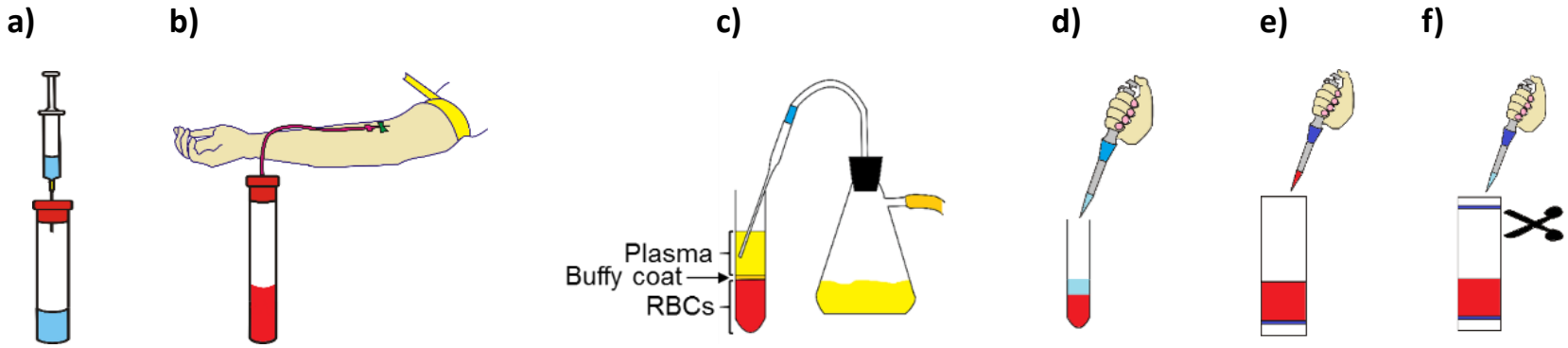

Figure 2.6 – Miniaturized blood collection and storage protocol. a) 1 mL of anti-coagulant solution (CPD, CP2D or CPDN) was injected into a non-heparinized vacuum tube; b) whole blood was drawn into each tube; c) after centrifugation, plasma and buffy coat were removed from the RBCs; d) AS was added to packed RBCs at a volume ratio 1:2. The combination of anticoagulant solution and AS followed FDA regulations (CPD/AS-1, CP2D/AS-3, CPD/AS-5) and their normoglycemic version (CPDN/AS-1N, CPDN/AS-3N, CPDN/AS-5N), respectively; e) an RBC suspension was aliquoted into sterilized PVC bags; f) for RBCs stored in normoglycemic solutions, the bags were opened weekly and a small amount of glucose saline (200 mM) solution was added to maintain the glucose concentration. (Copyright by Ruipeng Mu. Reprinted from Mu, R.; Chen, C.; Wang, Y.; Spence, D. M. analytical Methods 2016, 8, 6856 - 6864.)

2.2.2 Monitoring the Glucose Concentration

The glucose concentrations, both in the cell supernatant and in the cell fraction of the storage solutions, were determined weekly through 35 days of storage. To measure glucose in the storage supernatant, stored RBCs were centrifuged at 15,000 *g* for 15 min. The resulting supernatant from hyperglycemic storage conditions was diluted 1:1000 in distilled and deionized water (DDW), while supernatant from normoglycemic storage conditions was diluted 1:100 in DDW. Glucose standards were prepared by dilution from 100 mM glucose stock solution to a working range from 0 – 100 μM in DDW. Thus, different dilution factors were applied to bring the concentration of glucose into the assay calibration range. The glucose concentration was determined by an enzymatic fluorescence assay that required preparation of a mixture of glucose-6-phosphate dehydrogenase (G6PD, 0.9 U/mL), ATP (2 mM), magnesium chloride ($MgCl_2$, 2 mM), and hexokinase (HK, 1.7 U/mL) into triethanolamine (TEA) buffer (0.23 M, pH = 7.6). The supernatant (100 μL) was mixed with the enzyme assay mixture (100 μL) in a standard black 96-well plate, followed by incubation for 15 min at room temperature. The fluorescence from produced NADPH (excitation 340 nm; emission 460 nm) was detected by a plate reader (SpectraMax 4, Molecular Devices, Sunnyvale, CA, USA). To measure glucose in the cell fraction, the standard addition method was applied to eliminate matrix effects, especially those arising from the red color of Hb in the RBCs. Stored RBCs were centrifuged at 15,000 *g* for 15 min, followed by the removal of supernatant. Remaining packed RBCs at the bottom were lysed in DDW at a volume ratio of 1:100 for RBCs in hyperglycemic storage conditions and a 1:10 dilution ratio for RBCs in normoglycemic

storage conditions. The cell lysate was diluted in different glucose standard solutions (concentration range from 0 – 100 μM) at a 1:20 ratio (v/v). The resulting glucose concentration was determined by the enzymatic method described above.

2.2.3 Determining the Hemolysis Level

Percent hemolysis of stored RBCs was measured weekly, using a commercially available Drabkin's solution. Drabkin's solution was prepared from a kit, containing Drabkin's reagent and 30% Brij 35 solution. A vial of Drabkin's reagent, containing sodium bicarbonate, potassium ferricyanide, and potassium cyanide, was dissolved into 1000 mL of DDW with 0.5 mL of 30% Brij 35 solution. The solution was stored in an amber bottle, protecting it from light.

The hematocrit of the RBC samples was determined prior to the analysis of Hb concentration. It was measured by using microcapillary tubes to collect samples, and spinning them in a microhematocrit centrifuge (CritSpin, M960-22, Statspin). The volume percentage of RBCs in samples was obtained by visual quantification using a microcapillary reader (CritSpin, M960-22, Statspin).

Hb standards (concentration range from 0 – 0.8 g/L) were prepared by dissolving human Hb in Drabkin's reagent solution. Total Hb samples were prepared by adding RBC samples into Drabkin's solution at a ratio of 1:1000. Free Hb samples, which represent the concentration of Hb in the supernatant, were prepared by a 2-step centrifugation. RBC samples were first centrifuged at 2,000 *g* for 10 min, followed by a subsequent centrifugation at 15,000 *g* for 15 min. The resulting supernatant was diluted 1:10 in Drabkin's solution. Both samples and standards were incubated at room temperature and

darkness for 30 min, followed by measurement of absorbance at 550 nm using a standard, clear 96-well plate and plate reader. The calculation of the percent hemolysis is shown below:

$$\% \text{ Hemolysis} = (\text{Free Hb}) \times (100\% - \text{Hematocrit})/(\text{Total Hb})$$

2.2.4 Quantification of Sorbitol Accumulation

The amount of sorbitol accumulated in RBCs during storage was determined weekly by an enzymatic scheme utilizing a previously reported fluorometric detection method .[28] Here, 100 μL of stored RBCs were lysed in 500 μL of DDW, followed by the addition of 100 μL of 0.3 M zinc sulfate ($ZnSO_4$) solution and 100 μL of a 0.475 M sodium hydroxide (NaOH) solution to the cell lysate. The supernatant was obtained by centrifuging the sample at 2,000 *g* for 10 min. The sorbitol standards were prepared in a working range from 0 – 80 μM by dilution from a 20 mM sorbitol stock solution in physiological salt solution (PSS). The prepared sorbitol standards were treated in an identical manner to stored RBCs. The enzyme assay mixture was prepared by adding sorbitol dehydrogenase (SDH, 2kU/L), NAD^+ (3 mM) and disodium ethylenediaminetetraacetic acid (EDTA, 10 mM) into glycine-NaOH buffer (0.15 M, pH = 9.0). The blank assay was prepared similarly to the enzyme assay with the exception of the addition of SDH. The supernatants, resulting from samples and standards, were mixed with the enzyme assay and blank assay mixtures separately at a 1:1 ratio (v/v) in a standard, black 96-well plate. The mixture was incubated at 37 °C for 30 min, followed by fluorescence detection (excitation at 340 nm and emission at 460 nm) using a plate reader. As a control study, measurements of sorbitol in fresh RBCs from healthy donors were performed in the same manner as stored RBCs.

The Hb concentration in cell lysate was measured in conjunction with the sorbitol determination. The measurement was performed by using the Drabkin's method described in the Section 2.2.3. A minimal amount of cell lysate, 5 μL, was diluted in Drabkin's reagent solution at a 1:100 ratio (v/v). The sorbitol accumulation in stored RBCs was represented as nmol/g Hb.

2.2.5 Measuring Cell Osmotic Fragility

The standard osmotic fragility test is typically performed by measuring the concentration of sodium chloride (NaCl) solution required to lyse 50% of the RBCs in a sample. In this work, a simplified method was applied to quantify osmotic fragility of stored RBCs by measuring the percentage of lysis when placing RBC samples into a hypotonic solution.[30] Stored RBCs were warmed to room temperature before measurement, followed by the addition of25 μL aliquots of RBC samples to 500 μL of DDW, 0.45% NaCl solution and 0.9% NaCl solution, respectively. For RBCs, 0.9% NaCl is an isotonic solution that will not result in lysis, while 0.45% NaCl is a hypotonic solution where a certain portion of lysis will take place. RBC suspensions were gently mixed and then incubated for 30 min at room temperature. Afterwards, the suspensions were centrifuged at 1,500 *g* for 5 min. A 200 μL aliquot of the resulting supernatant from each sample was transferred to a standard clear 96-well plate. The absorbance of the supernatant (containing free Hb from lysed RBCs) was detected at 540 nm. The signal from RBCs in DDW was reported as 100% cell lysis, while the signal from RBCs in 0.9% NaCl solution was reported as no cell lysis. Therefore, the percent lysis in 0.45% NaCl solution was calculated using the equation:

$$\text{Percent lysis in 0.45\% NaCl solution} = (Abs_{0.45\%\ NaCl} - Abs_{0.9\%\ NaCl})/Abs_{DDW} \times 100$$

2.2.6 3D-Printed Fluidic Device: Design and Fabrication

The 3D-printed device applied in this study was designed using Autodesk Inventor 2014 student edition (Autodesk, San Rafael, CA). The base of the device is similar to our previous design.[49] As shown in Figure 2.7, the dimensions of the device are identical to a standard 96-well plate, enabling direct optical measurement in a plate reader. Twelve channels in the device make it suitable for parallel analysis. There are threaded ports at both ends of each channel, where male luer lock adapters can be integrated for connecting external Tygon tubes to the device. There is a single detection well above each channel, where removable trans-well membrane inserts can be positioned. The CAD file of the device was exported as a. STL file and printed by an Objet Connex350 Multi Material 3D Printing System (Stratasys, Eden Prairie, MN, USA), housed in the Department of Electrical and Computer Engineering at Michigan State University. The 3D device was made out of VeroClear (Stratasys), a transparent material, approximately comprised of isobornyl acrylate (15−30%), acrylic monomer (15−30%), urethane acrylate (10−30%), acrylic monomer (5−10; 10−15%), epoxy acrylate (5−10; 10−15%), acrylate oligomer (5−10; 10−15%), and photoinitiator (0.1−1; 1−2%). The printed device was cleaned manually by using a tip cleaner to remove supporting material, followed by sonication in 0.5 M sodium hydroxide (NaOH) solution. Prior to use, the device was rinsed with DDW and dried at room temperature.

2.2.7 Determination of Cell-Derived ATP Release

Flow-induced ATP release from stored RBCs was determined using the printed fluidic device described above. ATP standards (concentration range from 0 – 400 nM) were

prepared in different AS. Prior to use, stored RBCs were washed three times with the corresponding AS, and then diluted in the same AS, resulting in a 7% RBC suspension. The closed loop flow system was achieved by connecting a Tygon tube to both ends of a channel. Trans-well membrane inserts, containing 0.4 μm pore size polyester membranes, were placed into detection wells. ATP standards were circulated in the loops to generate calibration curves, followed by RBC suspensions in triplicate. The circulation was maintained by a peristaltic pump (IDEX Health & Science LLC, Oak Harbor, WA, USA) at a flow rate of 200 μL/min. A 100 μL volume of an AS were added into inserts to enable the collection of ATP from the channel via diffusion, as shown in Figure 2.8. The ATP, from the standards or RBC-derived, can diffuse through the membrane into the preloaded AS in the inserts, and is proportional to the amount of ATP in the channel. After circulating for 20 min at room temperature, the device was detached from the tubes and placed in the plate reader. The amount of ATP in the inserts was measured by the well-established luciferase/luciferin (L/L) chemiluminescence method.[48] The L/L assay solution was prepared by dissolving 2.0 mg of D-luciferin and 100 mg of firefly extract into 5 mL of DDW. Using a multichannel pipet, an aliquot of 10 μL of L/L assay solution was added simultaneously with additive solution into the trans-well insert. At 10 s after adding the assay solution, the device was vigorously shaken for 5 s by a plate reader, followed by the detection of chemiluminescence intensity. After each use, the device was cleaned by sonication in 10% bleach and rinsing with distilled water.

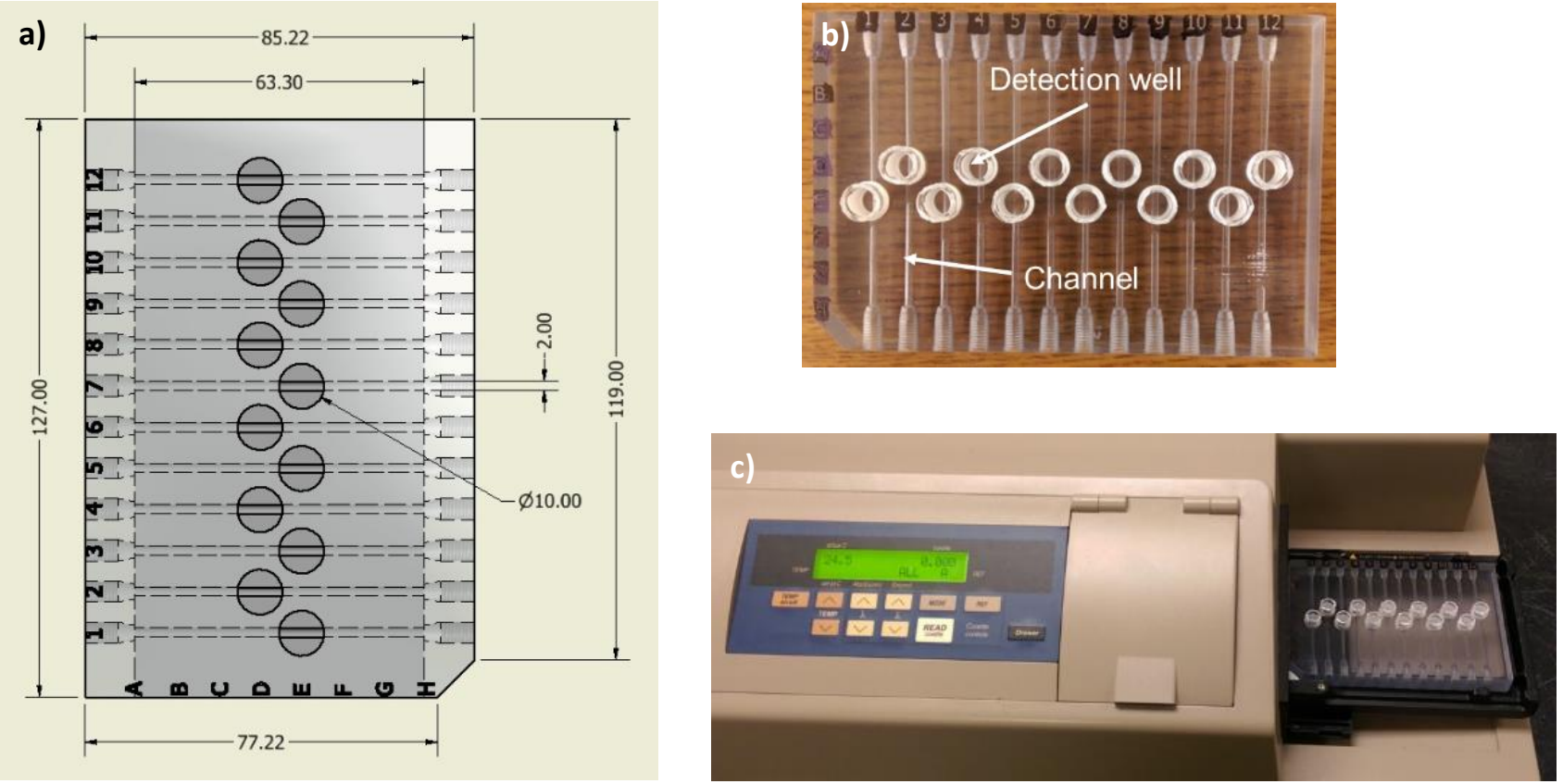

Figure 2.7 – The design of the 3D-printed device. a) Engineering sketch of the fluidic device with dimensions (mm); b) 3D-printed fluidic device in VeroClear material, with membrane inserts in detection wells; c) 3D-printed fluidic device is designed to fit into a commercial plate reader like a standard 96-well plate. (Copyright by Ruipeng Mu. Reprinted from Mu, R.; Chen, C.; Wang, Y.; Spence, D. M. analytical Methods 2016, 8, 6856 - 6864.)

a)

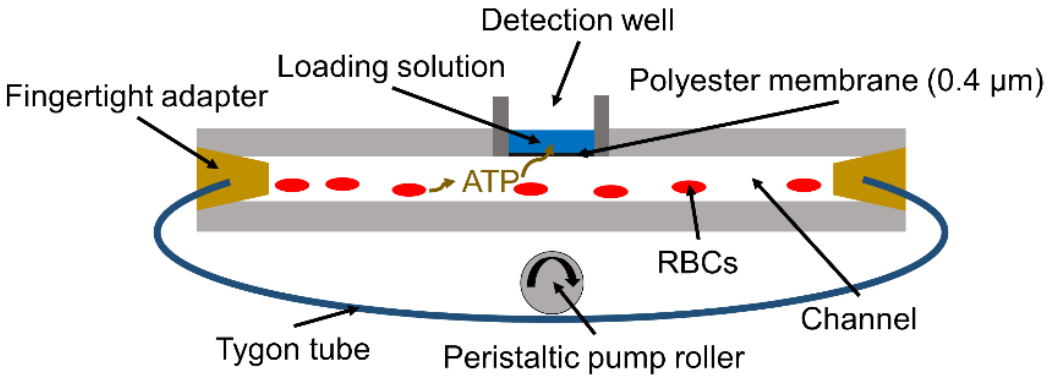

b)

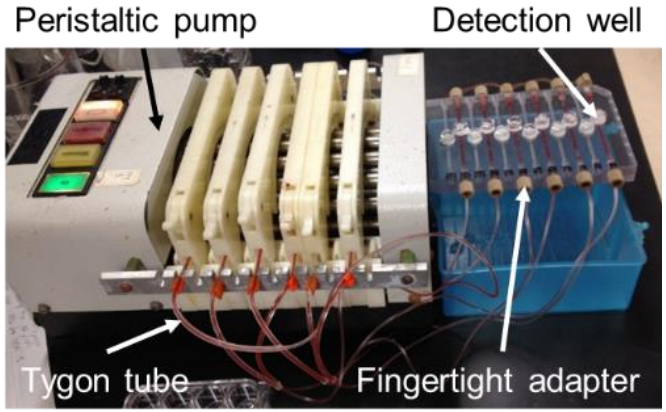

Figure 2.8 – The measurement of flow-induced ATP release from stored RBCs. a) A schematic cross section of RBCs circulated in a channel with membrane insert. The loop was closed by connecting Tygon tubing at both ends of a channel with a fingertight adapter. ATP released from RBCs will diffuse through the polyester membrane into the loading solution in the membrane insert; b) Stored RBC samples were diluted and loaded into 6 channels of the device. The flow was maintained by a peristaltic pump at a flow rate of 200 µL/min. (Copyright by Ruipeng Mu. Reprinted from Mu, R.; Chen, C.; Wang, Y.; Spence, D. M. analytical Methods 2016, 8, 6856 - 6864.)

2.3 Results

2.3.1 Glucose Concentration

The glucose levels in the stored RBCs was monitored weekly throughout the 35-day storage period. The results are shown in Figure 2.9. RBCs stored in hyperglycemic conditions are exposed to a high concentration of glucose throughout storage. For example, extracellular glucose level of RBCs stored in CPD/AS-1 on day 1 is 54.4 ± 2.6 mM (CP2D/AS-3: 40.2 ± 0.9 mM; CPD/AS-5: 35.7 ± 0.7 mM). While, on day 35, the glucose concentration in the supernatant is 51.1 ± 1.3 mM (CP2D/AS-3: 44.1 ± 0.4 mM; CPD/AS-5: 38.1 ± 2.6 mM). The glucose concentrations in the packed RBCs are similar to those found in the supernatants. For instance, for RBCs stored in CPD/AS-1, the glucose level in the cell fraction on day 1 is 44.6 ± 1.5 mM (CP2D/AS-3: 38.0 ± 0.9 mM; CPD/AS-5: 32.5 ± 1.0 mM). On day 35, it was 41.8 ± 1.7 mM (CP2D/AS-3: 40.5 ± 1.2 mM; CPD/AS-5: 34.8 ± 3.2 mM). On the other hand, for RBCs stored in our modified collection and storage solutions, including CPDN/AS-1N, CPDN/AS-3N and CPDN/AS-5N, the glucose level was maintained between 4 – 6 mM, for both cell fractions and solution supernatants.

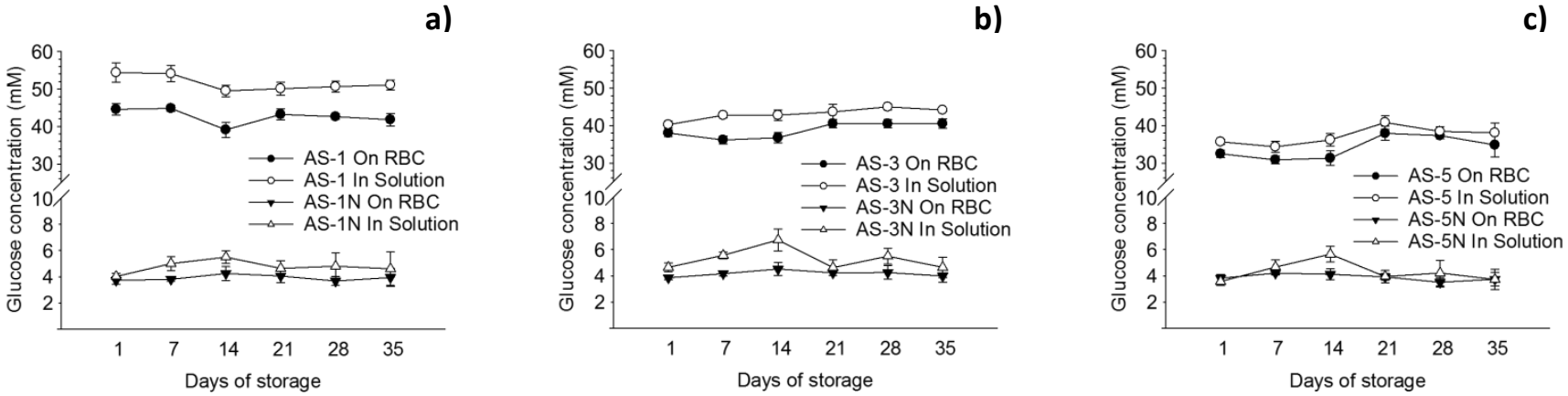

Figure 2.9 – Glucose concentrations in stored RBCs. Glucose levels in solution (blank) and on RBC (black), for RBCs stored in standard storage solutions (circle) and our normoglycemic storage solutions (triangle). a) RBCs stored in CPD/AS-1 and CPDN/AS-1N; b) RBCs stored in CP2D/AS-3 and CPDN/AS-3N; c) RBCs stored in CPD/AS-5 and CPDN/AS-5N. Glucose concentrations, both in solution and on the RBC, are higher for those stored in FDA approved solutions, in which CPD/AS-1 provides the highest level. However, in normoglycemic storage conditions, glucose concentration can be maintained between 4 ~ 6 mM, the blood glucose level in healthy humans, throughout a 35-day storage. Data represent mean ± s.e.m. (n = 4 humans for all). (Copyright by Ruipeng Mu. Reprinted from Mu, R.; Chen, C.; Wang, Y.; Spence, D. M. analytical Methods 2016, 8, 6856 - 6864.)

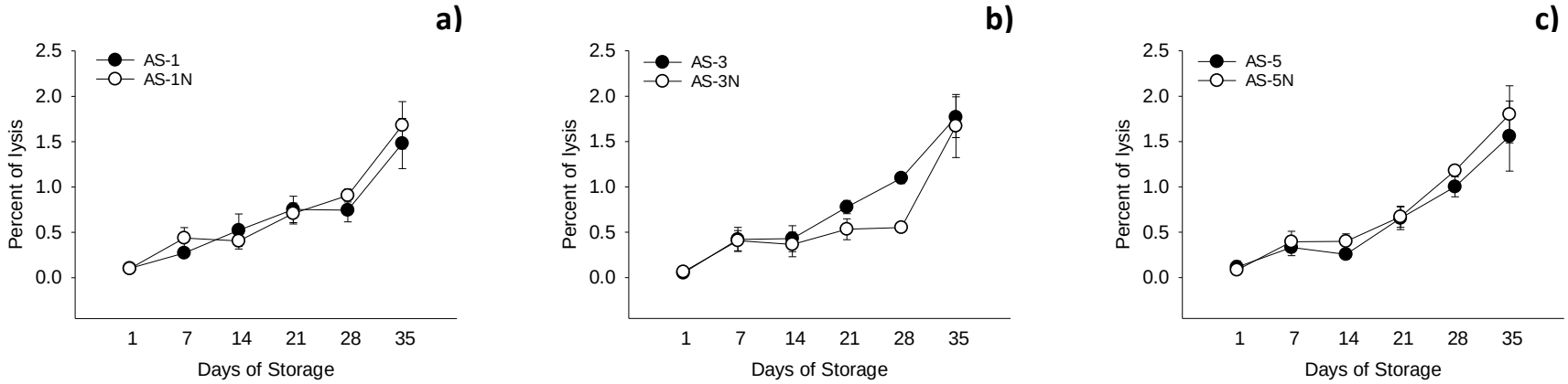

Figure 2.10 – Hemolysis level of stored RBCs. The percentage of hemolysis in the blood storage bags, including RBCs stored in high glucose environments (black circle) and low glucose environments (blank circle). a) RBCs stored in CPD/AS-1 and CPDN/AS-1N; b) RBCs stored in CP2D/AS-3 and CPDN/AS-3N; c) RBCs stored in CPD/AS-5 and CPDN/AS-5N. FDA requires the percent cell lysis less than 1% during RBC storage period. Stored RBCs meet the criteria until day 21, but exceed the threshold on day 35. The high percentage of hemolysis is partially due to the samples didn't pass through a leukofiltration membrane. Data represent mean ± s.e.m. (n = 4 humans for all).

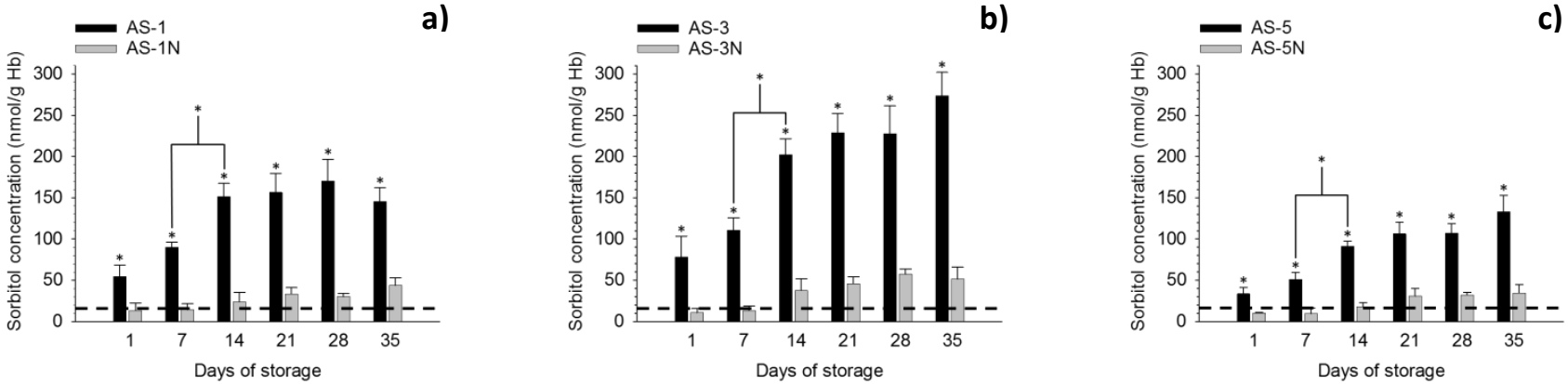

Figure 2.11 – Sorbitol accumulation in stored RBCs. Intracellular sorbitol produced when RBCs are stored in standard storage solutions (black bar) and normoglycemic storage solutions (grey bar). The dashed line represents the sorbitol level of fresh blood. a) RBCs stored in CPD/AS-1 and CPDN/AS-1N; b) RBCs stored in CP2D/AS-3 and CPDN/AS-3N; c) RBCs stored in CPD/AS-5 and CPDN/AS-5N. RBCs stored in standard solutions result in a significantly higher concentration of sorbitol accumulation in cells from day 1 through day 35. Notably, there is a significant increase of sorbitol concentration from day 7 to day 14 for RBCs stored in hyperglycemic conditions. This trend indicates permanent damage occurred during the first 2 weeks storage. Data represent mean ± s.e.m. (*$p < 0.01$, $n = 5$ humans for all). (Copyright by Ruipeng Mu. Reprinted from Mu, R.; Chen, C.; Wang, Y.; Spence, D. M. analytical Methods 2016, 8, 6856 - 6864.)

2.3.2 Hemolysis Level

The results of the cell lysis measurements during the storage period are shown in Figure 2.10. For RBCs stored in all different solutions, the percent lysis was less than 1% until day 21. However, on day 28, cells stored in three storage solutions exhibited higher percentage of hemolysis (CPD/AS-3: 1.10 ± 0.06%; CPD/AS-5: 1.00 ± 0.11%; CPDN/AS-5N: 1.18 ± 0.02%). All RBC products in this work had a level of hemolysis that would not be allowed FDA by the end of storage.

2.3.3 Sorbitol Accumulation

Figure 2.11 shows the results of weekly sorbitol accumulation in the stored bags containing RBCs. The dashed line represents the sorbitol level of fresh blood as a control (16.1 ± 2.0 nmol/g Hb). In comparison, sorbitol production in the RBCs stored under hyperglycemic conditions (CPD/AS-1: 54.7 ± 13.9 nmol/g Hb; CP2D/AS-3: 78.1 ± 25.2 nmol/g Hb; CPD/AS-5: 33.6 ± 7.8 nmol/g Hb) is statistically higher than the fresh blood control and RBCs stored under physiological glucose levels (CPDN/AS-1N: 13.5 ± 8.9 nmol/g Hb; CPDN/AS-3N: 10.8 ± 4.7 nmol/g Hb; CPDN/AS-5N: 10.4 ± 1.0 nmol/g Hb), at the first day of storage ($p < 0.01$). The intracellular sorbitol concentrations continually increased as a function of time. Notably, there is a significant increase of sorbitol concentration from day 7 to day 14 for RBCs stored in hyperglycemic ($p < 0.01$).

2.3.4 Osmotic Fragility

The results of the osmotic fragility measurements on stored RBCs are shown in Figure 2.12. Lower percent lysis in hypotonic solution indicates cells are more robust. The dashed line represents the result of the osmotic fragility test for RBCs obtained from fresh blood

(19.9 ± 5.2%). There is a significant difference of the percent lysis in 0.45% NaCl solution between RBCs stored in hyperglycemia and normoglycemia on day 1 and day 7 ($p < 0.05$). For example, for cells stored in CPD/AS-1 and CPDN/AS-1N, the percent lysis values are 63.4 ± 4.0% and 21.0 ± 3.1% on day 1. While on day 7, they became 56.6 ± 4.4% (CPD/AS-1) and 28.9 ± 1.4% (CPDN/AS-1N). There is no statistical significance from day 14.

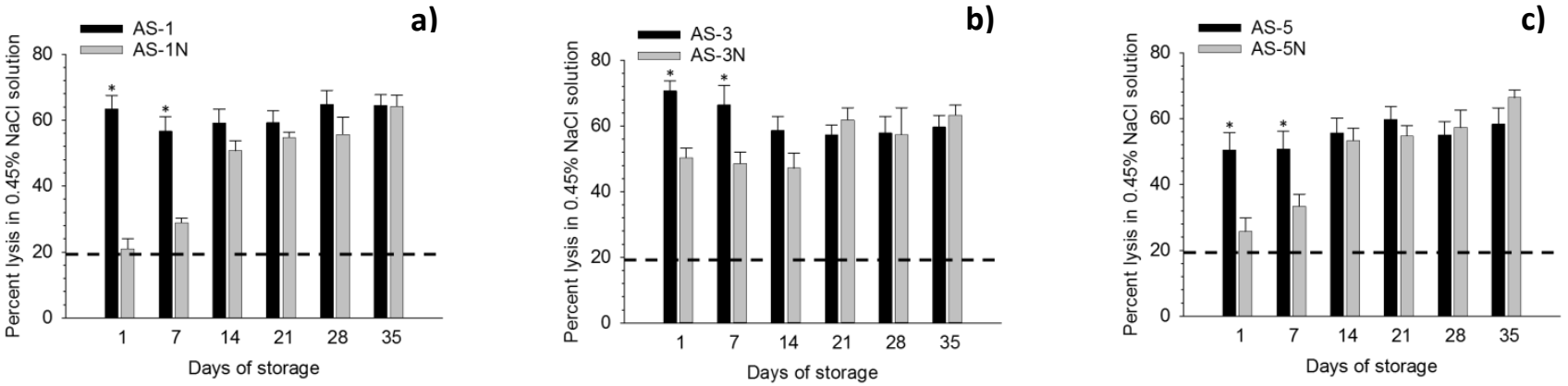

Figure 2.12 – Osmotic fragility of RBCs stored in hyperglycemic conditions (black bar) and normoglycemic conditions (grey bar). Dash line represents the ability of fresh RBCs to resist osmotic pressure. a) RBCs stored in CPD/AS-1 and CPDN/AS-1N; b) RBCs stored in CP2D/AS-3 and CPDN/AS-3N; c) RBCs stored in CPD/AS-5 and CPDN/AS-5N. RBCs stored in normoglycemic condition tend to be more rigid in the first week. However, after 2 weeks of storage, both hyperglycemic and normoglycemic storage show no difference, which further suggests that stored RBCs suffer from some permanent damage after 2 weeks in storage. Data represent mean ± s.e.m. (*$p < 0.05$, n = 5 humans). (Copyright by Ruipeng Mu. Reprinted from Mu, R.; Chen, C.; Wang, Y.; Spence, D. M. analytical Methods 2016, 8, 6856 - 6864.)

2.3.5 ATP Measurement

The results of flow-induced ATP release are shown in Figure 2.13. RBCs stored in normoglycemic storage solutions release significantly higher amounts of ATP compared to RBCs stored in commercialized hyperglycemic storage solutions throughout the 35-day storage ($p < 0.05$). RBC-derived ATP release slowly decreases with storage duration. On day 1, flow-induced ATP release from cells stored in normoglycemic environments is about 250 nM (CPDN/AS-1N, 251 ± 14 nM; CPDN/AS-3N, 252 ± 11 nM; CPDN/AS-5N, 254 ± 27 nM); whereas, it is about 150 nM when cells were exposed to high concentration of glucose (CPD/AS-1, 125 ± 2 nM; CP2D/AS-3, 145 ± 8 nM; CPD/AS-5, 165 ± 15 nM). On day 35, there is still approximately 200 nM of ATP release from RBCs stored in our modified solutions (CPDN/AS-1N, 173 ± 10 nM; CPDN/AS-3N, 219 ± 19 nM; CPDN/AS-5N, 165 ± 6 nM), which is close to fresh RBCs from healthy people (190 ± 10 nM). However, ATP release from the hyperglycemic stored RBCs is lowered down to below 100 nM (CPD/AS-1, 65 ± 8 nM; CP2D/AS-3, 97 ± 7 nM; CPD/AS-5, 48 ± 1 nM), which is close to our previous study involving diabetic RBCs (90 ± 10 nM).[50] Notably, there is a significant difference of ATP release between RBCs stored in CPDN/AS-1N on day 35 with RBCs stored in CPD/AS-1 on day 1 ($p < 0.05$). The same observation was also found when comparing CP2D/AS-3 and CPDN/AS-3N.

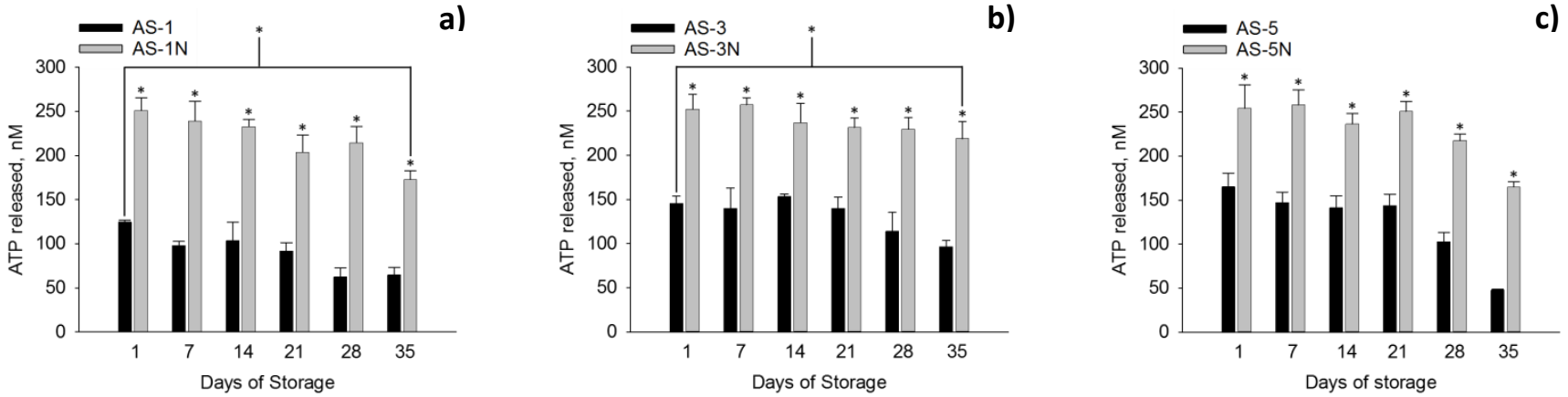

Figure 2.13 – Flow-induced ATP released from RBCs stored in standard storage solutions (black bar) and our modified storage solutions (grey bar). a) RBCs stored in CPD/AS-1 and CPDN/AS-1N; b) RBCs stored in CP2D/AS-3 and CPDN/AS-3N; c) RBCs stored in CPD/AS-5 and CPDN/AS-5N. During 35 days of storage, RBCs stored in our modified storage solutions keep their ability to release ATP, performing similar to fresh RBCs from healthy people (190 ± 10 nM). However, RBCs stored in standard storage solutions are only able to release about 50% of the ATP as typically measured from controls, thus resembling RBCs from people with diabetes. Data represent mean ± s.e.m. (*$p < 0.05$, n = 4 humans). (Copyright by Ruipeng Mu. Reprinted from Mu, R.; Chen, C.; Wang, Y.; Spence, D. M. analytical Methods 2016, 8, 6856 - 6864.)

2.4 Discussion

In order to study the effects of glucose, RBCs were collected and stored in both currently approved hyperglycemic storage solutions and our modified normoglycemic storage solutions. Three FDA approved storage solutions were applied in this work, CPD/AS-1, CP2D/AS-3 and CPD/AS-5, which were approved nearly three decades ago.[2] Recent studies have been focused on the quality of stored RBCs, possibly due to the prevalence of post-transfusion complications, especially when transfused RBCs have been stored more than 14 days.[51-54] Therefore, new storage solutions, which can improve the RBC storage and minimize post-transfusion related complications, are under high demand. Recently, our group has investigated CPDN/AS-1N and shown that storage solutions containing glucose concentrations at physiological levels have beneficial effects on stored RBCs.[20,21,55]

To further expand our prior reports, CP2D/AS-3 and CPD/AS-5, two other currently approved storage solutions were investigated. The storage process was identical to the FDA standard procedure, except for the handling of the buffy coat in the whole blood (removed by aspiration rather than filtration), and that collection and storage were performed on a scale of about 1:10. Normally, ~ 300 mL of purified RBCs are present in each unit, while only 1 mL was in our micro-unit. RBCs stored in normoglycemic conditions were fed with 10 μL of 200 mM glucose saline every 5 days to compensate for the consumption of glucose by cell metabolism and maintain the glucose level within 4 – 6 mM. Of course, this method of opening the bag would not be permitted clinically; but in order to demonstrate feasibility, here we open and reclose the bags.

There is a large amount of glucose molecules present in both anticoagulant solutions and AS. The high concentration of glucose that exists in stored RBCs is due to two reasons. First, a sufficient amount of glucose is required to last throughout the storage duration. Second, there is a historical element; as discussed in Chapter 1, whole blood was collected and stored in CPD before the development of components separation and AS.[56-58] In other words, glucose was added to stored RBCs twice during the collection and storage process. It is possible that when AS was first being developed, the necessity of containing glucose in anticoagulant solutions was not reevaluated.

The extracellular glucose level of RBCs stored in a normoglycemic environment can be successfully controlled between 4 – 6 mM, which is close to the healthy glucose level in the blood stream. However, standard storage solutions provide an extremely high concentration of glucose in the supernatant (CPD/AS-1, 50 – 55 mM; CP2D/AS-3, 40 – 45 mM; CPD/AS-5, 35 – 40 mM). Even compared to people with diabetes mellitus, who have an elevated blood glucose level (7 – 10 mM), RBCs stored in hyperglycemic solutions are subjected to constant fourfold increase in glucose. There is no notable decrease in extracellular glucose concentration during the storage duration. This is thought to be due to a decreased rate of cell metabolism, especially glycolysis, due to the acidic environment of storage solutions.[4] Moreover, the hemolysis of RBCs during storage releases intracellular glucose into the solution. The glucose concentration in the RBC fraction (glucose on the RBC), which refers to the glucose molecules either in the cell or attached to the outer layer of cell membrane, was also detected in this work.

Hyperglycemic storage environments lead to high concentrations of glucose on the stored RBCs, compared to our modified normoglycemic storage method.

The percent hemolysis of banked RBCs is higher than 1% at the 5-week storage mark, which makes stored RBCs no longer acceptable according to the FDA regulation. This undesirable phenomenon can be ascribed to that there is no leukofiltration process when collecting and storing RBCs. It has been shown that the extent of hemolysis can be reduced by 50% if white blood cells are removed.[24] Another factor that may contribute to the increased hemolysis percentage is the blood banking process were miniaturized. Compared to a commercial blood bag, which has a volume ~ 300 mL RBC suspension, the ratio of cells adhere on the side of the bags is higher in the miniaturized PVC bags. While, in a standard blood bag, most cells presented in the solution, instead of on the surface of the PVC. RBCs located on the side of the bags are prone to dry out and lyse.

Sorbitol, obtained by the reduction of glucose in the polyol pathway, is a well-known indicator of diabetes mellitus.[59] It has been found that the sorbitol concentration in RBCs is increased in diabetic subjects, and correlates with plasma glucose concentration.[26] The sorbitol levels in RBCs stored in hyperglycemic storage solutions is significantly higher than RBCs stored in normoglycemic storage solutions, even after 1 day of storage. There is a clear trend that sorbitol concentration increases in the cells as a function of storage time. Conversely, in our modified normoglycemic storage conditions, sorbitol concentrations in stored RBCs are similar to fresh RBCs from the blood stream. The mass production of sorbitol in stored RBCs is primarily due to two factors. First, there are elevated concentrations of glucose present in the storage solutions. Normally, RBCs break

down glucose through the glycolysis pathway to generate ATP as the cell energy source. The first step of this process is the phosphorylation of glucose via the enzyme hexokinase. Hexokinase would be saturated in the presence of excess glucose. Therefore, more glucose enters the polyol pathway, where it will be reduced by aldose reductase to form sorbitol. Second, glucose favors the polyol pathway instead of the glycolysis pathway in a relatively acidic storage environment. The pH of storage solutions is below 5.6 in order to avoid caramelization when they are being autoclaved.[60] After collecting blood into storage solutions, the resulting suspension has a pH between 7.0 – 7.2, which is lower than physiological pH (7.35).[61] Furthermore, the storage environment becomes increasingly acidic from protons that are produced when glucose is phosphorylated by hexokinase. The pH decreases down to 6.6 – 6.8 by the end of the storage. The optimal pH for hexokinase is 7.5 – 9.0, while its 6.2 – 6.8 for aldose reductase.[62,63] As the pH decreases during storage, the activity of hexokinase decreases, while aldose reductase production is favored. The enzyme sorbitol dehydrogenase converts sorbitol to fructose, making the pathway favor glycolysis, and the optimal pH for sorbitol dehydrogenase is 9.0 – 11.0.[28] Sorbitol concentration stays low for RBCs stored in normoglycemic storage solutions, since the glucose concentration is maintained at a physiological level. There is a small increase in sorbitol after two weeks of storage even when RBCs were stored in normoglycemic conditions. This is primarily due to the acidic environment discussed above. However, compared to the sharp increase that occurred in hyperglycemic storage conditions, this small increment is statistically insignificant. Overall, the mass production of sorbitol in RBCs stored in hyperglycemic storage solutions is mainly contributed to the

high concentration of glucose present around the cells, accompanied with the acidic environment of storage.

The high concentration of sorbitol accumulated in cells is anticipated to have adverse effects on stored RBCs. For example, NADPH is consumed when glucose is converted into sorbitol. NADPH is an important antioxidant molecule, protecting the cells against toxic reactive oxygen species (ROS). The consumption of NADPH would further accelerate the rate of antioxidant depletion, resulting in the cells suffering from high oxidative stress. Notably, there is a significant difference between day 7 and day 14 storage for RBCs stored in hyperglycemic conditions. Previously, our group has reported that the reversibility of RBC deformability is impaired after 1 to 2 weeks of storage.[64] The sorbitol study here might provide an explanation for that work. Due to the mass production of sorbitol, the cell membrane is subjected to ROS damage, especially the lipids and skeleton proteins that support the membrane structure, causing a permanent loss of cell deformability. Interestingly, many clinical retrospective studies indicate that the chance of post-transfusion related complications increases when patients receive blood shelved for more than two weeks.[51,54] Comparing this time line to the sorbitol study here indicates that sorbitol might play an important role in the complications using blood components stored for more than 2 weeks.

In addition to oxidative stress, the osmotic balance of the cells would be disrupted, because sorbitol is not able to pass through the cell membrane. Osmotic fragility represents the degree of cell lysis when RBCs are subjected to osmotic stress, reflecting abnormalities in the cell membrane. This test is commonly performed in hematology,

especially for the diagnosis of spherocytosis where RBCs are abnormally sphere-shaped instead of biconcave discs.[29] This shape change results in the loss of cell membrane associated with deformability, making RBCs more prone to rupture. Interestingly, stored RBCs also undergo shape change from biconcave discs to grossly abnormally shaped spheres, indicating that RBCs may become more fragile during the storage.[65]

RBCs stored in normoglycemic conditions tend to be less fragile, compared to RBCs stored in hyperglycemic conditions, in the first week of storage. This is especially true when RBCs were stored in CPDN/AS-1N and CPDN/AS-5N. However, the differences were not significant after 2 weeks of storage, which further supports deleterious effects of storage being permanent after 1 – 2 weeks.

On the first day of storage, the percent lysis of RBCs stored in CPDN/AS-1N and CPDN/AS-5N was 21 ± 3% and 26 ± 4%, and increased to 50 ± 3% in CPDN/AS-3N. A possible explanation behind this is proposed here. This unexpected increase in lysis might be caused by the storage components, especially citric acid, present in AS-3. When comparing AS-3 to AS-1 and AS-5, AS-3 provides a buffer system by adding citric acid and sodium citrate, while purposely lowering the concentration of chloride to balance the negative charges. In these conditions, the osmotic pressure will be balanced only if citrate can pass through the RBC membrane. However, the plasma membrane citrate transporters have been identified in human liver and brain, but not human RBC.[66,67] In addition, the RBC is different from many other types of cells due to a lack of cell nucleus and mitochondria, which are required for the citric acid cycle. Most pyruvic acid produced through glycolysis is converted to lactic acid instead of citric acid. Therefore, it is possible

that citrate transporters are not expressed on RBC membrane. As a consequence, RBCs may experience increased osmotic imbalance when processed using AS-3 compared to the other storage solutions.

A downstream of adverse effects caused by sorbitol accumulation is impaired ATP release from RBCs, because both oxidative damages and osmotic imbalance can affect cell mechanical properties. It has been reported that the RBC is a major determinant in regulating blood flow, in addition to its role in oxygen delivery.[68,69] The role of the RBC in controlling blood flow can be explained by two, somewhat competing, mechanisms. One describes the RBC's ability to release nitric oxide (NO), a well-known vasodilator, directly into the bloodstream.[68] The other mechanism describes how NO is produced by endothelial cells after stimulation by ATP released from RBCs.[69,70] In relation to the latter mechanism involving ATP, it has been reported by our group that RBCs stored in CPD/AS-1 release decreased amounts of ATP (80 ± 20 nM), similar to RBCs from patients with type 2 diabetes (90 ± 10 nM).[50] However, ATP released from RBCs processed in CPDN/AS-1N with feeding is significantly higher (232 ± 7 nM), which is close to the ATP released from fresh RBCs (210 ± 7 nM).[64,71] Impaired ATP release from stored RBCs, as well as ATP production, has also been reported by other groups. For example, Mcmahon group reported that impaired ATP release from stored RBCs promotes their adhesion to endothelial cells, but the issue can be improved if intracellular ATP production in banked RBCs was restored.[35,72]

To expand on previous work, flow-induced ATP released from RBCs processed using storage solutions CP2D/AS-3 and CPD/AS-5 have been investigated in this study. In

addition, polyjet 3D printing has been utilized in this work to replace the previous poly-dimethylsiloxane (PDMS) platform. The printed device, containing 12 channels, enables us to perform flow studies in parallel with improved precision. The robustness of the printed parts allows us to use only one device throughout the long term study, which minimized experimental and measurement variations. High-throughput optical detection has been achieved by fabricating the device to fit into a commercial plate reader.

RBCs stored in normoglycemic storage solutions release significantly higher amounts of ATP (CPDN/AS-1N, 251 ± 14 nM; CPDN/AS-3N, 252 ± 11 nM; CPDN/AS-5N, 254 ± 27 nM), compared to RBCs stored in commercialized hyperglycemic storage solutions (CPD/AS-1, 125 ± 2 nM; CP2D/AS-3, 145 ± 8 nM; CPD/AS-5, 165 ± 15 nM). This trend continues from the first day of storage to day 35. When comparing three hyperglycemic conditions on day 1, RBCs stored in CPD/AS-5 had the highest ATP release (165 ± 15 nM) while RBCs stored in CPD/AS-1 released the lowest amount (125 ± 2 nM). Interestingly, the ATP release from the stored RBCs was the lowest in CPD/AS-1, the storage solution with the highest glucose levels (Figure 2.9 c). This phenomenon implies that the most hyperglycemic storage solution has an immediate impact on the RBC's ability to release ATP, and the severity increases as the concentration increases. On the other hand, in hyperglycemic storage solutions, the RBCs were slowly losing their ability to release ATP regardless of the storage solutions used, indicating that long term stored cells suffer from permanent damage.

Modified normoglycemic storage solutions have increased ATP release in comparison to the hyperglycemic versions, even for long term storage. On day 35, the amount of ATP

released from RBCs stored in normoglycemic conditions was similar to fresh blood from healthy controls (190 ± 10 nM). Notably, in Figure 2.13 a) and b), ATP release from RBCs stored in normoglycemic conditions on day 35 (CPDN/AS-1N, 173 ± 10 nM; CPDN/AS-3N, 219 ± 20 nM) was higher than RBCs stored in hyperglycemic conditions on day 1 (CPD/AS-1, 125 ± 2 nM; CP2D/AS-3, 145 ± 8 nM). The difference was absent in Figure 2.13 c), where RBCs were stored in CPD/AS-5 and CPDN/AS-5N. This absence of difference was primarily due to the instant glucose effect discussed above, where CPD/AS-5 contained the least glucose level in hyperglycemic solutions.

Previously, it has been shown by Sprague *et al.* that total and upstream (arterial) rabbit pulmonary vascular resistance decreased significantly when 300 nM ATP in PSS was administrated to rabbit lung. However, the decrease was not significant when only 100 nM ATP was infused.[46] Reported by the same group, RBCs are required to demonstrate participation of NO in the regulation of rabbit pulmonary vascular resistance.[44] Moreover, work done by the Spence group in CPD/AS-1 and CPDN/AS-1N has demonstrated that the increased amount of RBC derived ATP can stimulate the NO production from endothelial cells by 25%.[55] Collectively considering the above results, RBCs stored in hyperglycemic conditions may experience a higher vascular resistance after transfusion, because they are only able to release less than 100 nM of ATP under flow condition. Although more direct evidence is needed, it is rational to hypothesize that RBCs stored in a normoglycemic environment may result in improved blood flow after transfusion, which may further enhance the NO bioavailability and reduce the chance of post-transfusion complications.

2.5 Conclusion

In this chapter, new versions of blood banking processing solutions were proposed, where the glucose concentrations were maintained at 4 – 6 mM. The modified collection and storage solutions were compared to current FDA approved solutions to explore the effects of glucose on stored RBCs in several different aspects. RBCs stored in standard solutions were exposed to an unfavorably high concentration of glucose throughout a 35-day storage. Whereas, glucose levels were successfully controlled within healthy range utilizing normoglycemic solutions with a continuous feeding protocol. The laboratory scale, miniaturized blood banking products were able to meet the FDA hemolysis requirement in the first 4 weeks of storage. The production of intracellular sorbitol was increased by over three fold in hyperglycemic conditions, which has detrimental effects on cells. For instance, hyperglycemic stored RBCs lost 50% of their capacity to release ATP when pumped through microfluidic channels. On the other hand, RBCs stored in high glucose environments are more fragile under osmotic pressure. However, the increased production of sorbitol can be avoided when processing RBCs using our modified normoglycemic solutions. Importantly, we demonstrated that the flow-induced ATP release can be maintained throughout storage in normoglycemic conditions, showing no statistically significant difference in comparison to healthy controls. This discovery implies that RBCs stored in normoglycemic conditions may have improved flow properties after transfusion, compared to current blood products. Additionally, RBCs stored in physiological levels of glucose tend to be more robust in the first week of storage. Notably, the significant changes measured in the sorbitol test occurred between 1 – 2 weeks of

storage, and indicate that hyperglycemia induces permanent damages to stored RBCs after 2 weeks. These results strongly suggest that the severity of storage lesion can be reduced in normoglycemic storage, therefore, potentially reducing the risk of post-transfusion complications.

REFERENCES

REFERENCES

(1) Whitaker, B. I., National Blood Collection and Utilization Survey Report; US Department of Health and Human Services2011.

(2) Hess, J. R. *Vox Sang* **2006**, *91*, 13-19.

(3) Hess, J. R. *J Proteomics* **2010**, *73*, 368-373.

(4) Hess, J. R. *Transfus Apher Sci* **2010**, *43*, 51-59.

(5) Qu, L.; Triulzi, D. J. *Cancer Control* **2015**, *22*, 26-37.

(6) Tinmouth, A.; Chin-Yee, I. *Transfus Med Rev* **2001**, *15*, 91-107.

(7) Dumont, L. J.; Yoshida, T.; AuBuchon, J. P. *Transfusion* **2009**, *49*, 458-464.

(8) Burns, J. M.; Yoshida, T.; Dumont, L. J.; Yang, X.; Piety, N. Z.; Shevkoplyas, S. S. *Blood Transfus* **2016**, *14*, 80-88.

(9) Yoshida, T.; AuBuchon, J. P.; Dumont, L. J.; Gorham, J. D.; Gifford, S. C.; Foster, K. Y.; Bitensky, M. W. *Transfusion* **2008**, *48*, 2096-2105.

(10) Yoshida, T.; Blair, A.; D'Alessandro, A.; Nemkov, T.; Dioguardi, M.; Silliman, C. C.; Dunham, A. *Blood Transfus* **2017**, *15*, 172-181.

(11) Yoshida, T.; AuBuchon, J. P.; Tryzelaar, L.; Foster, K. Y.; Bitensky, M. W. *Vox Sang* **2007**, *92*, 22-31.

(12) D'Alessandro, A.; Gevi, F.; Zolla, L. *Mol Biosyst* **2013**, *9*, 1196-1209.

(13) Administration, U. F. a. D., Ed., 2013.

(14) Dumont, L. J.; Cancelas, J. A.; Maes, L. A.; Rugg, N.; Whitley, P.; Herschel, L.; Siegal, A. H.; Szczepiorkowski, Z. M.; Hess, J. R.; Zia, M. *Transfusion* **2015**, *55*, 485-490.

(15) Cancelas, J. A.; Dumont, L. J.; Maes, L. A.; Rugg, N.; Herschel, L.; Whitley, P. H.; Szczepiokowski, Z. M.; Siegel, A. H.; Hess, J. R.; Zia, M. *Transfusion* **2015**, *55*, 491-498.

(16) Meryman, H. T.; Hornblower, M.; Keegan, T.; Syring, R.; Heaton, A.; Mesbah-Karimi, N.; Bross, J. *Vox Sang* **1991**, *60*, 88-98.

(17) Meryman, H. T.; Hornblower, M. *Vox Sang* **1991**, *60*, 99-104.

(18) Wang, Y.; Giebink, A.; Spence, D. M. *Integr Biol (Camb)* **2014**, *6*, 65-75.

(19) Liu, Y.; Chen, C.; Summers, S.; Medawala, W.; Spence, D. M. *Integr Biol (Camb)* **2015**, *7*, 534-543.

(20) Liu, Y. *DELIVERY OF A PANCREATIC BETA CELL-DERIVED HORMONE TO ERYTHROCYTES BY ALBUMIN AND DOWNSTREAM CELLULAR EFFECTS*. Michigan State University2015.

(21) Chen, C. *3D-PRINTED IN VITRO ANALYTICAL DEVICES FOR DIABETES THERAPEUTICS AND BLOOD BANKING STUDIES*. Michigan State University2015.

(22) McGarraugh, G. *Diabetes Technol Ther* **2009**, *11 Suppl 1*, S17-24.

(23) Hogman, C. F.; Meryman, H. T. *Transfusion* **2006**, *46*, 137-142.

(24) Hess, J. R.; Sparrow, R. L.; van der Meer, P. F.; Acker, J. P.; Cardigan, R. A.; Devine, D. V. *Transfusion* **2009**, *49*, 2599-2603.

(25) Somers, G.; Depoorter, I.; Sener, A.; Malaisse, W. J. *Diabetes Care* **1982**, *5*, 319-321.

(26) Aida, K.; Tawata, M.; Shindo, H.; Onaya, T. *Diabetes Care* **1990**, *13*, 461-467.

(27) McMillan, D. E.; Utterback, N. G.; La Puma, J. *Diabetes* **1978**, *27*, 895-901.

(28) Umeda, M.; Otsuka, Y.; Ii, T.; Matsuura, T.; Shibati, H.; Ota, H.; Sakurabayashi, I. *Ann Clin Biochem* **2001**, *38*, 701-707.

(29) Won, D. I.; Suh, J. S. *Cytometry B Clin Cytom* **2009**, *76*, 135-141.

(30) Abbas Meamarbashi, A. R. *Asian Journal of Experimental Biological Sciences* **2013**, *4*, 322-326.

(31) Bohlen, H. G.; Zhou, X.; Unthank, J. L.; Miller, S. J.; Bills, R. *Am J Physiol Heart Circ Physiol* **2009**, *297*, H1337-1346.

(32) Stamler, J. S.; Simon, D. I.; Osborne, J. A.; Mullins, M. E.; Jaraki, O.; Michel, T.; Singel, D. J.; Loscalzo, J. *Proc Natl Acad Sci U S A* **1992**, *89*, 444-448.

(33) Lundberg, J. O.; Weitzberg, E.; Gladwin, M. T. *Nat Rev Drug Discov* **2008**, *7*, 156-167.

(34) Gov, N.; Safran, S. A. *J Biol Phys* **2005**, *31*, 453-464.

(35) Kirby, B. S.; Hanna, G.; Hendargo, H. C.; McMahon, T. J. *Am J Physiol Heart Circ Physiol* **2014**, *307*, H1737-1744.

(36) Price, A. K.; Fischer, D. J.; Martin, R. S.; Spence, D. M. *Anal Chem* **2004**, *76*, 4849-4855.

(37) Edwards, J.; Sprung, R.; Sprague, R.; Spence, D. *Analyst* **2001**, *126*, 1257-1260.

(38) Erkal, J. L.; Selimovic, A.; Gross, B. C.; Lockwood, S. Y.; Walton, E. L.; McNamara, S.; Martin, R. S.; Spence, D. M. *Lab Chip* **2014**, *14*, 2023-2032.

(39) Raththagala, M.; Karunarathne, W.; Kryziniak, M.; McCracken, J.; Spence, D. M. *Eur J Pharmacol* **2010**, *645*, 32-38.

(40) Lockwood, S. Y.; Erkal, J. L.; Spence, D. M. *Nitric Oxide* **2014**, *38*, 1-7.

(41) Communi, D.; Raspe, E.; Pirotton, S.; Boeynaems, J. M. *Circ Res* **1995**, *76*, 191-198.

(42) Ignarro, L. J.; Byrns, R. E.; Wood, K. S. *Circulation Research* **1987**, *60*, 82-92.

(43) Carvajal, J. A.; Germain, A. M.; Huidobro-Toro, J. P.; Weiner, C. P. *Journal of Cellular Physiology* **2000**, *184*, 409-420.

(44) Sprague, R. S.; Stephenson, A. H.; Dimmitt, R. A.; Weintraub, N. L.; Branch, C. A.; McMurdo, L.; Lonigro, A. J. *Am J Physiol* **1995**, *269*, H1941-1948.

(45) Sprague, R. S.; Ellsworth, M. L.; Stephenson, A. H.; Lonigro, A. J. *Am J Physiol* **1996**, *271*, H2717-2722.

(46) Sprague, R. S.; Olearczyk, J. J.; Spence, D. M.; Stephenson, A. H.; Sprung, R. W.; Lonigro, A. J. *Am J Physiol Heart Circ Physiol* **2003**, *285*, H693-700.

(47) Kueng, A.; Kranz, C.; Mizaikoff, B. *Biosens Bioelectron* **2004**, *19*, 1301-1307.

(48) Spielmann, H.; Jacob-Muller, U.; Schulz, P. *Anal Biochem* **1981**, *113*, 172-178.

(49) Chen, C.; Wang, Y.; Lockwood, S. Y.; Spence, D. M. *Analyst* **2014**, *139*, 3219-3226.

(50) Carroll, J.; Raththagala, M.; Subasinghe, W.; Baguzis, S.; Oblak, T. D.; Root, P.; Spence, D. *Molecular Biosystems* **2006**, *2*, 305-311.

(51) Koch, C. G.; Li, L.; Sessler, D. I.; Figueroa, P.; Hoeltge, G. A.; Mihaljevic, T.; Blackstone, E. H. *N Engl J Med* **2008**, *358*, 1229-1239.

(52) Sanders, J.; Patel, S.; Cooper, J.; Berryman, J.; Farrar, D.; Mythen, M.; Montgomery, H. E. *Transfusion* **2011**, *51*, 2286-2294.

(53) Weinberg, J. A.; McGwin, G.; Griffin, R. L.; Huynh, V. Q.; Cherry, S. A.; Marques, M. B.; Reiff, D. A.; Kerby, J. D.; Rue, L. W. *J Trauma* **2008**, *65*, 279-282.

(54) Tinmouth, A.; Fergusson, D.; Yee, I. C.; Hebert, P. C.; Investigators, A.; Canadian Critical Care Trials, G. *Transfusion* **2006**, *46*, 2014-2027.

(55) Wang, Y. M.; Giebink, A.; Spence, D. M. *Integr Biol-Uk* **2014**, *6*, 65-75.

(56) Orlina, A. R.; Josephson, A. M. *Transfusion* **1969**, *9*, 62-69.

(57) Zuck, T. F.; Bensinger, T. A.; Peck, C. C.; Chillar, R. K.; Beutler, E.; Button, L. N.; McCurdy, P. R.; Josephson, A. M.; Greenwalt, T. J. *Transfusion* **1977**, *17*, 374-382.

(58) Hogman, C. F.; Hedlund, K.; Zetterstrom, H. *N Engl J Med* **1978**, *299*, 1377-1382.

(59) Malone, J. I.; Knox, G.; Benford, S.; Tedesco, T. A. *Diabetes* **1980**, *29*, 861-864.

(60) Hess, J. R. *Vox Sang* **2006**, *91*, 13-19.

(61) Bicalho, B.; Serrano, K.; Dos Santos Pereira, A.; Devine, D. V.; Acker, J. P. *Transfus Med Hemother* **2016**, *43*, 19-26.

(62) Sols, A.; Delafuente, G.; Villarpalasi, C.; Asensio, C. *Biochimica Et Biophysica Acta* **1958**, *30*, 92-101.

(63) Sands, J. M.; Schrader, D. C. *Journal of the American Society of Nephrology* **1991**, *2*, 212-218.

(64) Chen, C. P.; Wang, Y. M.; Lockwood, S. Y.; Spence, D. M. *Analyst* **2014**, *139*, 3219-3226.

(65) Lion, N.; Crettaz, D.; Rubin, O.; Tissot, J. D. *J Proteomics* **2010**, *73*, 374-385.

(66) Inoue, K.; Zhuang, L.; Ganapathy, V. *Biochem Biophys Res Commun* **2002**, *299*, 465-471.

(67) Gopal, E.; Miyauchi, S.; Martin, P. M.; Ananth, S.; Srinivas, S. R.; Smith, S. B.; Prasad, P. D.; Ganapathy, V. *Am J Physiol-Gastr L* **2007**, *292*, G402-G408.

(68) Allen, B. W.; Piantadosi, C. A. *Am J Physiol-Heart C* **2006**, *291*, H1507-H1512.

(69) Ellsworth, M. L. *Med Sci Sport Exer* **2004**, *36*, 35-41.

(70) Ellsworth, M. L.; Ellis, C. G.; Goldman, D.; Stephenson, A. H.; Dietrich, H. H.; Sprague, R. S. *Physiology* **2009**, *24*, 107-116.

(71) Subasinghe, W.; Spence, D. M. *Anal Chim Acta* **2008**, *618*, 227-233.

(72) Zhu, H. M.; Zennadi, R.; Xu, B. X.; Eu, J. P.; Torok, J. A.; Telen, M. J.; McMahon, T. J. *Critical Care Medicine* **2011**, *39*, 2478-2486.

Chapter 3 – Investigating the Feasibility of RBC Storage with Low Glucose Maintenance by an IV Piggyback System

3.1 Introduction

In the last chapter, three new versions of normoglycemic RBC collection and storage solutions were proposed. The effects of glucose on stored RBC properties were quantitatively investigated. The benefit of collecting and storing human RBCs under physiological levels of glucose has been highlighted. Specifically, using the modified blood storage solutions can help avoid the massive production of intracellular sorbitol during storage.

An apparent benefit from the low-glucose storage is that flow-induced ATP release from RBCs stored under normoglycemic conditions is maintained at levels comparable to that of fresh RBCs from healthy individuals throughout a five-week storage period. However, although the results in Chapter 2 seem promising, there are also two important issues that must be addressed prior to consideration of commercial use. First, to avoid bacteria contamination, the FDA does not allow the opening, closing, and reopening of blood bags during the storage period. Opening the bags and adding concentrated glucose saline solution to stored RBCs would not be an approved clinical method. Second, impaired ATP release from RBCs stored in hyperglycemic conditions was detected, but the mechanism behind this observation remains undetermined and a mode of action would probably be required for before widespread acceptance or investment by outside sources.

To overcome the first shortcoming (opening of the storage bag for feeding), a new method of blood banking is described that employs piggyback system similar to those

used in clinical settings to deliver a secondary solution (e.g., an antibiotic) to a saline or glucose drip prior to entering the patient's circulation. 3D-printed parts and PVC plastic will be used to create the blood bags. These new storage bags will allow minimal interference when adding glucose saline solution or taking out aliquots of sample to be analyzed. In addition to RBC storage, properties of the stored cells, such as cell deformability, will be quantitatively determined by a novel 3D-printed membrane based device. Shear stress is a major factor influencing cells under flow conditions and cellular deformation due to shear is capable of inducing ATP release. It is reasonable to hypothesize that the loss of cell deformability is a significant contributor to the observed decrease in RBC-derived ATP release from cells under storage.

The mechanical features of the RBC, especially cell deformability, are of great physiological and pathological significance. The importance of studying RBC deformability has been demonstrated in many other reports. For example, diabetic RBCs only have 50% of the relative deformability compared to healthy cells, which can induce insulin-dependent platelet aggregation.[1,2] The deformability of transfused RBCs is a potent effector of transfusion outcomes, and transfusing stored RBCs with decreased deformability can impede microvascular flow and result in complications and mortality.[3,4] Cell deformability is a critical component to over blood flow originating and flow resistance. For example, blood flows from the heart goes to the arteries, then to the arterioles and eventually the capillaries. The size of these blood vessels varies; for instance, the arteries have an inside diameter of about 25 mm, while the smallest capillaries only have a 5 μm channel for blood cells to pass through.[5-8] The diameter of a

mature RBC is approximately 6 – 8 μm, which is smaller than some capillaries. Thus, RBCs must change their shape when traversing through small size capillaries. Additionally, blood vessels are categorized as resistance vessels, where RBCs are subjected to shear stress as they pass through. RBCs experience a wide range of shear stress *in vivo,* which may result in a deformation of the cell. It has been experimentally observed that RBCs exhibit complicated dynamics, such as tumbling, tank-treading and swinging, under steady shear stress.[9-11] Deformation of cells can further induce the release of ATP, which has been investigated theoretically and experimentally.[12-15]

There are at least three suggested mechanisms of ATP release from different cell types, including transporter-mediated release through ATP-binding cassette (ABC) transporters, channel-mediated release and exocytosis-mediated release.[16] Since RBCs do not contain organelles such as the Golgi complex, the study of deformation-induced ATP release from RBCs focuses on the transporter-mediated and channel-mediated pathways.

One signal transduction pathway was proposed by Sprague *et al.*, as shown in Figure 3.1. It begins with a series of conformational changes in the G-protein coupled receptor (GPCR) located on the cell membrane, caused by mechanical deformation of the RBC. The GPCR that binds to the heterotrimeric G proteins activate Gi/Gs,[17,18] which can trigger the adenylate cyclase (AC) enzyme to convert ATP to cyclic adenosine monophosphate (cAMP). The production of cAMP will lead to the phosphorylation of the cystic fibrosis transmembrane conductance regulator protein (CFTR) by protein kinase A (PKA). ATP is then thought to be released through an undetermined nucleoside transporter channel.[19,20] There is evidence showing that CFTR is involved in the process of

deformation-induced ATP release, but the exact role of CFTR is still under debate.[21] In the proposed mechanism described here, CFTR acts as a regulator for ATP release. However, other experimental works support that CFTR is the conductance channel through which ATP can be released.[16,22] There is a hypothesis that CFTR may play two roles in the ATP release process, both as a regulator and transport channel.[23] Other possible channels that ATP may travel through are Pannexin 1 hemichannel, connexin 43 hemichannels, and the purinergic receptor P2X7.[24-29]

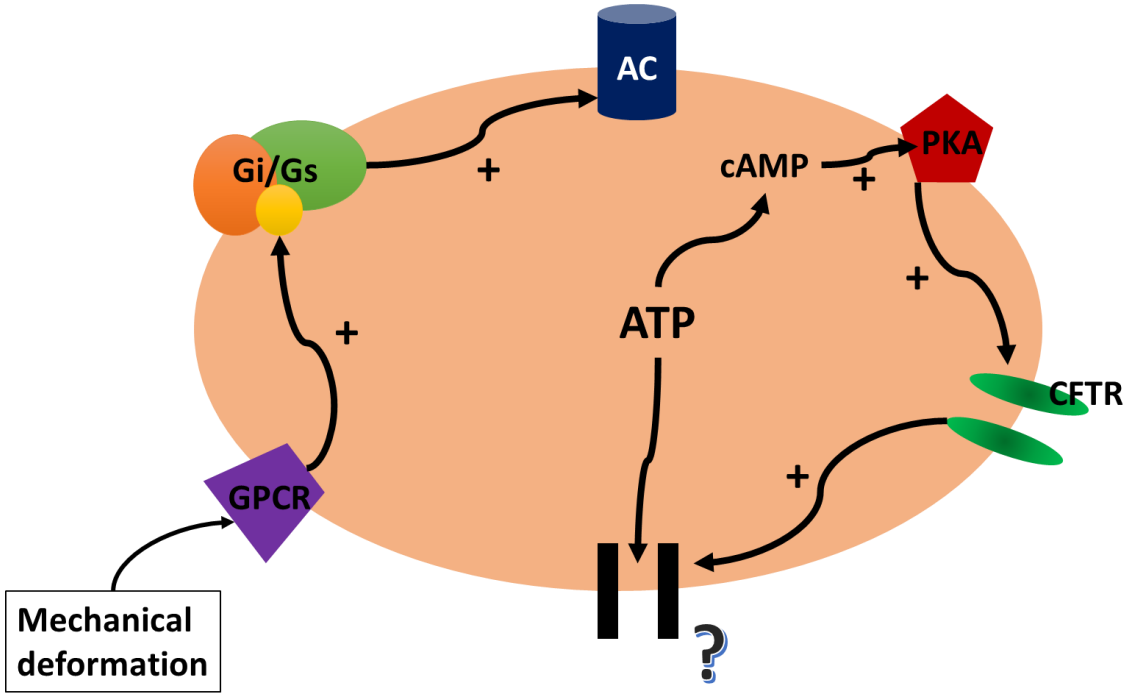

Figure 3.1 – The mechanism of deformation-induced stimulation of ATP release. The process is started by mechanical deformation of a G-protein coupled receptor (GPCR) on the cell membrane, which binds to and activates heterotrimeric G proteins, Gi/Gs. Then, G proteins will activate adenylate cyclase (AC) to produce cyclic adenosine monophosphate (cAMP) through activation of protein kinase A (PKA). This will result in the cystic fibrosis transmembrane conductance regulator protein (CFTR) to become phosphorylated and regulate ATP release through one or more undetermined channels. Two candidates of ATP release avenue are CFTR and Pannexin 1 hemichannel.

Information on cell deformability, a key component in the mechanical deformation-induced activation of G-proteins, can be obtained through multiple advanced analytical methods. For instance, accurate deformability measurement of individual cells can be performed by micropipette aspiration, atomic force microscopy (AFM), optical tweezers, magnetic twisting cytometry, quantitative phase imaging and dynamic light scattering.[30-34] Additionally, filtration methods, microfluidic filtration, and erythrocyte shape recovery are popular approaches for deformability measurements of multiple cells.[35-37] Among them, the filtration method is the most widely used technique because of the simplicity of its components and operating principle.[35]

The filtration method was the first method used for measuring RBC deformability. This approach is based on the ability of cells to pass through membrane filters that have pore sizes less than 6 μm (3 – 5 μm usually). The blood is passed through the holes in a membrane filter by applying positive or negative pressure. Quantification of the deformability can be achieved by measuring the time required to pass a certain volume of RBCs, the number of RBCs passing through within a fixed time, or a pressure-flow relationship. In this thesis, deformability measurements of stored RBCs were accomplished by counting the number of cells passed through a 3 μm polycarbonate membrane in a fixed time period. To facilitate these studies, an in-house device was made using 3D-printing technologies.

The benefits of employing 3D-printing techniques in biomedical engineering research have been demonstrated by our group in the utilization of detecting flow-induced ATP release.[38] Here, it was applied to the manufacturing of new blood storage bags and

creating a membrane based deformability device. The CAD software allows an application-orientated design. The semi-transparent material allows the flow of RBC suspensions to be visualized. The ruggedness of the material enables multiple usage of the device in a long term study. The combination of different materials generates broader applications. These advantages will be highlighted below.

3.2 Experimental

3.2.1 Storing RBCs in Newly Developed Bags

All reagents were purchased from Sigma-Aldrich (St. Louis, MO, USA) unless otherwise indicated. All syringes and needles were purchased from BD (Franklin Lakes, NJ, USA). The miniaturized blood collection and storage process is similar to that described in Section 2.2.1 with exceptions. It is the same as the previous storage method until adding AS to packed RBCs. After addition of AS, the RBC samples were stored in the new blood storage bags shown in Figure 3.2, which were fabricated from PVC rolls and 3D-printed parts.

The 3D-printing file was created in Autodesk Inventor 2014 (Autodesk, San Rafael, CA). Solid white material (Verowhite) and black rubbery material (TangoBlack) were employed in the printing process. When drawing the device in the CAD software, white material parts and black material parts were created in separate .ipt files, which are the Inventor standard part files. The different material parts were then assembled in another .iam file, which is the Inventor standard assembly file. Finally, the .iam file is exported as multiple .STL files, selecting one file per part option. There would be multiple .STL files with assembly information generated in this case. The .STL files were zipped and sent to

the Objet Connex350 Multi Material 3D Printing System. In this way, the two different materials for one part of the device can be printed together.

The PVC plastic piece was fixed to the 3D-printed piece using double-side tape. The surface of the 3D-printed part that faces the inside of the bag was covered by a layer of PVC plastic to avoid stored RBCs touching printed material. Teflon tape and super glue were used to seal the top part of the bag where the 3D-printed part was placed. The other three sides of the bag were sealed by an impulse sealer. Prior to use, the manufactured bags were sterilized by 70% ethanol and overnight exposure to UV light.

RBC suspension in AS were transferred into the bags by use of 5 mL syringes with 1.5 inch 22-gauge needles. The whole bag was placed in the refrigerator, where the temperature is 4 °C. On the days when experiments were performed, 1 mL of stored RBC samples was removed from the storage bags using 1 mL syringes with 1.5 inch 22-gauge needles. Instead of sacrificing unused sample, the rest of the sample was placed back into the refrigerator for further use at a later time. Since the deformability study of RBCs stored in CPD/AS-1 and CPDN/AS-1N has been performed by the Spence group, RBCs were collected and stored in CP2D/AS-3, CPDN/AS-3N, CPD/AS-5 and CPDN/AS-5N in this study.[39] Because of the minimal amount of blood being collected, RBC samples were collected separately for the deformability and sorbitol study.

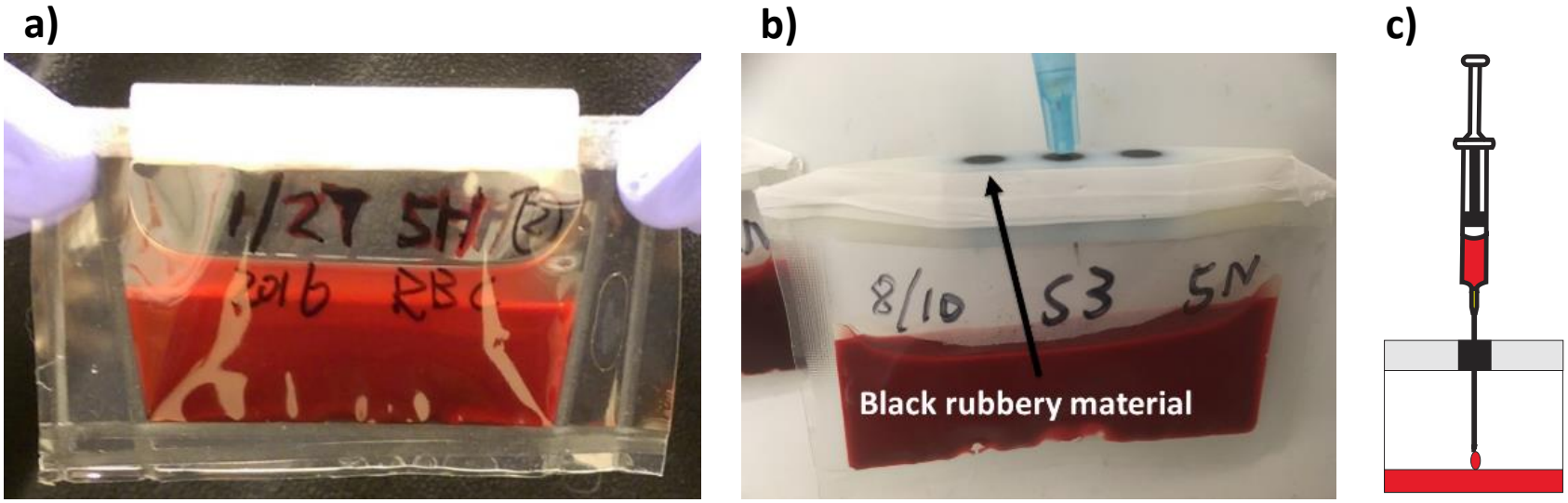

Figure 3.2 – New blood storage bags. a) A new blood storage bags with 5 mL RBC sample stored in CPD/AS-5. The bag contains two parts, a 3D-printed part and a PVC plastic part. Three sides of the bag were sealed by impulse sealer. The top part of the bag, where the two parts were attached, was sealed by double-side tape and Teflon tape; b) A picture of 5 mL RBC sample stored in CPDN/AS-5N with a needle punched through the 3D-printed part. Two different materials were used in the 3D printing process. One is a white solid material. The other one is a black rubbery material. The PVC plastic part was adhered to the white material. A needle can be inserted through the rubbery material, allowing concentrated glucose saline solution to be added to stored RBCs without opening bags; c) A schematic diagram of adding RBC sample into a blood bag. Utilizing the new blood storage bags, RBC samples were moved in or out from the bags using syringes. In this way, the process of opening, closing and reopening blood storage bags can be avoided.

3.2.2 The Creation of an IV-Piggyback Glucose Bag for Normoglycemic Cell Storage

The design and pictures of the piggyback bag system for storing RBCs under a normoglycemic environment is shown in Figure 3.3. The dimensions of the glucose reservoir and switch are illustrated in detail in Figure 3.3(a). The glucose reservoir was printed in white material, while the switch was printed in clear material. The switch was covered by a 1/2-inch layer of heat shrink tube (Insultab, Woburn, MA), and heated by a thermal blower at 200 °F. At this time, the channel in the switch was blocked by the heat shrink tube. To open the channel, holes were punched by using a steel wire heated by a propane torch. Vacuum grease was applied on the switch for better lubrication and sealing. Following that, the switch was inserted into the glucose reservoir part with an O-ring for controlling flow. The entire piggyback bag piece was connected to a 25-gauge needle by a Tygon tube. The sealing was achieved by applying Teflon tape and super glue. The needle can be used to penetrate through the rubbery material part on the blood bag. Glucose saline, 200 mM, was added into the glucose reservoir. The glucose reservoir was closed by a green rubbery cap (BD, Franklin Lakes, NJ, USA). When glucose was needed by the stored RBCs, the switch was turned to let concentrated glucose solution flow through the channel and needle into the bag. To stop the flow, the switch was simply turned back. All parts in this piggyback bag system were sterilized by autoclave and then 70% ethanol prior to use, with the exception of the Tygon tube, which was only decontaminated by ethanol. The whole set can be placed on the wall of the refrigerator, as shown in Figure 3.3.

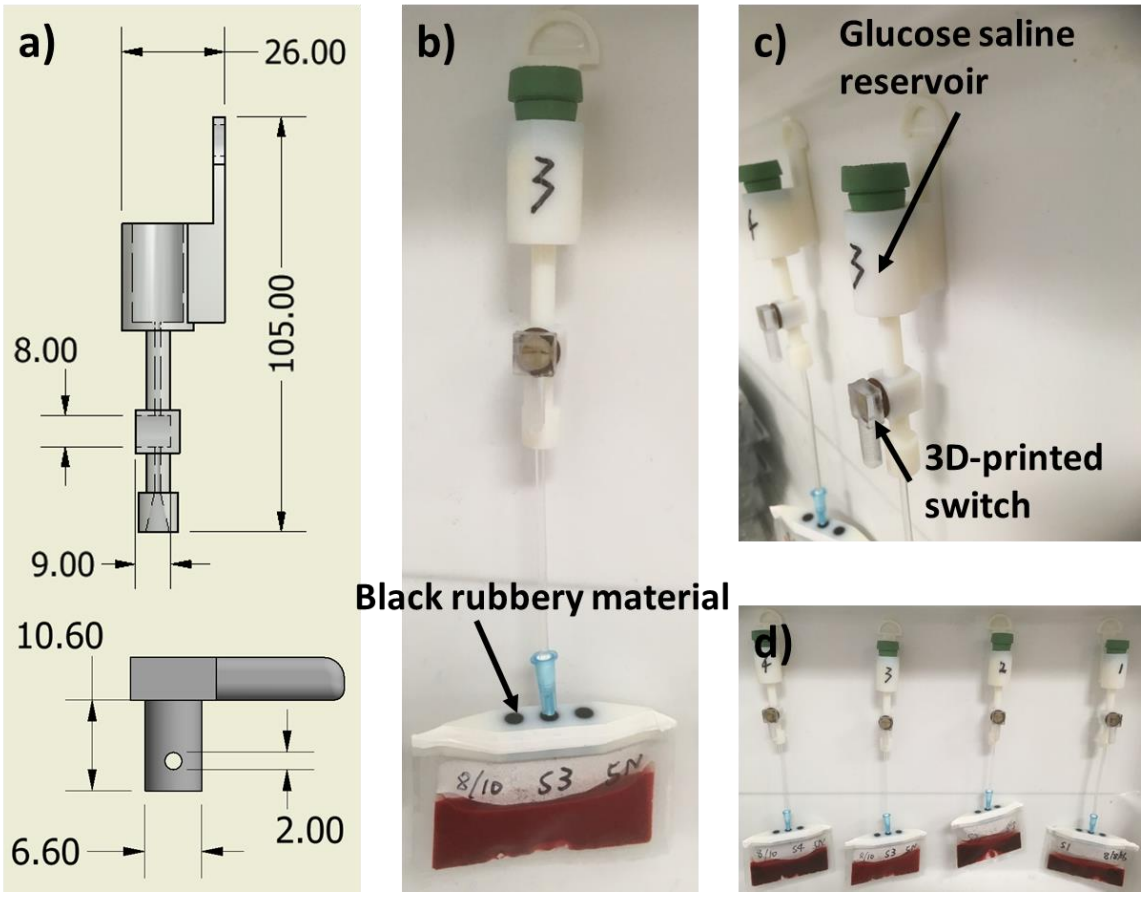

Figure 3.3 – Piggyback bag system for normoglycemic RBC storage. a) Engineering sketch of the glucose saline reservoir and switch with dimensions (mm); b) Storing RBCs under normal glucose levels using the piggyback bag system. The blood bag is connected to the 3D-printed piggyback bag by a Tygon tube and needle. The flow of glucose saline solution is controlled by the switch; c) A closer view of the 3D-printed glucose reservoir and switch. There is 2 mL of concentrated glucose saline solution in the container; d) Four sets of piggyback bag system fixed on the wall of a refrigerator. The blood samples were from four different donors.

Table 3.1 – Prediction of extracellular glucose concentration increment (mM)

Number of drops	RBC sample volume (mL)				
	5	4	3	2	1
1	0.25	0.31	0.41	0.62	1.24
2	0.50	0.62	0.83	1.24	2.48
3	0.74	0.93	1.24	1.86	3.72
4	0.99	1.24	1.65	2.48	4.96
5	1.24	1.55	2.07	3.10	6.20
6	1.49	1.86	2.48	3.72	7.44
7	1.74	2.17	2.89	4.34	8.68
8	1.98	2.48	3.31	4.96	9.92
9	2.23	2.79	3.72	5.58	11.16

3.2.3 Glucose Feeding Guideline

The glucose levels in the solution supernatant of RBCs stored in normoglycemic conditions were determined twice each week using a glucose meter to ensure the glucose concentration was within a normoglycemic range (4 – 6 mM). Concentrated glucose saline solution, 200 mM, was added to stored RBCs if the glucose level was close to or below 4 mM. The volume of glucose solution added was estimated by the number of drops. Each drop is approximately 6.20 μL. Table 3.1 provides a guide for feeding glucose to cells. It describes the correlation between the number of drops added with the prediction of extracellular glucose concentration increment, at different volume of RBC sample remaining in the blood bag.

3.2.4 The Design and Fabrication of 3D-printed Membrane Based Device

The 3D-printed device applied in this study is made of two different materials, a semi-transparent clear material (VeroClear) and a black rubbery material (TangoBlack). The assembly method for multiple materials, introduced in Section 3.2.1, was applied in the manufacturing of this deformability device. The idea behind this design is similar to the filtration device previously created in our group and was introduced in Figure 1.7. The membrane-based device consists of two parts, an upper part and a lower part. The dimensions of the two parts, both front view and side view, are shown in Figure 3.4. The projecting areas with black materials on the upper part of the device is the inserting part. While, there are hollow areas with black materials on the lower part of the device where the upper part can be inserted. The printed device was cleaned manually by using a tip

cleaner (HARRIS, Mason, OH, USA) to remove supporting material. Prior to use, the device was rinsed with DDW and dried at room temperature.

3.2.5 Determination of Cell Deformability

A physiological saline solution (PSS), which has a glucose concentration of 5.5 mM and a hyperglycemic version of PSS, which has a glucose concentration of 40 mM, were prepared. RBC samples (approximately 1 mL volumes) were obtained from storage bags using 1 mL syringes with 1.5 inch 22-gauge needles. Three different samples were prepared for deformability measurements. *S*amples were prepared from RBCs stored in normal glucose condition and suspended in normal PSS (labeled as "N" samples). *S*amples were also prepared from RBCs stored in high glucose condition and suspended in hyperglycemic PSS (H samples). Finally, samples were prepared from RBCs stored in high glucose conditions but suspended in normal PSS (HR samples). All RBC samples were washed using one of the PSS versions at least three times. The hematocrit of the samples was measured using a microhematocrit centrifuge (CritSpin, M960-22, Statspin) after the final wash. RBC suspensions with 5% hematocrit were prepared using their corresponding PSS for deformability determinations.

Polycarbonate membranes (Sterlitech, Kent, WA) with a 3 μm pore size were placed on the black materials on the lower part of the device after being wetted by PSS. Vacuum grease was applied on the side of the inserting part on the upper part of the device, while avoiding touching the black material areas. The two parts of the device were assembled tightly, fixed by six binder-clips. The device was rinsed by DDW prior to deformability measurements. RBC suspensions were loaded into 1 mL syringes in triplicate for each

different sample. Syringes were connected to the device using luer lock adapters and Tygon tubing. RBC samples were pumped through the membrane at 10 μL/min for 5 min, utilizing a syringe pump with a rack for multiple syringes (Chemyx, Stafford, TX). Cells passing through the membrane with PSS were collected into plastic tubes. The collection was further diluted 100-fold into PBS before cell counting using a flow cytometer (Accuri C6, BD Biosciences, San Jose, CA). The cell counting on the flow cytometer was accomplished by counting the cells in a fixed volume (10 μL). The density plots in generated during the flow cytometry measurement portion were gated at 600k – 1,600k for forward-scattered light (FSC) and 0 – 1,000k for side-scattered light (SSC), where the most RBCs were located. The device was cleaned by DDW and bleach after each experiment. The membranes were used once and replaced for every new experiment.

3.2.6 Measuring Hemolysis, Glucose and Sorbitol Levels

The determinations of hemolysis levels, glucose concentrations, and intracellular sorbitol accumulation were performed on the same day as the deformability measurements. The analytical methods for percent lysis and sorbitol concentration are described in detail in Sections 2.2.3 and 2.2.4. The glucose concentration in the solution supernatants was measured using a commercial glucose meter (Accu-Chek Aviva, Roche Diabetes Care, Inc. Indianapolis, IN). The measurements can be performed by simply inserting detection strips into the glucose meter and adding a small drop of blood sample on the tip of the strips. The results in mg/dL are reported after 5 seconds.

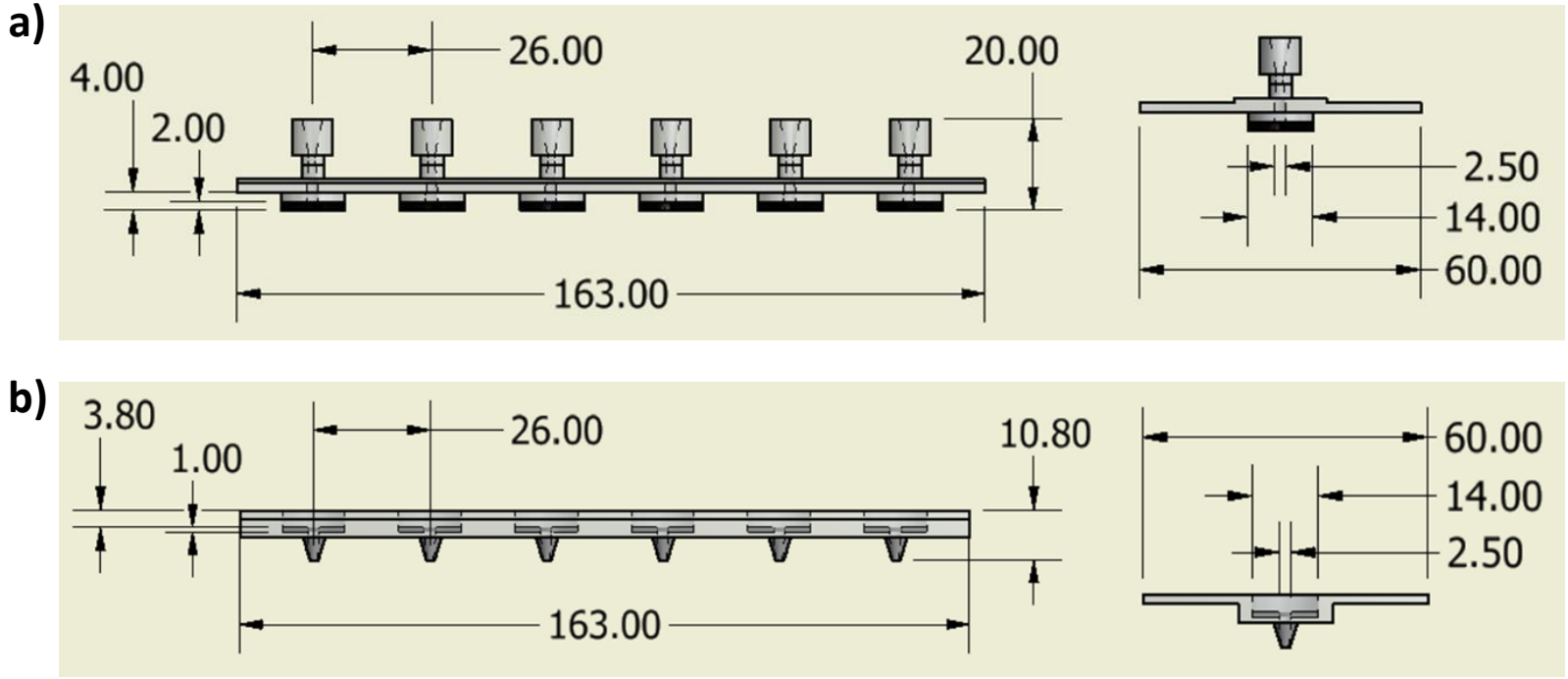

Figure 3.4 – The design of the membrane based deformability analysis device. a) Engineering sketch of the upper part of the device with dimensions (mm); b) Engineering sketch of the lower part of the device with dimensions. The printed device is composed of two different materials, a semi-transparent clear material and a black rubbery material. Polycarbonate membranes were placed on the black material areas. The two parts can be assembled together before deformability measurements. There are 6 ports on the device, enabling a high throughput deformability analysis. The diameter of the channels is 2.5 mm, which means the area of filtering RBCs is approximately 19.6 mm^2.

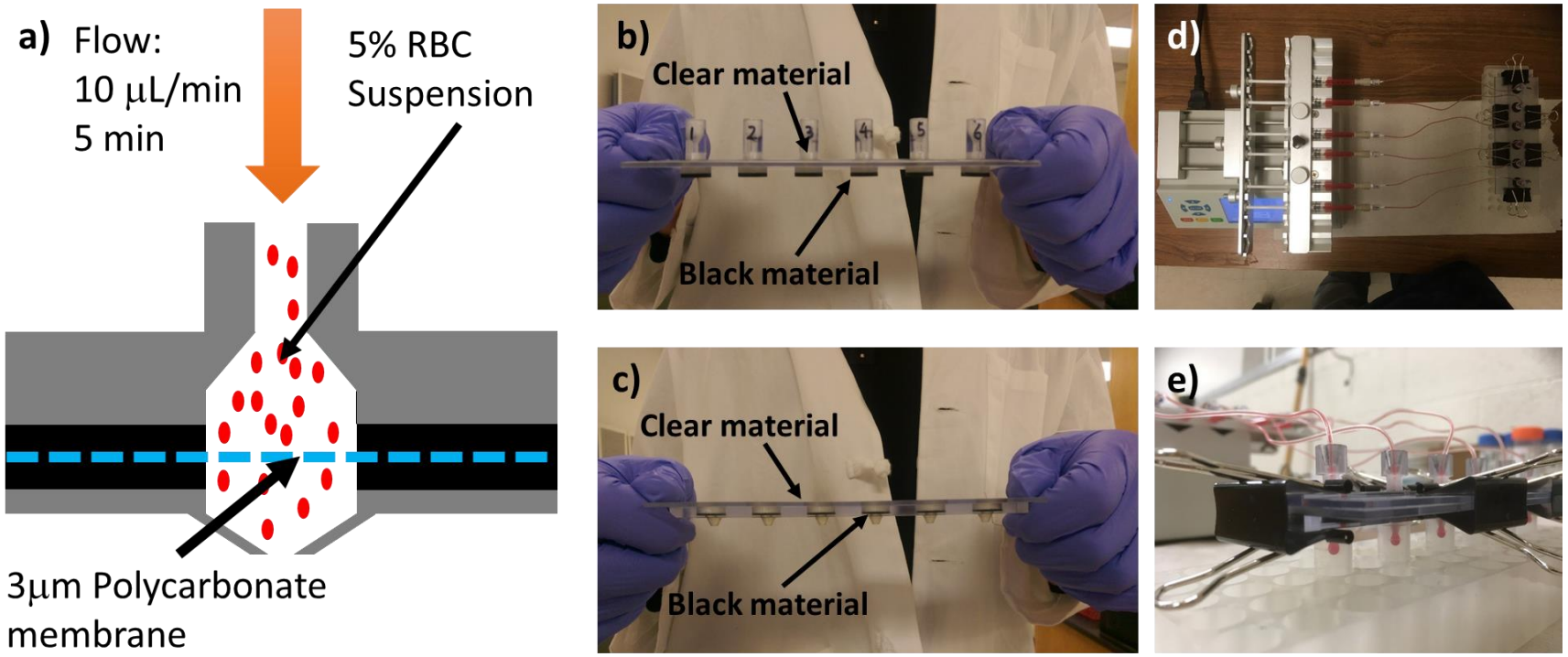

Figure 3.5 – The determination of cell deformability applying 3D-printed device. a) A schematic illustration of measuring RBC deformability by filtration method. Diluted RBC suspension is pumped through a polycarbonate membrane with a pore size smaller than the diameter of RBCs. More deformable cells will be able to pass the membrane, while less deformable cells will be blocked; b) and c) Pictures of the printed membrane based device using clear material and black material; d) High throughput RBC deformability analysis using a syringe pump and printed device; e) A close view of RBC suspensions passing through membranes and being collected in tubes.

3.3 Results

3.3.1 Quantification of Hemolysis, Glucose and Sorbitol Levels

The results from percent cell lysis determinations are shown in Figure 3.6. RBCs were stored for 4 weeks, and the hemolysis level was measured weekly. Black dots represent RBCs collected and stored in CPDN/AS-5N, while white dots represent RBCs processed using CPD/AS-5. The percent cell lysis is less than 1% throughout the storage period, which meets the FDA criteria for blood products. On day 28, the percentage of lysed cells is 0.54 ± 0.12% for normoglycemic storage and 0.56 ± 0.10 for hyperglycemic storage. There is no difference between the hyperglycemia and normoglycemia cell storage.

Figure 3.7 exhibits the glucose concentrations in the solution supernatant for RBCs stored in CPDN/AS-5N using piggyback bag system. The glucose level was monitored using a commercial glucose meter. It is well maintained at 4 – 6 mM, which is the healthy glucose level in the bloodstream, during a 28-day storage.

The bar graph in Figure 3.8 is the detection result of intracellular sorbitol accumulation. Black bars represent RBCs stored in the modified CPDN/AS-5N collection and storage solutions. White bars represent RBCs stored in FDA approved CPD/AS-5. The intracellular sorbitol concentration in fresh RBCs is 16.1 ± 2.0 nmol/g Hb, as reported in Chapter 2. Sorbitol production from RBCs stored in CPD/AS-5 is significantly higher than RBCs stored in CPDN/AS-5N throughout the 28-day storage period ($p < 0.05$). It exceeded 150 nmol/g Hb on the first day of storage (168.1 ± 12.1 nmol/g Hb), and was kept until the end of storage (145.3 ± 16.5 nmol/g Hb). For RBCs stored under normal glucose conditions, the sorbitol level increased slowly as a function of time. There is no statistical difference

between fresh blood and RBCs stored in CPDN/AS-5N on day 1 (19.5 ± 7.0 nmol/g Hb), day 7 (31.1 ± 7.6 nmol/g Hb) and day 14 (37.4 ± 9.9 nmol/g Hb).

3.3.2 Comparison of Cell Deformability

Results of RBC deformability and reversibility of deformation capacity measurements are shown in Figure 3.6. The results were demonstrated in the way of normalization, showing percentage in the y axis. For RBC samples from the same donor but different storage length and conditions, the number of cells passing through the membrane from RBCs stored in normoglycemia on day 1 was considered as 100% deformability, to which all other results were normalized. Black bars represent RBCs stored in normoglycemic condition, and suspended in normal PSS. Lighter grey bars represent RBCs stored in hyperglycemic condition, and suspended in high glucose PSS. Darker grey bar represent RBCs stored in hyperglycemic environment, but suspended in normal glucose level PSS. This process is trying to mimic a real blood transfusion situation, where the high concentration of glucose is diluted in patients' bloodstream.

RBCs stored in normal glucose level were able to keep their ability of deformation close to 100% throughout the 28-day storage time, showing no statistical difference between day 1 and day 28 (CPDN/AS-3N: 96.01 ± 2.98%; CPDN/AS-5N: 95.97 ± 2.78%). For hyperglycemia RBC storage, cells lost their deformability on the first day of storage (CP2D/AS-3: 82.14 ± 4.19%; CPD/AS-5: 82.88 ± 6.06%). The loss of deformability was continued until the end of storage (CP2D/AS-3: 81.58 ± 3.76%; CPD/AS-5: 87.46 ± 0.60%). There are significant differences between the black bars and lighter grey bars from day 1 to day 28 ($p < 0.05$). When cells were stored in high glucose environment but suspended

back into normal glucose condition, there is a clear trend of deformability decreasing as a function of storage length. For RBCs stored in both CP2D/AS-3 and CPD/AS-5 on day 1, their deformability can be reversed back to a healthy level (CP2D/AS-3: 100.66 ± 2.10%; CPD/AS-5: 105.61 ± 4.51%). On day 7, they still can be reversed (CP2D/AS-3: 94.41 ± 3.55%; CPD/AS-5: 98.62 ± 3.93%), but there is no statistical difference between the high glucose bar and reverse bar for RBCs stored in CPD/AS-5. However, starting from day 14, RBCs stored in CPD/AS-5 tend to lose all their ability to reverse (91.61 ± 4.90%). The same difference was observed on day 21 when RBCs were stored in CP2D/AS-3 (86.58 ± 3.78%).

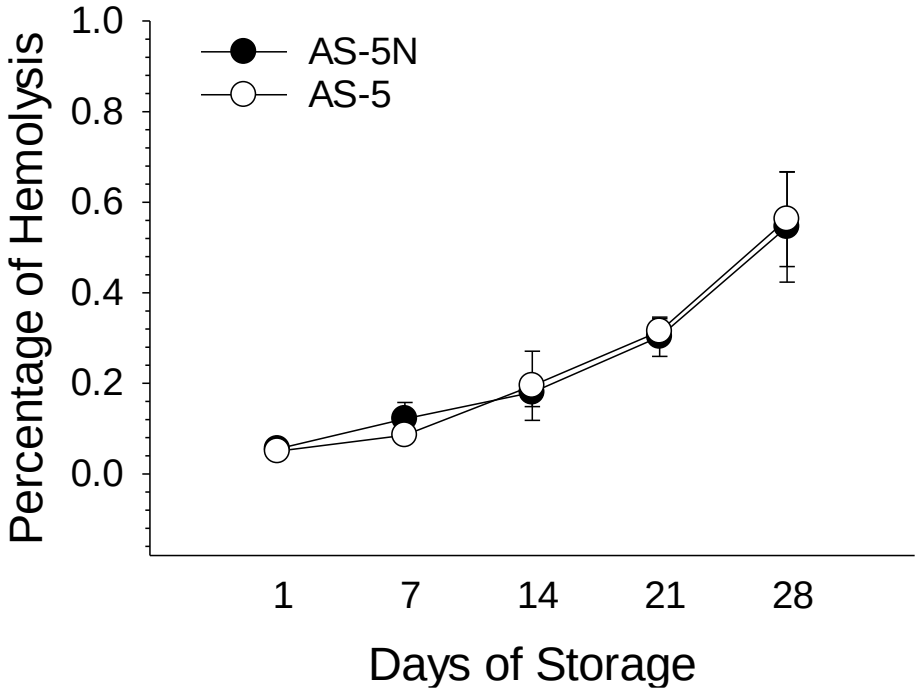

Figure 3.6 – Hemolysis level of RBC stored in new blood bags. Black dots represent RBCs collected and stored in CPDN/AS-5N, which has physiological level of glucose. White dots represent RBCs processed using CPD/AS-5, which is the standard high glucose storage solution. RBCs were stored for 4 weeks in this study. The percent cell lysis is less than 0.8% throughout the storage period, which meets the FDA criteria for blood products. There is no difference between the hyperglycemia and normoglycemia cell storage. Data represents mean ± s.e.m. (n = 4 humans for all).

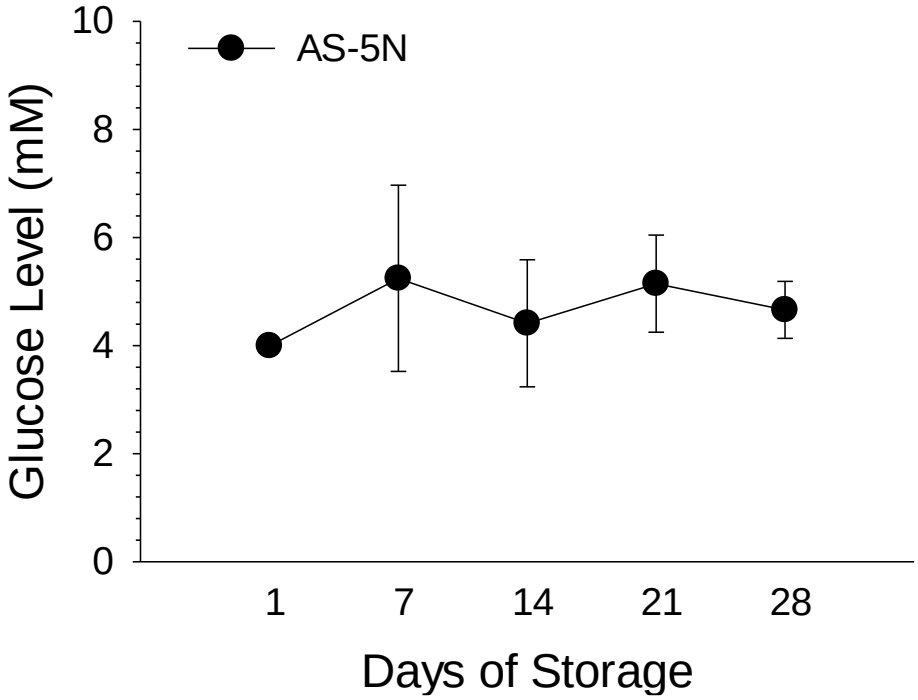

Figure 3.7 – Extracellular glucose concentration of storing RBCs using piggyback bag system. The glucose concentration in the solution supernatants was detected by a commercial glucose meter. It was well maintained at 4 – 6 mM, which is the healthy glucose level in bloodstream, during a 28-day storage. A successful controlling of the extracellular glucose level can be achieved by using the piggyback bag system. Data represents mean ± s.e.m. (n = 4 humans for all).

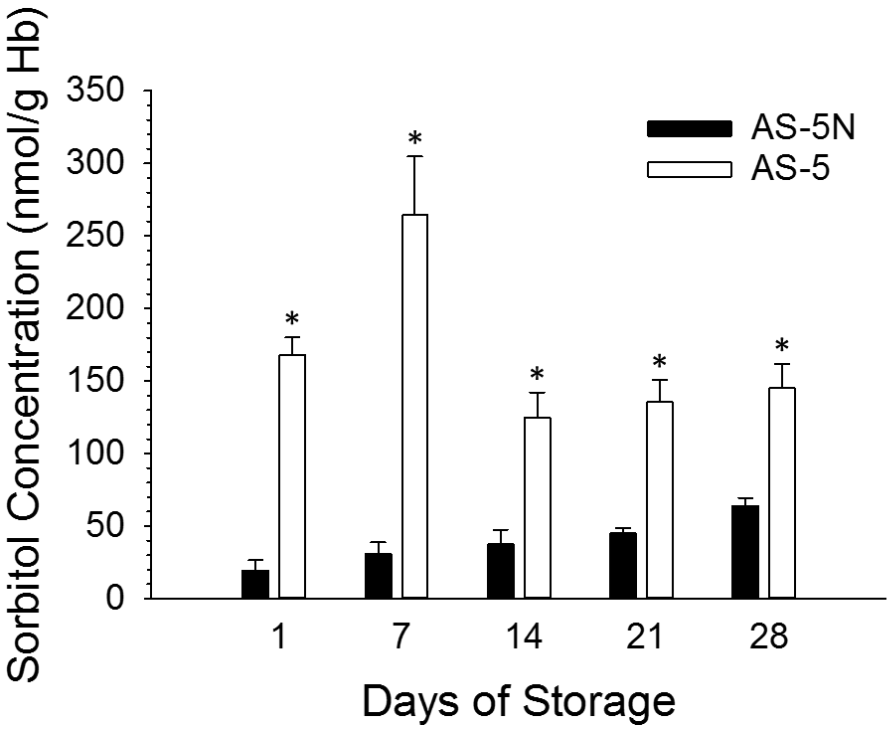

Figure 3.8 – Sorbitol accumulation in stored RBCs. Black bars represent RBCs stored in the modified CPDN/AS-5N collection and storage solutions. White bars represent RBCs stored in FDA approved CPD/AS-5. Sorbitol production in RBCs stored in the high glucose environment is significantly higher than RBCs stored in the normal glucose condition, from the first day of storage. There is a slow increment of sorbitol concentration as a function of time, when cells were stored in CPDN/AS-5N. Data represents mean ± s.e.m. (*$p < 0.05$, n = 5 humans for all).

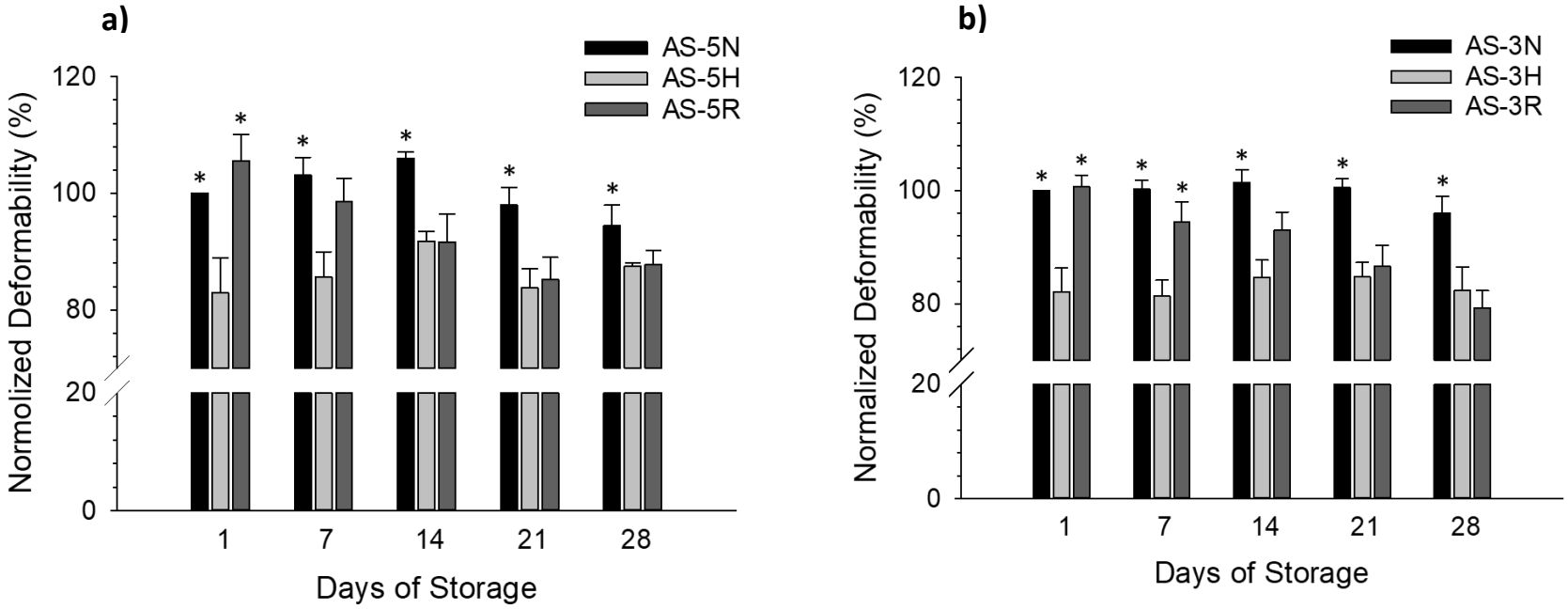

Figure 3.9 – Deformability measurements of stored RBCs. Black bars represent RBCs stored in normoglycemic conditions, and suspended in normal PSS. Lighter grey bars represent RBCs stored in hyperglycemic conditions, and suspended in high glucose PSS. Darker grey bar represent RBCs stored in hyperglycemic conditions, but suspended in normal glucose level PSS. This process is trying to mimic a real blood transfusion situation, where the high concentration of glucose is diluted in patients' bloodstream. All results from deformability measurements were normalized to the result from cells stored in normoglycemia on day 1. RBCs stored in hyperglycemic environments lost 10 – 20% of their deformability from the first day of storage. However, cell deformability can be maintained close to 100% when the modified storage solutions were utilized. Moreover, RBCs stored in standard storage solutions lost their reversibility of deformability after two weeks of storage. Data represents mean ± s.e.m. (*$p < 0.05$ when compared to the lighter grey bar, n = 4 humans for all).

3.4 Discussion

In this chapter, a new version of a miniaturized blood bag was created using 3D printing techniques. RBC suspensions in AS were successfully stored in the recently developed bags. The purpose of combining 3D-printed parts with PVC plastic is to avoid opening the bags during the storage, when obtaining samples for analysis each week. The black rubbery material on the 3D-printed parts allows the use of syringes to transfer RBC samples in and out from the bags, as shown in Figure 3.2 b) and c). Previously, in Chapter 2, samples were stored in several bags, and one bag was opened each week. Using different bags may induce variations for analytical study, especially for cells stored in normoglycemic conditions, because it is highly challenging to guarantee that RBCs in different bags are exposed to the exact same concentration of glucose. But using the newly developed bags, RBC samples from the same donor, following the same processing procedures, can be stored in one bag.

In the clinical field, a piggyback bag is a 50 to 150 mL small bag containing medications, such as antibiotic, electrolyte or steroid. It is usually plugged into a patient's existing intravenous administration system. Here, applying the piggyback bag concept, a new method of maintaining glucose level of RBCs stored in normal glucose environments was invented. The glucose reservoir and switch were produced by 3D printing. Because the printed material is not smooth enough to prevent leakage, the switch was covered by a layer of PVC heat shrink tube. Successful liquid sealing was achieved after covering the PVC tube and applying vacuum grease. The blood bags with rubbery material also allow for adding glucose saline to stored RBCs without opening and reclosing bags. The blood

bag is connected to the 3D-printed piggyback bag by a Tygon tube and needle, as shown in Figure 3.3 b). The whole set of normoglycemic blood storage, placed on the wall of a refrigerator, enables controlling glucose concentration in stored RBCs with minimal temperature changes. RBCs collected in CPD/AS-5 and CPDN/AS-5N were successfully stored for 28 days utilizing the piggyback bag system and latest version of miniaturized blood storage bag.

Several *in vitro* cell analyses were performed to evaluate the new method of blood storage and further investigate the benefits of normoglycemia RBC storage. Hemolysis level was determined weekly in this study to ensure the quality of blood products. As shown in Figure 3.6, the percent cell lysis is less than 1% throughout the storage period, which meets the FDA requirement for blood products. There is no difference between the hyperglycemia and normoglycemia cell storage. The glucose concentration in normoglycemic RBCs storage was monitored every week, and the results are shown in Figure 3.7. The glucose level was well maintained at 4 – 6 mM, which is the healthy glucose level in the bloodstream. This result highly suggests that a successful controlling of the extracellular glucose level can be achieved by using the piggyback bag system. In addition, the usage of a commercialized glucose detector in this study allows fast analysis and minimal amount of sample consumption.

Since there is a new miniaturized blood storage method, intracellular sorbitol accumulation, which has been discovered in Chapter 2, was measured again. As shown in Figure 3.8, there is a significant difference in sorbitol concentration between RBCs stored in high glucose conditions and normal glucose conditions throughout the whole storage

period ($p < 0.05$). Sorbitol results from RBCs stored in CPDN/AS-5N show no difference to fresh blood control within the first two weeks of storage. There is a slow increment of sorbitol concentration as a function of storage length, which is primarily due to the acidic storage environment discussed in Chapter 2 before. However, when RBCs were stored in hyperglycemic conditions, the sorbitol level is close to 150 nmol/g Hb from the beginning to the end of storage. When considered with the results from Section 2.3.3, it is reasonable to state that the massive production of intracellular sorbitol is due to the excess amount of glucose. Notably, in Figure 2.11, there is a significant increase of sorbitol concentration from day 7 to day 14 for RBCs stored in hyperglycemic conditions. This difference is not observed in Figure 3.8. The elements behind are still under investigation. More importantly, this work further proves that high concentration of glucose in stored RBCs will induce massive production of sorbitol, which may cause adverse effects to cells, such as loss of deformability.

Previously in Chapter 2, RBC-derived ATP release under flow conditions was studied. Mechanical deformation of cells was considered to be the main contributor to the release of ATP. The importance of studying RBC deformability has been demonstrated by multiple outstanding works.[1-4,40-42] Here, stored RBC deformability was analyzed by the filtration method. Although the filtration method has several drawbacks, including variation in pore size and potential occlusion of pores, it was chosen because it is cost effective and simple to perform. A membrane based device was manufactured by 3D printing techniques for filtering RBCs through a polycarbonate membrane.

There are several dimensions shown in Figure 3.4 that need to be noted. The length, width, and positions of ports are identical. This allows the two parts matching each other to be easily assembled together. Polycarbonate membranes can be placed on the black material areas. The diameter of the circle shape rubbery area is 14 mm, which is slightly larger than the diameter of the membrane, 13mm. The membrane can be placed at the center of the black material area easily. The diameter of the channels is 2.5 mm, which means the area of filtering RBCs is approximately 19.6 mm^2. There are 6 ports on the device, allowing simultaneous cell deformability studies. Notably, at the bottom of the upper part, there are 2 mm of clear material and 2 mm of black material, which means there are 4 mm of projecting areas that can be inserted into the lower part of the device when assembling. Meanwhile, at the hollows of the lower part, there are only 3.8 mm space with 1 mm black material. The 0.2 mm room is left for placing membranes. More importantly, the 0.2 mm difference allows the membranes to be sealed between black materials, preventing leakage. Figure 3.5 shows the pictures of the printed device and deformability measurement. Compared to the previous deformability experiments performed in our group, high-throughput cell analysis was achieved by printing 6 ports on the device. Additionally, instead of using a peristaltic pump, a more accurate and stable syringe pump was applied in this study. Moreover, the semi-transparent clear material allows visualizing of the flow of RBC suspensions.

The results of determining stored RBC deformability are shown in Figure 3.9. In order to further illustrate the feasibility of the printed device, RBCs stored in CP2D/AS-3 and CPDN/AS-3N were employed. The results from both bar graphs show similar trend. RBCs

stored in normoglycemia are able to keep their deformation ability close to 100% during the 4 weeks of cold storage, showing no statistical difference between day 1 and day 28. However, 15 – 20% of deformability was lost on the first day of storage when cells are exposed to high concentrations of glucose. For the reversibility study, there is a trend of decreasing deformability of stored RBCs, which means cells are losing their reversibility as the duration of storage increases. Interestingly, RBCs stored in high glucose conditions tend to lose their ability to reverse their deformability back to normal level after two weeks' mark. Taking into consideration previous works from the Spence group and other clinical retrospective studies, two weeks shelf life might be a turnover point for blood products' quality.[39,43-46] When comparing Figure 3.9 a) and b), RBCs stored in CP2D/AS-3 tend to lose more deformability to RBCs stored in CPD/AS-5, although there is no statistical significance. This observation indicates that the loss of deformability is positively correlated to the extracellular glucose level, since the glucose concentration in C2PD/AS-3 is higher than CPD/AS-5 (Figure 2.9).

The deformability study here provides an explanation for the ATP results in Chapter 2. The loss of cell deformation capacity is a main mechanism causing the decrease in ATP release from stored RBCs under flow condition. Although the elements developing the loss of deformability remain unknown, a possible interpretation is proposed. The massive produced intracellular sorbitol, resulting from the high glucose environment, causes the cells to suffer from oxidative stress. Those reactive oxygen species may react with lipids and skeleton proteins that are responsible for cell deformation on the cell membrane.

The glycation or oxidation products might induce cell membrane malfunction, resulting in loss of deformability.

3.5 Conclusion

In this chapter, a new method of miniaturized blood storage was developed. Applying 3D printing techniques, a new blood bag and piggyback back system were manufactured. The new method allows transferring blood samples and feeding glucose saline without opening and reclosing bags. This feature is essential for applying for an FDA license for normoglycemic RBC storage in the future, since blood bags cannot be opened during the storage to avoid bacteria contamination. Multiple cell properties were analyzed for RBCs stored in new blood bags. Results from hemolysis measurements indicate that the piggyback bag system for RBC storage has great potential to follow the FDA criteria. The glucose level in blood bags can be controlled within physiological levels using the piggyback glucose bags. Additionally, RBC deformability was quantified by a 3D-printed membrane based device. RBCs stored in normal glucose environments are able keep their deformability, while RBCs stored in high glucose environments tend to lose their deformability throughout the whole storage period. Notably, RBCs exposed to high concentrations of glucose lose their ability to reverse back to normal after two weeks. One possible contributor to the loss of deformability is the extensive production of intracellular sorbitol. 3D printing techniques were applied several times here, including the producing of blood bags, piggyback bags, and the deformability device. The assembly feature in the CAD software allows printing two different material on one part. Customer

oriented design enables realizing researchers' creative ideas quickly and cost effectively. 3D printing can be, and will be an extremely functional tool for analytical chemistry.

REFERENCES

REFERENCES

(1) McMillan, D. E.; Utterback, N. G.; La Puma, J. *Diabetes* **1978**, *27*, 895-901.

(2) Vague, P.; Juhan, I. *Diabetes* **1983**, *32 Suppl 2*, 88-91.

(3) Ho, J.; Sibbald, W. J.; Chin-Yee, I. H. *Crit Care Med* **2003**, *31*, S687-697.

(4) Barshtein, G.; Pries, A. R.; Goldschmidt, N.; Zukerman, A.; Orbach, A.; Zelig, O.; Arbell, D.; Yedgar, S. *Microcirculation* **2016**, *23*, 479-486.

(5) Mao, S. S.; Ahmadi, N.; Shah, B.; Beckmann, D.; Chen, A.; Ngo, L.; Flores, F. R.; Gao, Y. L.; Budoff, M. J. *Acad Radiol* **2008**, *15*, 827-834.

(6) Kwon, K. Y.; Park, K. K.; Chang, E. S. *J Korean Med Sci* **1991**, *6*, 234-245.

(7) Guntheroth, W. G.; Luchtel, D. L.; Kawabori, I. *Chest* **1992**, *101*, 1131-1134.

(8) Glazier, J. B.; Hughes, J. M.; Maloney, J. E.; West, J. B. *J Appl Physiol* **1969**, *26*, 65-76.

(9) Fischer, T. M.; Haest, C. W.; Stohr-Liesen, M.; Schmid-Schonbein, H.; Skalak, R. *Biophys J* **1981**, *34*, 409-422.

(10) Abkarian, M.; Faivre, M.; Viallat, A. *Phys Rev Lett* **2007**, *98*, 188302.

(11) Noguchi, H. *Phys Rev E Stat Nonlin Soft Matter Phys* **2009**, *80*, 021902.

(12) Wan, J.; Ristenpart, W. D.; Stone, H. A. *Proc Natl Acad Sci U S A* **2008**, *105*, 16432-16437.

(13) Gov, N. S.; Safran, S. A. *Biophys J* **2005**, *88*, 1859-1874.

(14) Fischer, D. J.; Torrence, N. J.; Sprung, R. J.; Spence, D. M. *Analyst* **2003**, *128*, 1163-1168.

(15) Price, A. K.; Fischer, D. J.; Martin, R. S.; Spence, D. M. *Anal Chem* **2004**, *76*, 4849-4855.

(16) Sabirov, R. Z.; Okada, Y. *Purinergic Signal* **2005**, *1*, 311-328.

(17) Olearczyk, J. J.; Stephenson, A. H.; Lonigro, A. J.; Sprague, R. S. *Am J Physiol-Heart C* **2004**, *286*, H940-H945.

(18) Olearczyk, J. J.; Stephenson, A. H.; Lonigro, A. J.; Sprague, R. S. *Med Sci Monit* **2001**, *7*, 669-674.

(19) Sprague, R. S.; Ellsworth, M. L.; Stephenson, A. H.; Lonigro, A. J. *Am J Physiol-Cell Ph* **2001**, *281*, C1158-C1164.

(20) Sprague, R. S.; Ellsworth, M. L.; Stephenson, A. H.; Kleinhenz, M. E.; Lonigro, A. J. *Am J Physiol-Heart C* **1998**, *275*, H1726-H1732.

(21) Sprague, R. S.; Ellsworth, M. L.; Stephenson, A. H.; Kleinhenz, M. E.; Lonigro, A. J. *Am J Physiol* **1998**, *275*, H1726-1732.

(22) Linsdell, P.; Evagelidis, A.; Hanrahan, J. W. *Biophys J* **2000**, *78*, 2973-2982.

(23) Schwiebert, E. M. *Am J Physiol* **1999**, *276*, C1-8.

(24) Locovei, S.; Bao, L.; Dahl, G. *Proc Natl Acad Sci U S A* **2006**, *103*, 7655-7659.

(25) Cotrina, M. L.; Lin, J. H.; Alves-Rodrigues, A.; Liu, S.; Li, J.; Azmi-Ghadimi, H.; Kang, J.; Naus, C. C.; Nedergaard, M. *Proc Natl Acad Sci U S A* **1998**, *95*, 15735-15740.

(26) Parpura, V.; Scemes, E.; Spray, D. C. *Neurochem Int* **2004**, *45*, 259-264.

(27) Forsyth, A. M.; Wan, J.; Owrutsky, P. D.; Abkarian, M.; Stone, H. A. *Proc Natl Acad Sci U S A* **2011**, *108*, 10986-10991.

(28) Liu, H. T.; Sabirov, R. Z.; Okada, Y. *Purinergic Signal* **2008**, *4*, 147-154.

(29) Sridharan, M.; Adderley, S. P.; Bowles, E. A.; Egan, T. M.; Stephenson, A. H.; Ellsworth, M. L.; Sprague, R. S. *Am J Physiol Heart Circ Physiol* **2010**, *299*, H1146-1152.

(30) Evans, E. A.; La Celle, P. L. *Blood* **1975**, *45*, 29-43.

(31) Kamruzzahan, A. S.; Kienberger, F.; Stroh, C. M.; Berg, J.; Huss, R.; Ebner, A.; Zhu, R.; Rankl, C.; Gruber, H. J.; Hinterdorfer, P. *Biol Chem* **2004**, *385*, 955-960.

(32) Svoboda, K.; Block, S. M. *Annu Rev Biophys Biomol Struct* **1994**, *23*, 247-285.

(33) Puig-de-Morales-Marinkovic, M.; Turner, K. T.; Butler, J. P.; Fredberg, J. J.; Suresh, S. *Am J Physiol Cell Physiol* **2007**, *293*, C597-605.

(34) Park, Y.; Best-Popescu, C. A.; Dasari, R. R.; Popescu, G. *J Biomed Opt* **2011**, *16*, 011013.

(35) Reid, H. L.; Barnes, A. J.; Lock, P. J.; Dormandy, J. A.; Dormandy, T. L. *J Clin Pathol* **1976**, *29*, 855-858.

(36) Wang, R.; Ding, H.; Mir, M.; Tangella, K.; Popescu, G. *Biomed Opt Express* **2011**, *2*, 485-490.

(37) Dobbe, J. G.; Streekstra, G. J.; Strackee, J.; Rutten, M. C.; Stijnen, J. M.; Grimbergen, C. A. *IEEE Trans Biomed Eng* **2003**, *50*, 97-106.

(38) Chen, C.; Wang, Y.; Lockwood, S. Y.; Spence, D. M. *Analyst* **2014**, *139*, 3219-3226.

(39) Chen, C. *3D-PRINTED IN VITRO ANALYTICAL DEVICES FOR DIABETES THERAPEUTICS AND BLOOD BANKING STUDIES*. Michigan State University2016.

(40) Wan, J.; Forsyth, A. M.; Stone, H. A. *Integr Biol (Camb)* **2011**, *3*, 972-981.

(41) van der Heyde, H. C.; Nolan, J.; Combes, V.; Gramaglia, I.; Grau, G. E. *Trends Parasitol* **2006**, *22*, 503-508.

(42) McMillan, D. E.; Gion, K. M. *Horm Metab Res Suppl* **1981**, *11*, 108-112.

(43) Koch, C. G.; Li, L.; Sessler, D. I.; Figueroa, P.; Hoeltge, G. A.; Mihaljevic, T.; Blackstone, E. H. *N Engl J Med* **2008**, *358*, 1229-1239.

(44) Tinmouth, A.; Fergusson, D.; Yee, I. C.; Hebert, P. C.; Investigators, A.; Canadian Critical Care Trials, G. *Transfusion* **2006**, *46*, 2014-2027.

(45) Liu, Y. *DELIVERY OF A PANCREATIC BETA CELL-DERIVED HORMONE TO ERYTHROCYTES BY ALBUMIN AND DOWNSTREAM CELLULAR EFFECTS*. Michigan State University2015.

(46) Wang, Y. M.; Giebink, A.; Spence, D. M. *Integr Biol-Uk* **2014**, *6*, 65-75.

Chapter 4 – Studying the RBC Membrane Lipid Glycation During Storage

4.1 Introduction

In the last chapter, applying 3D printing techniques allowed for the creation of new blood storage bags and an IV-piggyback approach to maintenance of glucose levels during storage. The new blood storage bags, containing a black rubbery material, enabled removal of aliquots of stored blood samples and adding concentrated glucose solution with minimal interferences. The glucose level was maintained within the healthy range during storage using the IV-piggyback bag system. These features proved that maintenance of normoglycemic cell storage may be a possible clinical application.

In addition, the changes in cell deformability were quantitatively investigated using a 3D-printed membrane based filtration device. The results demonstrated that RBCs stored in high glucose conditions lose 15 – 20% of their deformability after the first day of storage. This deformability study provides a possible explanation for the reduced ATP release discussed in Chapter 1, since deformability is one of the main mechanisms of RBC-derived ATP release. However, more evidence is needed to explain the reasons behind the loss of RBC deformability. Considering that the only difference between normoglycemia and hyperglycemia cell storage is the level of glucose to which the RBCs are exposed, it is reasonable to hypothesize that the non-enzymatic glycation of cell membrane lipids and proteins plays an important role in the development of the storage lesion. In this chapter, the phosphatidylethanolamine (PE), a lipid, glycation of RBC membranes under storage conditions will be quantitatively studied using a high resolution orbitrap mass analyzer with a Nano-electrospray ionization (nESI) source.

Mature RBCs are deformable and flexible.[1,2] Since there is no nucleus or other cell organelles in the RBC, the cell membrane plays an important role in cellular functions. As shown in Figure 4.1, the RBC membrane is composed of three layers: the glycocalyx, a glycoprotein covering that surrounds the cell membranes on the exterior; the lipid bilayer, which contains many transmembrane proteins; and the spectrin-based cytoskeleton, a structural network of proteins located on the inner surface of the lipid bilayer. There are two classes of membrane proteins: integral and peripheral proteins. Integral proteins are embedded in the membrane via hydrophobic interactions with lipids. Examples of integral proteins are glycophorin and band 3. Peripheral proteins are located on the inner side of the lipid bilayer. They are anchored via integral proteins and are responsible for cell deformation. Peripheral proteins, including spectrin, ankyrin, actin, band 4.1 and band 4.2, form the cell cytoskeleton.

Lipids are mainly comprised of cholesterol and phospholipids. There are five major phospholipids, including phosphatidylcholine (PC), sphingomyelin (SM), phosphatidylethanolamine (PE), phosphatidylserine (PS) and phosphatidylinositol (PI). The chemical structures of the above lipids are shown in Figure 4.2. Notably, PC and SM are located on the outer monolayer of cell membrane, while PE, PI and PS are distributed in the inner layer. This asymmetric distribution of lipids among the bilayer is an important part of the overall RBC function. For instance, research has shown that macrophages recognize and phagocytose RBCs that expose PS at their outer surface.[3]

Damages to the RBC membrane, caused by oxidation, glycation, or both, may adversely affect cell deformability. Proteomic studies have revealed that the oxidation of proteins

occur in the first week of RBC storage, specifically cytoskeletal proteins like band 4.1, band 4.2 and spectrin.[4-6] Also, membrane protein oxidation and the breakdown of actin filaments were observed when RBCs were exposed to high concentrations of glucose (>25 mM).[7]

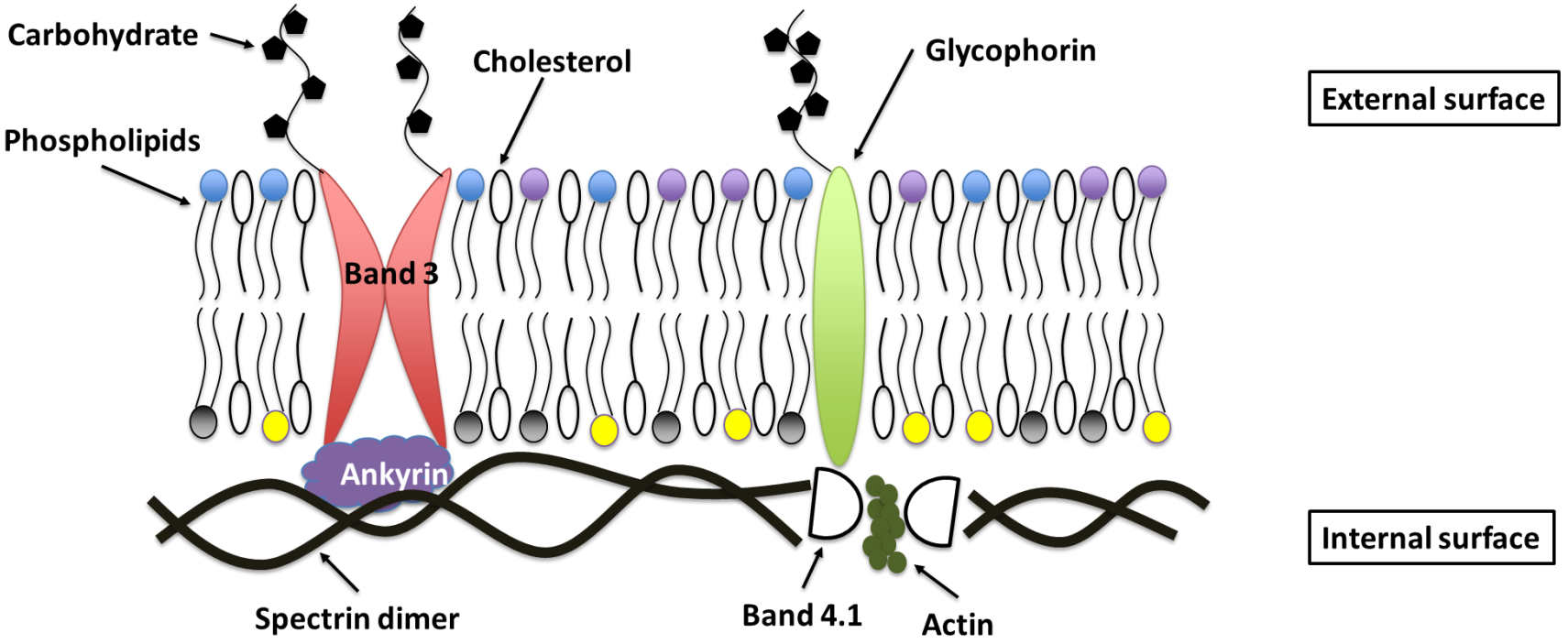

Figure 4.1 – Diagram of RBC membrane structure. The RBC membrane is composed of three layers: a glycocalyx layer, which is rich in carbohydrates, on the exterior; a lipid bilayer, which is composed of cholesterol and phospholipids; and cytoskeleton proteins, a structural network of proteins located on the inner surface of the lipid bilayer. There are two kinds of membrane proteins. Integral proteins, which are embedded in the membrane via hydrophobic interactions with lipids. Such as, glycophorin and band 3. The other kind of membrane proteins are peripheral proteins, which are located on the inner side of lipid bilayer. Those proteins, including spectrin, ankyrin, actin and band 4.1, are responsible for cell deformation.

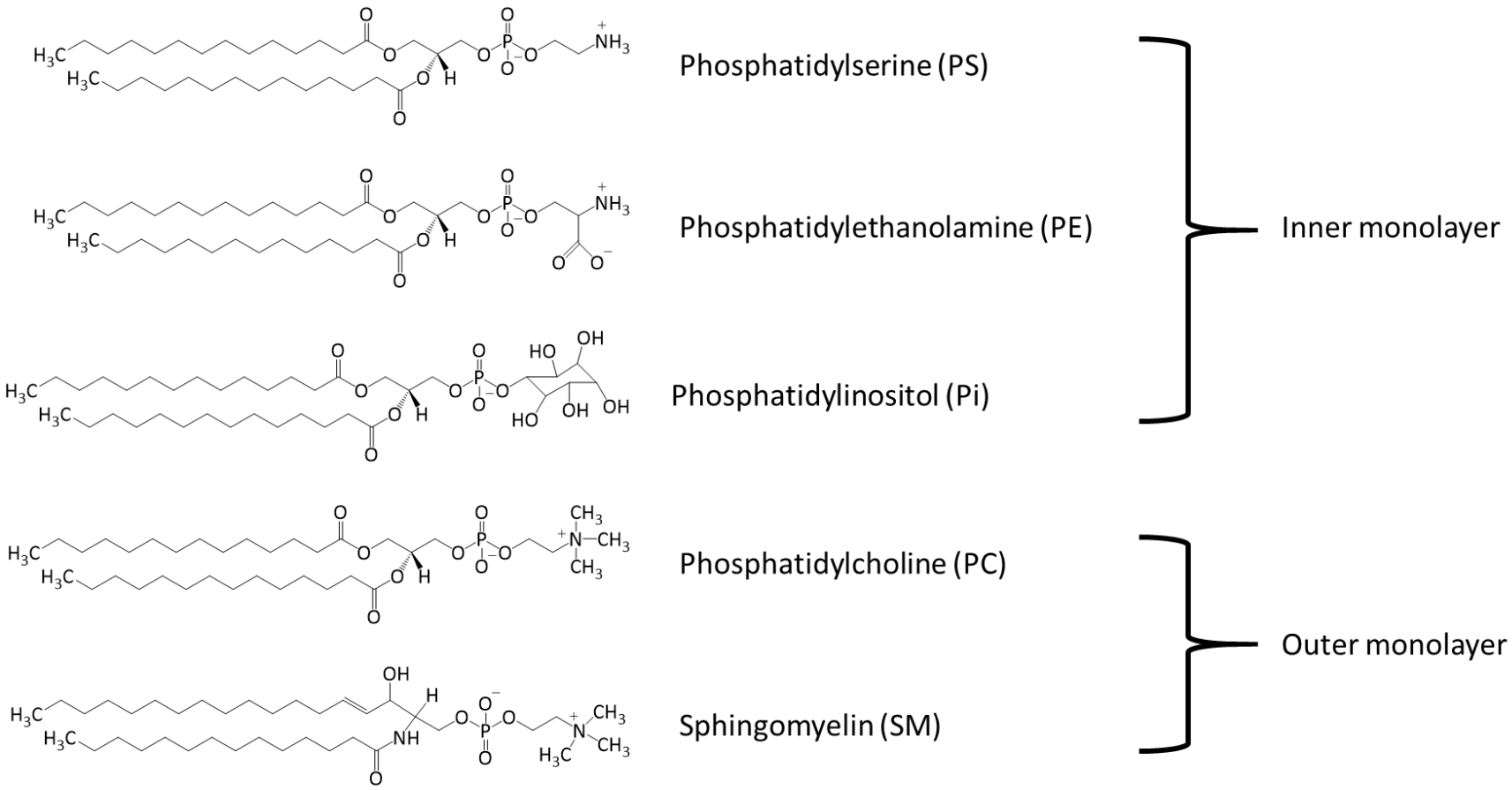

Figure 4.2 – Chemical structures of RBC membrane lipids. There are five major phospholipids on RBC membranes, including phosphatidylcholine (PC) and sphingomyelin (SM), which are located on the outer monolayer of cell membrane; and phosphatidylethanolamine (PE), phosphatidylserine (PS) and phosphatidylinositol (PI), which are distributed in the inner layer. Notably, PE and PS, both containing an amino group, can react with glucose to form glycation products.

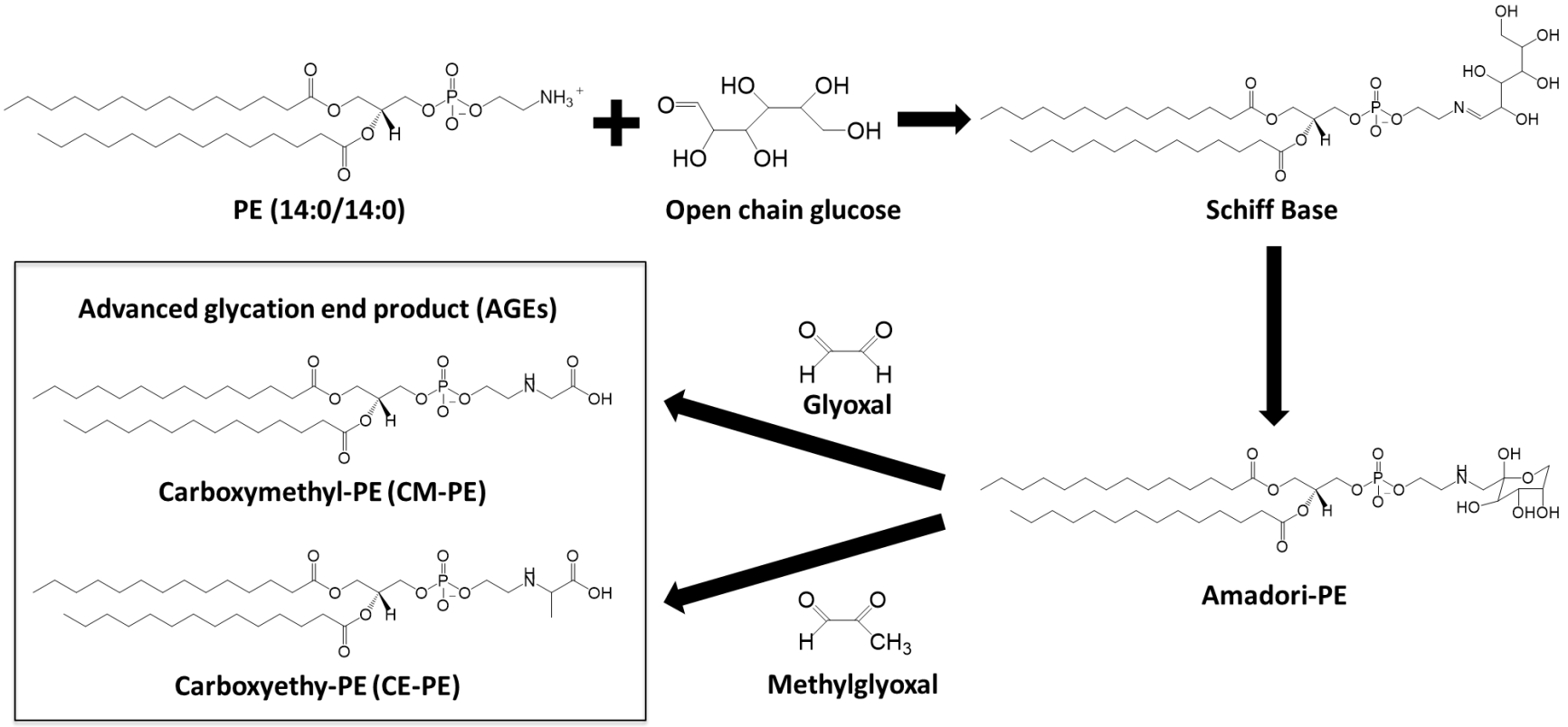

Figure 4.3 – Non-enzymatic glycation reactions of PE. Glucose chemically reacts with primary amine groups on PE, forming a reversible Schiff base within minutes. After that, the Schiff base product undergoes an Amadori rearrangement to form Amadori-PE, a more stable ketoamine compound. Once Amadori-PE is formed, it can further undergo complex reactions to form PE-linked advanced glycation end products (AGE-PE), such as carboxymethyl-PE (CM-PE) and carboxyethyl-PE (CE-PE).

In addition to oxidative stress, the hyperglycemic environments of RBC storage solutions may induce damage to the cell membrane by forming glycation products.[8-10] Because there is an excess amount of glucose acting as a reducing agent in stored RBCs, proteins and lipids with amino groups can react non-enzymatically with sugar molecules through a series of reactions. These reactions form Schiff bases and Amadori products, which then produce advanced glycation end products (AGEs). This process is called the Maillard reaction, which describes amino acids being heated in the presence of reducing sugars and developing a yellow-brown color.[11] The series of reactions are well illustrated in Figure 4.3, using PE and glucose as an example.[12] Of importance is the formation of highly reactive intermediate carbonyl groups during the Amadori rearrangement. These compounds are known as α-dicarbonyls, which include products such as 3-deoxyglucosone and methylglyoxal.[13-15] It has been implicated that methylglyoxal can lead to hyperglycemia-induced damage in diabetes.[16,17] Functional groups in proteins, including amino, sulfhydryl and guanidine, may be attacked by the highly reactive carbonyl groups, resulting in protein denaturation or cross-linking.[18] If oxidation occurs simultaneously with glycation, glycoxidation products are formed, such as N^{ε}-(carboxymethyl)lysine (CML).

Currently, there is no universal method to detect glycation products, including AGEs and Amadori products. Although it is confirmed that AGEs are accumulated in stored RBCs, it is difficult to compare results between laboratories.[19,20] Moreover, a number of AGEs, which are structurally heterogeneous, make the measurement of glycation products more challenging. The lack of internal standards increases measurement variations.

Common methods utilized for AGE determination are HPLC, Enzyme-Linked ImmunoSorbent Assay (ELISA) and immunohistochemistry.[21-25] Miyazawa developed a LC-MS/MS method with a QTRAP quadrupole/linear ion-trap tandem mass spectrometer to quantify Amadori-PE, as well as AGE-PE in human RBC and blood plasma.[26] Amadori-PE, CM-PE and CE-PE standards were synthesized *in vitro* for their work.[27,28] Here, instead of using LC coupled with a relative low resolution mass spectrometer, Amadori-PE from stored human RBC samples were measured by a high resolution mass spectrometer without LC separation.

4.2 Experimental

4.2.1 Sample Preparation

Standard PE (14:0/14:0) was purchased from Avanti Polar Lipids (Alabaster, AL, USA). All solvents used in this study were HPLC grade. Water and Isopropanol were purchased from Sigma-Aldrich (St. Louis, MO, USA); Methanol was purchased from Macron Fine Chemicals, Avantor Performance Materials (Center Valley, PA, USA); Chloroform ($CHCl_3$) was purchased from Omnisolv, EMD Millipore (Billerica, MA, USA). Glass tubes (15.5 mL) and caps for lipid extraction were purchased from Sigma-Aldrich. Glass vials (2 mL) and caps for sample storage were purchased from Thermo Fisher Scientific (Waltham, MA, USA). Prior to use, all glassware was baked overnight in a 500 °C oven, which is available in the Department of Biochemistry, Michigan State University. Internal standard, 100 μM of PE (14:0/14:0) was prepared by dissolving 3.22 mg of PE powder into 1 mL of $CHCl_3$ to make a 5 mM PE solution, followed by a 50-fold dilution in $CHCl_3$. The internal standard was kept in - 80 °C freezer until use. The prepared internal standard solution was used for all

RBC lipid extract samples. Ammonium bicarbonate (10 mM) was prepared by dissolving 158 mg into 200 mL of water.

In this study, RBCs were stored in CPD/AS-1 and CPDN/AS-1N using the newly developed blood storage method described in the previous chapter. Cell membrane lipid extractions, applying the Rose and Oklander method, were performed on days 1, 7, 14 and 35 of storage.[29] On each day, approximately 1 mL of stored RBC sample was removed from both the high glucose and the low glucose storage bags. In order to remove any extracellular lipids, RBC samples were washed using 5 mL of phosphate buffer saline (PBS) at least three times. Samples were centrifuged at 1500 *g* for 5 min, followed by the removal of the supernatant by aspiration. If a light pink color is still visible after the third wash, more washes were added until a clear supernatant was obtained. Then, 250 μL of packed RBCs were added to a glass tube containing 500 μL of water. RBCs were lysed under vigorous vortex and placed on ice for 15 min. Next, 2.25 mL of 80% isopropanol were slowly added into cell lysates with continued vortex mixing. Samples were incubated on ice for 1 hr with occasional vortex mixing. An internal standard 2.5 μL of 100 μM PE (14:0/14:0), was added into the sample mixture with 1.75 mL of $CHCl_3$. The sample mixture was combined by vigorous vortex and remained on the ice for another hour. The phase separation was achieved by centrifugation at 2000 *g* for 30 min. The lower phase (organic phase) was collected using a glass pipette. In order to pursue a higher efficiency lipid extraction, 1.75 mL of $CHCl_3$ was added into the sample mixture, followed by the mixing, incubation and centrifugation process. The lower phases from the two-time lipid extractions were pooled together. Next, samples were dried overnight under N_2. For the purpose of removing any

unwanted salts from the extracted lipids, samples were washed using 1 mL of 10 mM ammonium bicarbonate 5 times. After drying the samples again under N_2, the resultant lipid extracts were re-constituted into a 250 μL solvent mixture of isopropanol, methanol and $CHCl_3$ (4:2:1, v/v/v) containing 0.01% of butylated hydroxytoluene (BHT) for anti-oxidation. The lipid samples were stored in a - 80 °C freezer. Fresh blood samples were also collected as controls. They were treated in the same manner as the stored RBCs.

4.2.2 *In vitro* Synthesis of Amadori-PE

The *in vitro* synthesis of Amadori-PE was performed by following the procedure described by Miyazawa.[27] Phosphate buffer (0.1 M) was prepared by adding 0.31 g $NaH_2PO_4 \bullet H_2O$ and 1.09 g Na_2HPO_4 into 100 mL of water. Then, 17.2 mg standard PE (14:0/14:0) and 0.3603 g D-glucose were mixed in 30 mL 0.1 M phosphate buffer/methanol (2:1, v/v, pH = 7.4). The reaction took place in a Talboys incubating shaker (Thorofare, NJ) at 37 °C for 30 days. On day 30, 3 mL of sample were transferred into 12 mL of $CHCl_3$/methanol (2:1, v/v) for lipid extraction. The lower phase was collected after centrifugation at 3000 *g* for 5 min. The sample was dried under N_2, followed by reconstituting into 250 μL of isopropanol, methanol and $CHCl_3$ (4:2:1, v/v/v) solvent mixture containing 0.01% BHT. The synthesized Amadori-PE was stored in a - 80 °C freezer until use.

4.2.3 Optimizing PE and Amadori-PE Determination

A method for analyzing PE and Amadori-PE with direct infusion high resolution/accurate mass spectrometry and tandem mass spectrometry was developed. The mass spectrometry platform was a Thermo LTQ Orbitrap Velos (San Jose, CA). The ionization source was an Advion Triversa Nanomate nESI source (Advion, Ithaca, NY). High resolution

MS and MS/MS spectra were acquired using the FT analyzer operating at 100,000 mass resolving power. Ion mapping Higher-Energy Collision Induced Dissociation (HCD) MS/MS product ion spectra were acquired to confirm lipid head groups and acyl chain compositions.

Standard PE (14:0/14:0) and synthesized Amadori-PE were diluted by a factor of 10, and introduced to the mass spectrometer under nESI+ conditions to determine the molecular ions, as well as the loss of head groups in tandem MS. Then, RBC membrane extract samples were diluted by different folds and injected into the mass spectrometer to determine optimal detection signal. In order to eliminate the influence from PI, an isomer of Amadori-PE, RBC membrane extract samples were also detected using the nESI – mode. After excluding the potential overlap between PI and Amadori-PE peaks, a list of PE and Amadori-PE that will be discovered in stored blood samples was generated.

4.2.4 PE and Amadori-PE Determination of Stored RBCs

All quantitative analyses of PE and Amadori-PE from stored RBC extracts were performed by the Thermo Fisher LTQ Velos orbitrap mass spectrometer. Samples were directly infused to the mass spectrometer by nESI using the Advion Triversa Nanomate nESI source with a spray voltage of 1.4 kV and a gas pressure of 0.3 psi. High resolution MS spectra were acquired in positive ionization modes using the FT analyzer operating at 100,000 mass resolving power.

For each analysis, 30 μL of lipid extract were transferred to an Eppendorf twin-tec 96-well plate (Sigma Aldrich), and evaporated under N_2. The dried lipid film was then resuspended in isopropanol, methanol and $CHCl_3$ (4:2:1 v/v/v) containing 20 mM ammonium formate

and sealed with Teflon Ultra-Thin Sealing Tape (Analytical Sales and Services, Pompton Plains, NJ).

Lipids were identified using the Lipid Mass Spectrum Analysis (LIMSA) v.1.0 software linear fit algorithm, in conjunction with a user-defined database of hypothetical lipid compounds for automated peak finding and correction of ^{13}C isotope effects. Relative quantification of abundance between samples was performed by normalization of target lipid ion peak areas to the PE (14:0/14:0) internal standard.

4.3 Results

4.3.1 Optimization of PE and Amadori-PE Detection

The positive mode of nESI provides lipid peaks in the form of $[M+H]^{1+}$. The results of high resolution MS and MS/MS spectra acquired from standard PE (14:0/14:0) and synthesized Amadori-PE (14:0/14:0) are shown in Figure 4.4. The standard PE (14:0/14:0) peak at m/z = 636.44 and synthesized Amadori-PE peak at m/z = 798.51 were observed in the MS spectrum. The difference between the two peaks, which has a m/z = 162.07, represents a glucose molecule bonded to PE and a loss of one water molecule. After using tandem MS to fragment those two molecular ions, the same product ion was obtained. The di-glyceride product ion peak at m/z = 495.44 further confirmed that the two peaks, m/z = 636.44 and m/z = 798.51, have the same acyl chain composition but different head groups. The measurement of lipid extract from stored RBC samples was determined using a direct infusion method without any further dilution. Table 4.1 lists the target PE and Amadori-PE, after eliminating the influence from PI overlapping.

4.3.2 PE Glycation in Stored RBCs

RBCs were stored in CPD/AS-1, which is a hyperglycemic condition, and CPDN/AS-1N, which is a normoglycemic condition. Figure 4.5 shows the results of MS quantitation of Amadori-PE to PE ratio in percentage from the first set of RBC samples. The black bar represents fresh blood control (0.26 ± 0.03%). On day 1, the ratio of Amadori-PE/PE was higher in stored RBCs (CPD/AS-1: 0.77 ± 0.10%; CPDN/AS-1N: 0.55 ± 0.07%) than fresh blood. The ratio of Amadori-PE/PE decreases as the storage duration increases. The ratio decreases faster when RBCs were stored in normal glucose conditions. On day 14, there was a statistical difference between the ratios from hyperglycemia storage and normoglycemia storage ($p < 0.05$). The ratio of Amadori-PE/PE is significantly higher than fresh blood level ($p < 0.05$), when RBCs were stored in CPD/AS-1 on day 1 and day 14 (0.51 ± 0.06%).

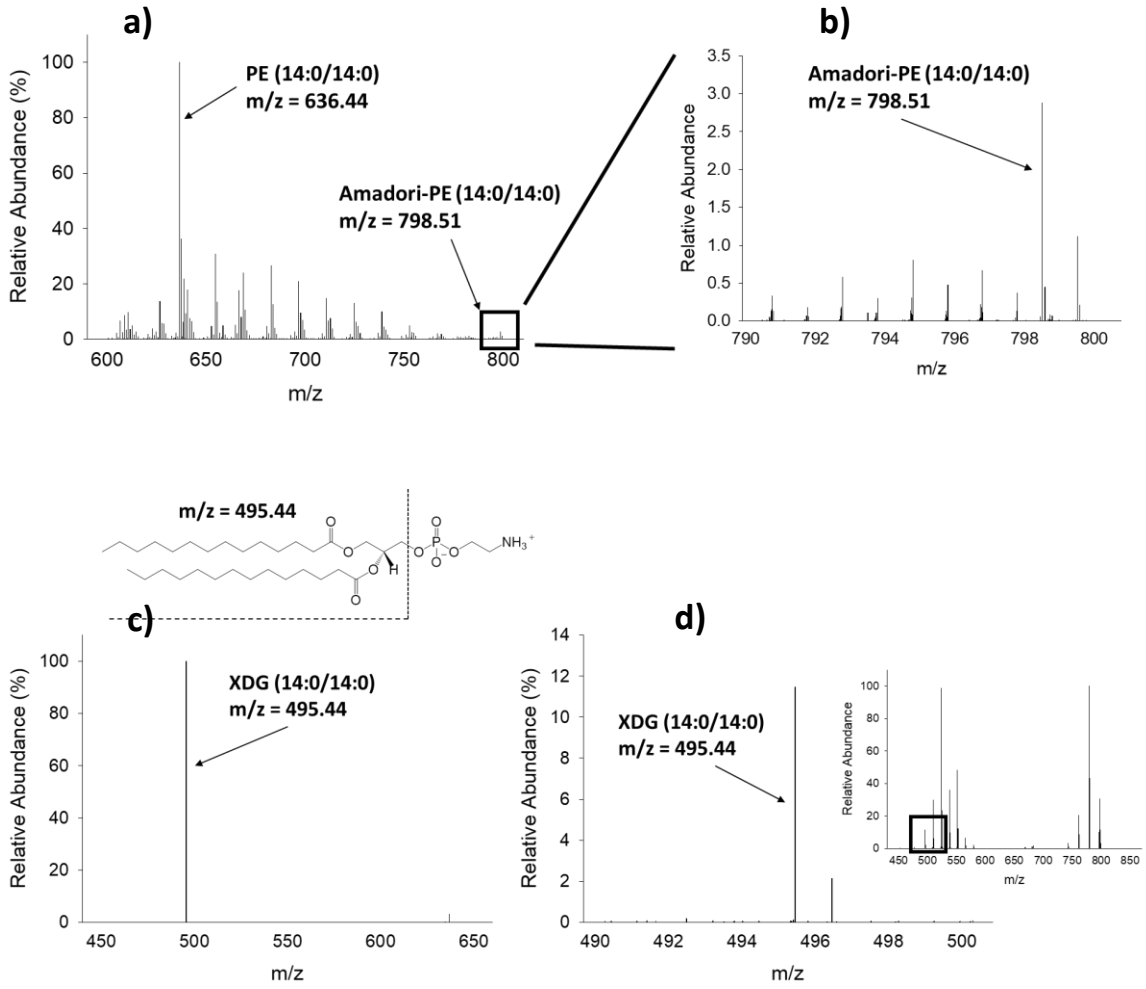

Figure 4.4 – MS and MS/MS scan of standard PE (14:0/14:0) and synthesized Amadori-PE (14:0/14:0). a) MS scan of synthesized Amadori-PE sample. Standard PE (14:0/14:0) shows a peak at m/z = 636.44. Synthesized Amadori-PE peak is located at m/z = 798.51; b) A zoomed-in spectrum of synthesized Amadori-PE sample at range m/z = 790 to m/z = 800; c) MS/MS detection of standard PE (14:0/14:0). A di-glyceride product ion peak at m/z = 495.44 was acquired. The fragmentation of PE, as well as the structure of XDG is presented; d) MS/MS detection of synthesized Amadori-PE (14:0/14:0). The same XDG peak at m/z = 495.44 was obtained.

Table 4.1 – List of PE and Amadori-PE targeted in stored RBC lipid extract

PE	Formula	m/z	Amadori PE	Formula	m/z
28:00	$C_{33}H_{66}NO_8P$	636.4598	28:00	$C_{39}H_{70}NO_{13}P$	798.5127
32:01	$C_{37}H_{72}NO_8P$	690.5068	32:01	$C_{43}H_{76}NO_{13}P$	852.5596
34:01	$C_{39}H_{76}NO_8P$	718.5381	34:01	$C_{45}H_{80}NO_{13}P$	880.5909
34:02	$C_{39}H_{74}NO_8P$	716.5224	34:02	$C_{45}H_{78}NO_{13}P$	878.5753
36:01	$C_{41}H_{80}NO_8P$	745.5622	36:01	$C_{47}H_{84}NO_{13}P$	901.5680
36:02	$C_{41}H_{78}NO_8P$	744.5537	36:02	$C_{47}H_{82}NO_{13}P$	906.6066
36:04	$C_{41}H_{74}NO_8P$	739.5152	36:04	$C_{47}H_{78}NO_{13}P$	895.5211
38:04	$C_{43}H_{78}NO_8P$	768.5537	38:04	$C_{49}H_{82}NO_{13}P$	930.6066
38:05	$C_{43}H_{76}NO_8P$	766.5381	38:05	$C_{49}H_{80}NO_{13}P$	928.5909
38:06	$C_{43}H_{74}NO_8P$	763.5152	38:06	$C_{49}H_{78}NO_{13}P$	919.5211

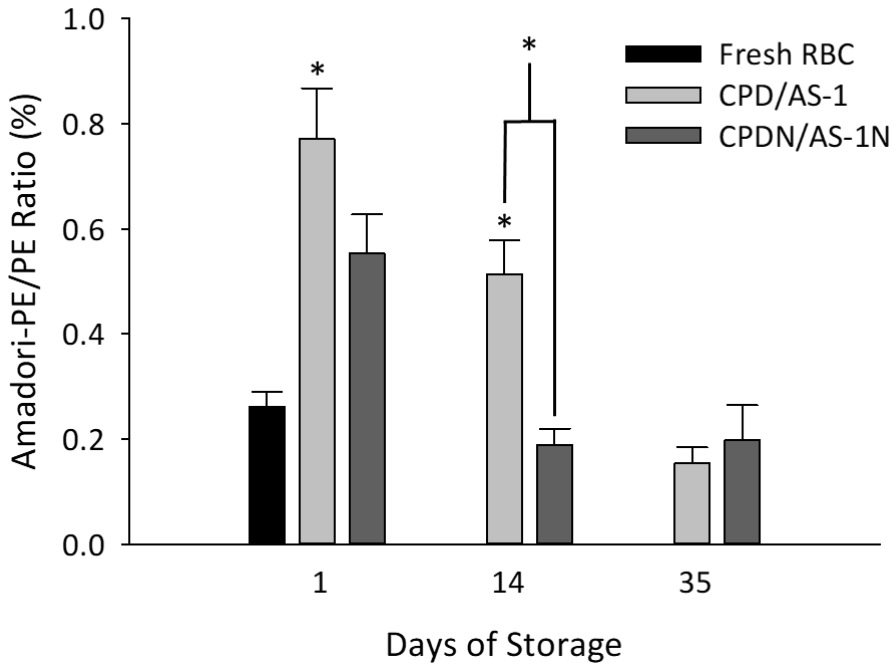

Figure 4.5 – MS results of Amadori-PE to PE ratio in stored RBC lipid extract. The black bars represent fresh blood control. The light grey bars represent RBCs collected and stored in CPD/AS-1, which is a high glucose environment. The dark grey bars represent RBCs collected and stored in CPDN/AS-1N, which is a normal glucose environment. Data is displayed as the ratio of Amadori-PE to PE in percentage at different storage length. On day 1, the ratio of Amadori-PE/PE is higher in stored RBC than fresh blood. The ratio decreases as a function of time. When RBCs were stored in physiological level of glucose, the ratio decreases faster. There is a significant difference between the two bars on day 14. In addition, the ratio of Amadori-PE/PE is significantly higher than the fresh blood level, when RBCs were stored in CPD/AS-1 on day 1 and day 14. Data represents mean ± s.e.m. (*$p < 0.05$, n = 4 ~ 6 humans).

The normalized ratio of Amadori-PE to PE is shown in Figure 4.6. The ratios of Amadori-PE to PE at different storage lengths were normalized to the result obtained from the same storage condition on day 1. The normalized ratios of Amadori-PE/PE, on day 14 (CPD/AS-1: 63.22 ± 4.6%; CPDN/AS-1N: 38.54 ± 2.1%) and day 35 (CPD/AS-1: 18.65 ± 5.7%; CPDN/AS-1N: 24.19 ± 8.4%), were significantly lower than day 1, from both normoglycemia and hyperglycemia cell storage. After two weeks, there was a significant difference between the results from RBCs stored in CPD/AS-1 and CPDN/AS-1N. The same trend is demonstrated in Figure 4.5 where the Amadori-PE/PE ratio decreases as a function of time.

Figure 4.7 represents the results of normalized Amadori-PE to PE ratios from the second set of stored RBC samples. Compared to Figure 4.6, the same trend occurred when RBCs were stored in a normal glucose environment. The normalized ratio decreases as a function of time. The results from day 1 are significantly higher than results from day 14 (46.25 ± 6.3%) and day 35 (28.18 ± 7.4%). However, the results are not reproducible to that from the first set of RBC samples when cells were stored in CPD/AS-1. The normalized ratio does not change with the storage length. Additionally, on day 35, there is a statistical difference between the results from RBCs stored in a high glucose environment (107.78 ± 7.2%) and a normal glucose environment.

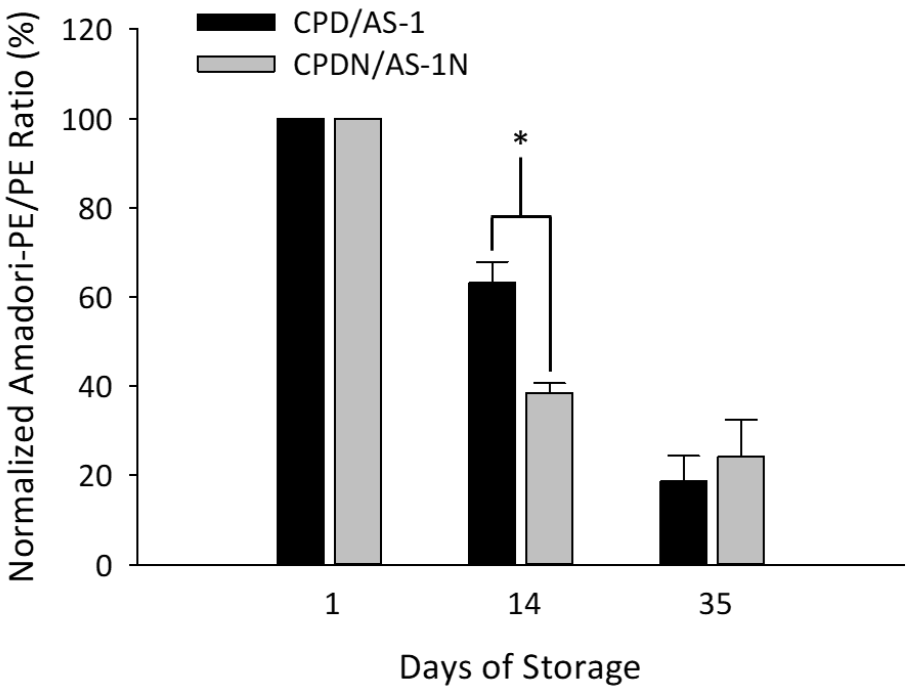

Figure 4.6 – Normalized Amadori-PE to PE ratios in stored RBCs. The black bars represent RBCs collected and stored in CPD/AS-1, which is a hyperglycemic condition. The grey bars represent RBCs collected and stored in CPDN/AS-1N, which is a normoglycemic condition. The ratios of Amadori-PE to PE at different storage lengths were normalized to the ratio on day 1, in order to have an improved visualization of trend and eliminate some human variations. The normalized ratios of Amadori-PE/PE, on day 14 and day 35, are significantly lower than day 1, from both normoglycemia and hyperglycemia cell storage. There was a significant difference observed on day 14 between the samples from CPD/AS-1 and CPDN/AS-1N. The trend of decreasing Amadori-PE/PE ratio, which was found in Figure 4.5, is also demonstrated in this bar graph. Data represents mean ± s.e.m. (*$p < 0.05$, n = 4 humans).

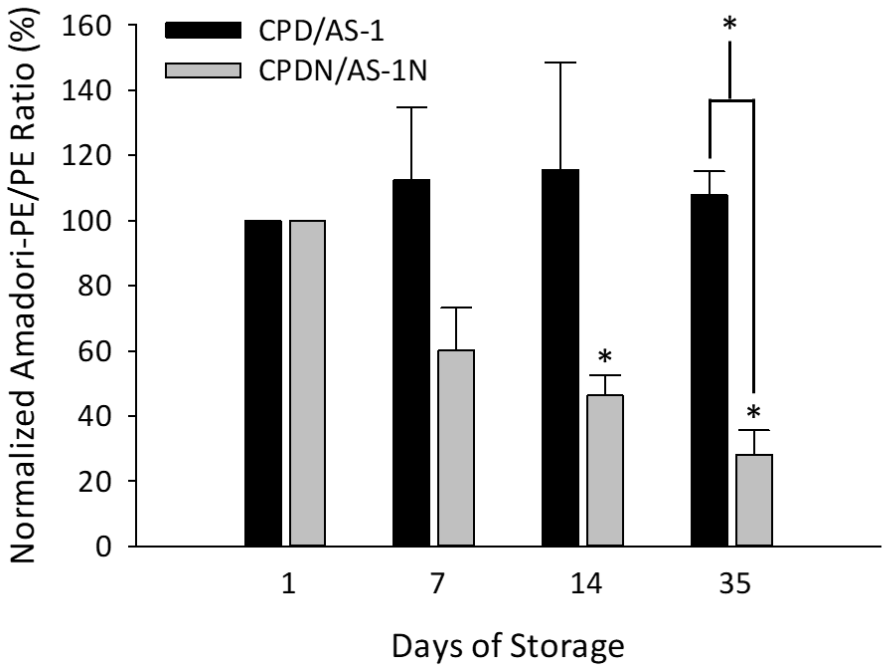

Figure 4.7 – Normalized Amadori-PE to PE ratios from the second set of RBC samples. The black bars represent RBCs collected and stored in CPD/AS-1. The grey bars represent RBCs collected and stored in CPDN/AS-1N. The ratio of Amadori-PE to PE at different storage length was normalized to the ratio on day 1. Compared to Figure 4.6, the same trend was observed here when RBCs were collected and stored in normal glucose condition. The normalized ratio decreases as the function of time. The results from day 1 were significantly higher than results from day 14 and day 35. However, the results are not reproducible to that from the first set of RBC samples when cells were stored in high glucose condition. Here, the normalized ratio does not change with the storage length. Additionally, there was a significant difference between the results on day 35. Data represents mean ± s.e.m. (*$p < 0.05$, n = 4 humans).

4.4 Discussion

The correlation between AGEs and diabetic complications has been studied for years, which is reflected by the abundance of works and reviews.[30-34] Since diabetic RBCs and stored RBCs are both exposed to high concentrations of glucose, it is reasonable to hypothesize that non-enzymatic glycation reactions are also happening in RBC storage. Indeed, it has been reported by Mangalmurti *et al.* that AGEs are being produced during the storage of RBCs.[19] Preliminary results from Spence group and Reid group has shown that total protein glycation of stored RBCs keeps increasing as a function of time (data not shown).

In order to further study glycation reactions happening in blood storage, PE and Amadori-PE in stored RBC lipid extract were determined in this work. These two lipids were selected as the starting point of discovering stored RBC glycation for two reasons. First, there are amino groups on PE molecules that can potentially non-enzymatically react with glucose. Second, PE and Amadori-PE from human RBCs have been successfully measured on a LC-MS/MS platform.[26] Instead of using the developed LC-MS/MS method, a new direct infusion approach was investigated with a high resolution/accurate mass spectrometer. This new detection method enables fast spectra acquiring (~3 min for each sample). Compared to a typical 30 min LC-MS/MS experiment, the efficiency was dramatically improved. The Nano-electrospray ionization source allowed for higher efficiency in the ionization process, as well as lower sample consumption. Also, less chemical waste was generated because HPLC solvents were saved, which is beneficial for

environment protection. Importantly, the high resolution mass analyzer provided not only quantitative but also qualitative information.

As shown in Figure 4.4, the orbitrap mass analyzer was able to capture molecular ions of PE and Amadori-PE efficiently. Ion mapping HCD-MS/MS product ion spectra helped to confirm lipid head groups and acyl chain compositions. The m/z difference between Amadori-PE and PE that have the same acyl chain is 162.07, suggesting that the difference is due to a glucose molecule bonded to PE and a loss of one water molecule. The XDG peaks in MS/MS spectrum further supported that the difference was because of the change at lipid head groups.

When processing data, the ratio of Amadori-PE to PE was calculated first, instead of using absolute lipid concentration directly. This was due to the variations contributed by sample preparation and detection. The number of cells that were extracted from the recovery percentage of lipid extraction, and the efficiency of ionization process were all error sources. The Amadori-PE/PE ratio was further normalized to the result on day 1, because of the variations contributed by different human subjects. Notably, the normalization method was different from analyzing deformability results in Chapter 3, where all results were normalized to the RBCs stored in normoglycemic conditions on day 1. Here, the ratio was normalized to the result on day 1 that was from the same storage condition. The normalized ratio provided a better view of the trend when analyzing the changes of Amadori-PE to PE ratio.

Previously, the content of Amadori-PE from diabetic human RBCs and blood plasma was demonstrated to be statistically higher than cells and plasma from healthy people.[26] Since

diabetic RBCs and RBCs stored in hyperglycemic conditions are similar in some aspects, it is rational to assume that there will be more Amadori-PE if cells are stored in high glucose level, compared to our modified normoglycemia RBC storage. Moreover, the concentration of Amadori-PE is supposed to increase as a function of time, because more glycation reactions may take place during a long term storage. Surprising, the results showed an inverse trend.

The experiments of PE and Amadori-PE quantification from stored RBCs were performed twice. Two sets of stored RBC from different human subjects were used in these studies. When RBCs were collected and stored in our modified CPDN/AS-1N, the Amadori-PE to PE ratio decreased during storage as shown in Figure 4.6 and Figure 4.7. This discovery meant there was a reduced amount of Amadori-PE on the stored RBC membrane, especially for a longer storage length. Although the mechanism behind this phenomenon is still under investigation, possible explanations are discussed here. Amadori-PE might be further converted to AGE-PE, such as CM-PE and CE-PE. It is less possible during the first two weeks of storage, because the process of AGE formation occurs over a period of weeks.[35] On the other hand, forming Schiff base and Amadori products are usually within minutes and reversible.[36] Since RBCs are exposed to physiological level of glucose when stored in CPDN/AS-1N, Amadori-PE molecules may by hydrolyzed to produce PE and glucose molecules. Another highly possible mechanism is stored RBCs clean damaged lipids by shedding microvesicles into environment. It has been suggested that RBCs releasing microvesicles might be a salvage progress.[37]

The results from hyperglycemia cell storage are not identical between two sets of human samples. In the first set of samples, it acted similar to normoglycemic stored cells but decreased slower, shown in Figure 4.6. There is a significant difference on day 14 between the ratios from high glucose and normal glucose RBC storage ($p < 0.05$). However, the ratio of Amadori-PE to PE doesn't change with time in the second set of human subjects, shown in Figure 4.7. Although a larger size of sample is needed to further confirm the trend of cell membrane Amadori-PE change during high glucose storage, the results here suggest that RBCs stored in hyperglycemic conditions have more Amadori-PE relative to total PE. Since there is excess amount of glucose presented in storage solutions, Amadori-PE molecules are unlikely to participate in hydrolysis reactions. Also, more Amadori-PE might be generated during a long term storage. Glycation is concentration-dependent in the early stage rather than later, so the formation of AGE-PE may be favored but not guaranteed.[38,39] Therefore, the most possible mechanism of reducing the Amadori-PE percentage is releasing microvesicles. It has been discussed in Chapter 1 that the rate of metabolism in stored RBC is slower than cells in the bloodstream. Less ATP was generated during the cold storage.[40] The lack of energy supply may affect the cell capacity to clean damaged lipids, such as PE, resulting in the Amadori-PE/PE ratio to decrease slower or remain unchanged.

Comparing the fresh blood control to stored RBCs results, Amadori-PE/PE ratio is higher in RBCs stored in both high glucose and physiological glucose levels, as shown in Figure 4.5. The Amadori-PE percentage was back to fresh blood level after one week of normoglycemic storage. These discoveries suggest that there was a strike of increasing

Amadori-PE content during the first day of storage, even when cells are processed and stored under healthy glucose range. This may be caused by dramatic environmental changes from *in vivo* to *in vitro*, when RBCs leave the bloodstream and enter into storage solutions. In the future, it would be better to normalize the results to a fresh blood control instead of stored RBCs on day 1, which may provide more information about changes during cell collection in processing solutions.

4.5 Conclusion

In this chapter, Amadori-PE and PE were quantified from human RBC lipid extract. Utilizing the high resolution/accurate mass spectrometer with a direct infusion method under nESI + mode, the percentage of Amadori-PE occupying in total RBC membrane PE was determined at different time point during RBC storage. Compared to a typical LC-MS/MS experiment with a relatively low resolution mass analyzer, the developed method significantly increased the productivity. Also, less LC solvents were used, which reduced the amount of chemical waste generated. The results of Amadori-PE to PE ratio from each sample were represented in percentage, after normalizing to the result obtained from the same storage condition on day 1. For RBCs processed in normal glucose environment, the Amadori-PE/PE ratio decreased as the storage length increased. The results are reproducible between the two sets of human RBC samples. When standard storage solutions were used, the trend from the two sets of human subjects are not consistence. The ratio of Amadori-PE/PE decreased as a function of time in the first set of human samples. While, it does not change during the cold storage in the second set of lipid extract. This was mainly due to the relatively small sample size, as well as human

variability. However, the results of Amadori-PE/PE ratio from hyperglycemic stored RBCs highly suggest that RBCs exposed to high concentration of glucose are less healthy.

REFERENCES

REFERENCES

(1) Zhu, H. M.; Zennadi, R.; Xu, B. X.; Eu, J. P.; Torok, J. A.; Telen, M. J.; McMahon, T. J. *Critical Care Medicine* **2011**, *39*, 2478-2486.

(2) Kirby, B. S.; Hanna, G.; Hendargo, H. C.; McMahon, T. J. *Am J Physiol Heart Circ Physiol* **2014**, *307*, H1737-1744.

(3) Connor, J.; Pak, C. C.; Schroit, A. J. *J Biol Chem* **1994**, *269*, 2399-2404.

(4) D'Amici, G. M.; Rinalducci, S.; Zolla, L. *J Proteome Res* **2007**, *6*, 3242-3255.

(5) Kriebardis, A. G.; Antonelou, M. H.; Stamoulis, K. E.; Economou-Petersen, E.; Margaritis, L. H.; Papassideri, I. S. *Transfusion* **2007**, *47*, 1212-1220.

(6) Bosman, G. J.; Lasonder, E.; Luten, M.; Roerdinkholder-Stoelwinder, B.; Novotny, V. M.; Bos, H.; De Grip, W. J. *Transfusion* **2008**, *48*, 827-835.

(7) Resmi, H.; Akhunlar, H.; Temiz Artmann, A.; Guner, G. *Cell Biochem Funct* **2005**, *23*, 163-168.

(8) Hunt, J. V.; Bottoms, M. A.; Mitchinson, M. J. *Biochem J* **1993**, *291 (Pt 2)*, 529-535.

(9) Pokharna, H. K.; Pottenger, L. A. *J Surg Res* **2000**, *94*, 35-42.

(10) Dolhofer-Bliesener, R.; Lechner, B.; Gerbitz, K. D. *Eur J Clin Chem Clin Biochem* **1996**, *34*, 355-361.

(11) John, W. G.; Lamb, E. J. *Eye (Lond)* **1993**, *7 (Pt 2)*, 230-237.

(12) Nawale, R. B.; Mourya, V. K.; Bhise, S. B. *Indian J Biochem Biophys* **2006**, *43*, 337-344.

(13) Skovsted, I. C.; Christensen, M.; Breinholt, J.; Mortensen, S. B. *Cell Mol Biol (Noisy-le-grand)* **1998**, *44*, 1159-1163.

(14) Wells-Knecht, K. J.; Brinkmann, E.; Wells-Knecht, M. C.; Litchfield, J. E.; Ahmed, M. U.; Reddy, S.; Zyzak, D. V.; Thorpe, S. R.; Baynes, J. W. *Nephrol Dial Transplant* **1996**, *11 Suppl 5*, 41-47.

(15) Baynes, J. W.; Thorpe, S. R. *Diabetes* **1999**, *48*, 1-9.

(16) Sima, A. A.; Sugimoto, K. *Diabetologia* **1999**, *42*, 773-788.

(17) Nishikawa, T.; Edelstein, D.; Du, X. L.; Yamagishi, S.; Matsumura, T.; Kaneda, Y.; Yorek, M. A.; Beebe, D.; Oates, P. J.; Hammes, H. P.; Giardino, I.; Brownlee, M. *Nature* **2000**, *404*, 787-790.

(18) Lo, T. W.; Westwood, M. E.; McLellan, A. C.; Selwood, T.; Thornalley, P. J. *J Biol Chem* **1994**, *269*, 32299-32305.

(19) Mangalmurti, N. S.; Chatterjee, S.; Cheng, G.; Andersen, E.; Mohammed, A.; Siegel, D. L.; Schmidt, A. M.; Albelda, S. M.; Lee, J. S. *Transfusion* **2010**, *50*, 2353-2361.

(20) Berg, T. J.; Clausen, J. T.; Torjesen, P. A.; Dahl-Jorgensen, K.; Bangstad, H. J.; Hanssen, K. F. *Diabetes Care* **1998**, *21*, 1997-2002.

(21) Sell, D. R.; Monnier, V. M. *J Clin Invest* **1990**, *85*, 380-384.

(22) Makita, Z.; Radoff, S.; Rayfield, E. J.; Yang, Z.; Skolnik, E.; Delaney, V.; Friedman, E. A.; Cerami, A.; Vlassara, H. *N Engl J Med* **1991**, *325*, 836-842.

(23) Papanastasiou, P.; Grass, L.; Rodela, H.; Patrikarea, A.; Oreopoulos, D.; Diamandis, E. P. *Kidney Int* **1994**, *46*, 216-222.

(24) Munch, G.; Keis, R.; Wessels, A.; Riederer, P.; Bahner, U.; Heidland, A.; Niwa, T.; Lemke, H. D.; Schinzel, R. *Eur J Clin Chem Clin Biochem* **1997**, *35*, 669-677.

(25) Soulis, T.; Thallas, V.; Youssef, S.; Gilbert, R. E.; McWilliam, B. G.; Murray-McIntosh, R. P.; Cooper, M. E. *Diabetologia* **1997**, *40*, 619-628.

(26) Shoji, N.; Nakagawa, K.; Asai, A.; Fujita, I.; Hashiura, A.; Nakajima, Y.; Oikawa, S.; Miyazawa, T. *J Lipid Res* **2010**, *51*, 2445-2453.

(27) Oak, J.; Nakagawa, K.; Miyazawa, T. *FEBS Lett* **2000**, *481*, 26-30.

(28) Utzmann, C. M.; Lederer, M. O. *Carbohydr Res* **2000**, *325*, 157-168.

(29) Rose, H. G.; Oklander, M. *J Lipid Res* **1965**, *6*, 428-431.

(30) Wolff, S. P.; Jiang, Z. Y.; Hunt, J. V. *Free Radic Biol Med* **1991**, *10*, 339-352.

(31) Miyazawa, T.; Nakagawa, K.; Shimasaki, S.; Nagai, R. *Amino Acids* **2012**, *42*, 1163-1170.

(32) Bucala, R.; Tracey, K. J.; Cerami, A. *J Clin Invest* **1991**, *87*, 432-438.

(33) Singh, V. P.; Bali, A.; Singh, N.; Jaggi, A. S. *Korean J Physiol Pharmacol* **2014**, *18*, 1-14.

(34) Wautier, J. L.; Wautier, M. P.; Schmidt, A. M.; Anderson, G. M.; Hori, O.; Zoukourian, C.; Capron, L.; Chappey, O.; Yan, S. D.; Brett, J.; et al. *Proc Natl Acad Sci U S A* **1994**, *91*, 7742-7746.

(35) Singh, R.; Barden, A.; Mori, T.; Beilin, L. *Diabetologia* **2001**, *44*, 129-146.

(36) Nakagawa, K.; Oak, J. H.; Higuchi, O.; Tsuzuki, T.; Oikawa, S.; Otani, H.; Mune, M.; Cai, H.; Miyazawa, T. *J Lipid Res* **2005**, *46*, 2514-2524.

(37) Delobel, J.; Barelli, S.; Canellini, G.; Prudent, M.; Lion, N.; Tissot, J.-D. *ISBT Science Series* **2016**, *11*, 171 - 177.

(38) Furth, A. J. *Br J Biomed Sci* **1997**, *54*, 192-200.

(39) McCance, D. R.; Dyer, D. G.; Dunn, J. A.; Bailie, K. E.; Thorpe, S. R.; Baynes, J. W.; Lyons, T. J. *J Clin Invest* **1993**, *91*, 2470-2478.

(40) Hess, J. R. *J Proteomics* **2010**, *73*, 368-373.

Chapter 5 – Conclusions and Future Directions

5.1 Conclusions

5.1.1 Storing RBCs in Physiological Levels of Glucose Can Reduce Storage Lesion

Transfusion of stored RBCs has become one of the most frequently performed medical interventions in hospitals and other clinical institutes. Although it has been developing for more than 100 years, risks still accompany this therapeutic process. Mortality and morbidity cannot be 100% avoided. Adverse changes occurring to stored RBCs during the storage period has been indicated as the major element contributing to post-transfusion related complications. New blood collection and storage solutions that can reduce the storage lesion are under high demand. Previously, the Spence group has shown that RBCs stored under normoglycemic conditions could potentially increase NO bioavailability during and after transfusion.[1]

In order to further promote the benefits of normoglycemic cell storage, three new versions of blood banking processing solutions were proposed in this thesis. They are CPDN/AS-1N, CPDN/AS-3N and CPDN/AS-5N. Using a solution containing 200 mM glucose in saline to feed the cells, the glucose levels in our miniaturized RBC storage bags were controlled successfully within 4 – 6 mM during a 35-day storage. However, RBCs stored in standard solutions were exposed to an unfavorably high concentration of glucose throughout the 35-day storage, shown in Figure 2.9 (CPD/AS-1, 50 – 55 mM; CP2D/AS-3, 40 – 45 mM; CPD/AS-5, 35 – 40 mM). When compared to people with diabetes mellitus, who have an elevated blood glucose level (7 – 10 mM), RBCs stored in hyperglycemic

solutions are subjected to constant fourfold increases in glucose. The excess amount of glucose is regarded as a main contributor to the development of the RBC storage lesion. The modified collection and storage solutions were compared to current FDA approved solutions to explore the effects of glucose on stored RBC properties. For the laboratory scale, miniaturized blood banking products were able to meet the FDA hemolysis requirements in the first 4 weeks of storage. However, all RBC products in this work had a non-ideal level of hemolysis, over 1%, by the end of storage, which makes them expired according to FDA regulations.[2] The percent cell lysis could potentially be reduced by 50% if leukofiltration was performed.[3]

The high concentration of glucose in the solution's supernatant leads to massive production of intracellular sorbitol through the polyol pathway. Elevated sorbitol level is a well-known feature of people with diabetes mellitus, which has been found to be correlated with plasma glucose levels.[4,5] The generation of sorbitol in stored RBCs might cause osmotic imbalance and result in cellular oxidative stress. In our modified normoglycemic storage conditions, intracellular sorbitol concentrations are similar to fresh RBCs. Conversely, sorbitol concentrations in RBCs stored in standard storage solutions are statistically higher than fresh RBCs (16.1 ± 2.0 nmol/g Hb), and RBCs stored in our modified storage solutions, throughout the 35-day storage period ($p < 0.01$). Sorbitol concentrations increase in the cells as a function of storage time, especially for RBCs stored in hyperglycemic environments. There is a significant increase in sorbitol levels from day 7 to day 14 for RBCs stored in hyperglycemic conditions, which has been illustrated in Figure 2.11 ($p < 0.01$). Considering other studies, including both clinical

retrospective and *in vitro,* two weeks might be a turnover point for the quality of blood products.[6-8]

The massive production of intracellular sorbitol can result in some detrimental effects on stored RBCs. For example, RBCs stored in normoglycemic conditions tend to be less fragile, compared to RBCs stored in hyperglycemic conditions, in the first week of storage, as shown in Figure 2.12 ($p < 0.05$). This is especially true when RBCs were stored in CPDN/AS-1N and CPDN/AS-5N, since their osmotic fragility test results are close to fresh blood samples on day 1 (CPDN/AS-1N: 21.0 ± 3.1%; CPDN/AS-5N: 25.7 ± 4.1%; fresh blood: 19.9 ± 5.2%). However, the differences disappeared after 2 weeks of storage, which implies that those deleterious effects to stored RBCs become permanent after 1 – 2 weeks.

Another adverse change that occurs to stored RBCs, possibly caused by the polyol pathway, is decreased cell deformability. The mechanical features of RBCs, especially cell deformability, are of great physiological and pathological significance.[9-15] Because the diameter of a mature RBC is approximately 6 – 8 μm, RBCs need to squeeze and deform when traversing through small-size capillaries. The flow properties of RBCs are crucial for cells to function properly. Impaired RBC deformability might cause problematic blood flow. In Figure 3.9, RBCs stored in normoglycemic conditions are able to keep their deformability close to 100% during the four-week storage duration, showing no statistical difference between day 1 and day 28. However, 15 – 20% of deformability was lost on the first day of storage when cells were exposed to high concentrations of glucose (CP2D/AS-3: 82.14 ± 4.19%; CPD/AS-5: 82.88 ± 6.06%) ($p < 0.05$). This trend continues until the end of the storage period (CP2D/AS-3: 81.58 ± 3.76%; CPD/AS-5: 87.46 ± 0.60%). Furthermore,

RBCs stored in high glucose conditions lost their reversibility of deformation capacity as the duration of storage increased. Notably, they lost their ability to reverse their deformability back to normal levels after two weeks of storage.

The decrease in mechanical deformation can consequently impair ATP release from stored RBCs under flow conditions. In this work, since there are no chemical effects on RBCs, shear stress is the only physical factor that affects cells under flow conditions. Deformation is responsible for inducing ATP release. In addition to its role in oxygen delivery, it has been reported that the RBC is a major determinant in regulating blood flow.[16,17] As shown in Figure 2.13, hyperglycemic stored RBCs lost 50% of their capacity to release ATP when pumped through microfluidic channels (CPD/AS-1, 125 ± 2 nM; CP2D/AS-3, 145 ± 8 nM; CPD/AS-5, 165 ± 15 nM). On the other hand, normoglycemic stored RBCs release significantly higher amounts of ATP (CPDN/AS-1N, 251 ± 14 nM; CPDN/AS-3N, 252 ± 11 nM; CPDN/AS-5N, 254 ± 27 nM) ($p < 0.05$). This trend continues from day 1 to day 35. Notably on day 35, the amount of ATP released from RBCs stored in our modified solutions (CPDN/AS-1N, 173 ± 10 nM; CPDN/AS-3N, 219 ± 19 nM; CPDN/AS-5N, 165 ± 6 nM) is still close to fresh RBCs from healthy people (190 ± 10 nM).[18] However, RBCs stored in FDA approved collection and storage solutions (CPD/AS-1, 65 ± 8 nM; CP2D/AS-3, 97 ± 7 nM; CPD/AS-5, 48 ± 1 nM) act similarly to type 2 diabetic RBCs (90 ± 10 nM).[19] Previous work done by the Spence group has demonstrated that the decreased amount of RBC-derived ATP release results in lower NO production from endothelial cells.[1] Thereby, the above results strongly suggest that RBCs stored in normoglycemic conditions may have improved blood flow during and after transfusion.

Overall, when applying normoglycemic collection and storage solutions, the storage lesion can be reduced, therefore potentially reducing the risk of post-transfusion complications.

5.1.2 Low Glucose Storage of RBC can be Achieved by Implementing a Piggyback Bag System

In this thesis, blood samples were collected and stored on a miniaturized scale to reduce sample consumption. At the beginning, RBCs were stored in micro-unit PVC bags. In order to maintain the glucose concentration for cells stored in normal glucose conditions, bags were opened and reclosed several times during the 35-day storage period.[20] This procedure is prohibited by the FDA for the purpose of preventing bacteria contamination. In order to make the glucose feeding process potentially acceptable by clinical institutes, new blood storage bags and piggyback glucose bags were created.

The new blood bag can hold a 5 mL blood sample. It contains two parts, a 3D-printed part and a PVC plastic part. The combination of the 3D-printed part with the PVC plastic part allows the user to avoid opening the bag during the storage, when obtaining samples for weekly analysis. The black rubbery material on the 3D-printed part allows the use of syringes to transfer RBC samples in and out of the bags. The 3D-printed part at the top of the bag also enables addition of concentrated glucose saline to stored RBCs with minimal interference. Instead of opening the bags and using pipettes to add a glucose solution, a piggyback bag system was implemented. A piggyback bag is a small bag containing medications, which is usually plugged into a patient's existing intravenous administration system. Launching this concept, a glucose reservoir and switch were manufactured by 3D

printing. The blood bag is connected to the 3D-printed piggyback bag by a Tygon tube and needle. The flow of glucose-saline solution is controlled by the switch. The amount of glucose added to the stored RBCs is estimated by the number of drops of concentrated glucose saline. RBC suspensions in AS were successfully stored in the new blood storage bags. Importantly, the glucose level was successfully maintained within the healthy range using the piggyback bag system when RBCs were stored in CPDN/AS-3N and CPDN/AS-5N.

5.1.3 3D-Printed Devices Are Useful Tools for Analytical Scientists

3D-printed devices were widely used throughout the experiments in this thesis and there are several advantages of applying 3D printing techniques. First, the CAD software is very customer-friendly and customer-orientated. It allows researchers to pursue creative ideas quickly and cost effectively. Second, there are multiple materials that can be chosen for use. Vero Clear material, which is semi-transparent, makes the blood flow in the device's channel visible. Tango Black material, which is a rubbery kind plastic, acts like a septum. The assembly feature in the CAD software enables printing two different materials on one part. Third, the printed devices are very robust, so one device can be used for years. This reduces the variations in analytical measurements that are due to the use of different devices, and is therefore a significantly improvement. Fourth, the 3D printing process has a great potential to become a gold standard of manufacturing fluidic devices. The CAD files can be shared between labs. As the process becomes more standardized, the complexity and difficulty in the manufacturing process can be reduced.

A 3D-printed device was applied to determine RBC-derived ATP release from stored cells under flow conditions. The printed device, containing 12 channels, enables us to perform

flow studies in parallel with improved precision. Optical detection has been achieved by fabricating the device to fit into a commercial plate reader. In addition, a membrane based device was produced to measure cell deformability changes. The filtration device is composed of two different materials, a semi-transparent clear material and a black rubbery material. Polycarbonate membranes were placed on the black material areas. The device contains two parts, which can be assembled together before deformability measurements. There are 6 ports on the device, enabling a high throughput deformability analysis. Moreover, as was discussed in the Section 5.1.2, 3D-printed parts were also used in the development of the new blood storage method.

5.2 Future Directions

For the purpose of improving transfusion medicine, more work needs to be done in understanding RBC collection and storage under physiological levels of glucose.

In Chapter 2, the significant differences between normoglycemic and hyperglycemic RBC storage have been illustrated with the use of multiple methods. People may argue that instead of maintaining glucose concentrations in the solution supernatant within the healthy range, simply decreasing the amount of glucose added in the storage solutions might be able to reduce storage lesion. As long as the extracellular glucose level is guaranteed to be above 4 mM by the end of storage, the percent cell lysis shouldn't be a problem. In this way, the process of feeding glucose saline to stored RBCs can be saved, which makes the storage procedure less complicated.

While this is a good argument, problems still remain. In order to maintain cell integrity and correct functions, stored RBCs constantly break down glucose through glycolysis

pathway to produce ATP. The rate of glucose consumption is fast in the first two weeks, but slows down as the storage duration length increases. According to the author's experience, the extracellular glucose concentration reduces by ~ 1 mM every day in the first week of storage. In the last two weeks of storage, the rate of glucose consumption is approximately 2 mM per week. If RBCs are stored for 42 days, the total amount of glucose metabolized by cells can be estimated to be ~ 20 – 25 mM. Considering that the glucose level by the end of storage still needs to be higher than 4 mM, the glucose concentration in blood bags can be estimated to be 27 mM on day 1. Compared to current standard storage solutions, 27 mM is smaller than all storage solutions, but still much higher than a healthy individual. Although stored RBCs might be exposed to physiological levels of glucose by the end of storage, they still suffer from high concentrations of glucose in the first three weeks of storage. Recall that many adverse changes that occur to stored RBCs become permanent after two weeks. Also, stored RBCs might be used anytime during their storage period, but not by the end of storage. Therefore, storing RBCs in storage solutions with slightly lower glucose levels will act similarly to current blood products, in theory. However, in order to prove it experimentally, it is worthwhile to store RBCs at different but lower concentrations of glucose, such as 15 mM, 20 mM and 25 mM, and compare them to normoglycemic RBC storage strategies.

In Chapter 3, a new miniaturized blood storage method was developed, which allowed the transfer of blood samples and adding glucose saline without opening and reclosing the bags. In order to apply for a license through the FDA for our piggyback blood storage system, RBCs needs to be stored on the accepted volume scale (hundreds of milliliters)

instead of the miniaturized scale. The feasibility of using a piggyback glucose-bag to feed 300 mL of stored RBCs needs to be evaluated. Importantly, leukofiltration for storing RBCs is very much needed when collecting cells on a standard scale.

Also, the biocompatibility and toxicity of 3D-printed plastic remains unknown. It is possible that some toxic molecules are being released into the glucose-saline or stored RBCs. Therefore, replacing 3D-printed materials by other medically acceptable materials will be beneficial. The application of 3D-printed parts in this thesis is partially due to the laboratory scale, miniaturized blood storage system. The volume of blood bags and piggyback IV-bags on the market is about 50 – 300 mL. The blood bags and piggyback bags developed in-house during this thesis work only hold 2 – 5 mL of liquid. It has been proposed by members of our group to feed the stored RBCs automatically. Instead of manually controlling a switch, the flow of concentrated glucose solution to the blood bag can be quantitatively managed by a programmable peristatic pump. With a programed pump, the time and volume in which to dispense glucose saline will be accurate and automated.

In Chapter 4, the Amadori products of PE on stored cell membranes were quantified by a direct infusion orbitrap MS method. The ratio of Amadori-PE to PE decreases as a function of time. The next step for the PE glycation study is to determine the extent of AGE-PEs on cell membranes, especially CM-PE and CE-PE. It has been reported by Miyazawa that human RBC CM-PE and CE-PE can be analyzed by LC-MS/MS with an isocratic mobile phase of methanol-water (99:1, v/v; containing 5 mM ammonium acetate).[21] Also, microvesicles, originating from stored RBCs, have been reported to increase progressively

during the storage period.[22,23] Microvesicles typically range from 100 – 1000 nm in size, and are composed of high membrane phospholipid content.[24] It has been suggested that microvesicles shed from stored RBCs could be regarded as a potential mechanism to get rid of damaged molecules.[25] Therefore, studying the lipid composition of microvesicles might provide an explanation for the decrease of Amadori-PE/PE ratio.

Since there are two kinds of lipids on the RBC membrane that can react with glucose, the study of PS glycation is essential to fully understand the lipid glycation of stored RBCs. Another research study focused on PS, which is of great interest, to detect the PS exposure on the outer layer of cell membranes. The exposure of PS has been proven to be correlated with cell clearance.[26] It has been shown that PS translocation to the cell surface increases during storage, resulting in progressive adherence of RBCs to endothelial cells.[27] In addition to lipid study, protein glycation will be the next step to further investigate the effects of glucose on stored RBCs.[28]

There is one storage solution currently approved by FDA not studied in this thesis, CPD/AS-7. These new storage solutions include two satellite containers with different solutions, container A with Additive Solution A and container B with Additive Solution B. Contents in container B are completely drained into container A and mixed well before adding the combined solutions to the RBCs. The separation into two solutions, where solution B is an acidic glucose solution and solution A contains other components, allows sterilization of the solutions.[29] Because the components of the two different Additive Solutions have not been fully released to public, AS-7 has been excluded from my work. AS-7 is the first basic additive solution for RBCs that has been demonstrated to reduce

RBC storage lesion.[30] Considering that the acidic environment promotes intracellular sorbitol production, it is rational to assume that RBCs stored in CPD/AS-7 favor the glycolysis pathway instead of the polyol pathway. However, the glucose concentration in AS-7 itself is 80 mM. Based on estimation, RBCs collected and stored in CPD/AS-7 are exposed to about 40 mM of glucose. RBCs would possibly benefit from the physiological pH values, but still suffer from excess amounts of glucose. In order to fully demonstrate the benefits of normoglycemic RBC storage, it is necessary to modify CPD/AS-7 to CPDN/AS-7N. Cellular analyses, such as ATP release, deformability changes and membrane glycation, are required for cells stored in the two new storage solutions.

REFERENCES

REFERENCES

(1) Wang, Y. M.; Giebink, A.; Spence, D. M. *Integr Biol-Uk* **2014**, *6*, 65-75.

(2) Hogman, C. F.; Meryman, H. T. *Transfusion* **2006**, *46*, 137-142.

(3) Hess, J. R.; Sparrow, R. L.; van der Meer, P. F.; Acker, J. P.; Cardigan, R. A.; Devine, D. V. *Transfusion* **2009**, *49*, 2599-2603.

(4) Malone, J. I.; Knox, G.; Benford, S.; Tedesco, T. A. *Diabetes* **1980**, *29*, 861-864.

(5) Aida, K.; Tawata, M.; Shindo, H.; Onaya, T. *Diabetes Care* **1990**, *13*, 461-467.

(6) Koch, C. G.; Li, L.; Sessler, D. I.; Figueroa, P.; Hoeltge, G. A.; Mihaljevic, T.; Blackstone, E. H. *N Engl J Med* **2008**, *358*, 1229-1239.

(7) Tinmouth, A.; Fergusson, D.; Yee, I. C.; Hebert, P. C.; Investigators, A.; Canadian Critical Care Trials, G. *Transfusion* **2006**, *46*, 2014-2027.

(8) Chen, C. P.; Wang, Y. M.; Lockwood, S. Y.; Spence, D. M. *Analyst* **2014**, *139*, 3219-3226.

(9) Wan, J.; Forsyth, A. M.; Stone, H. A. *Integr Biol (Camb)* **2011**, *3*, 972-981.

(10) McMillan, D. E.; Utterback, N. G.; La Puma, J. *Diabetes* **1978**, *27*, 895-901.

(11) Vague, P.; Juhan, I. *Diabetes* **1983**, *32 Suppl 2*, 88-91.

(12) van der Heyde, H. C.; Nolan, J.; Combes, V.; Gramaglia, I.; Grau, G. E. *Trends Parasitol* **2006**, *22*, 503-508.

(13) Ho, J.; Sibbald, W. J.; Chin-Yee, I. H. *Crit Care Med* **2003**, *31*, S687-697.

(14) Barshtein, G.; Pries, A. R.; Goldschmidt, N.; Zukerman, A.; Orbach, A.; Zelig, O.; Arbell, D.; Yedgar, S. *Microcirculation* **2016**, *23*, 479-486.

(15) McMillan, D. E.; Gion, K. M. *Horm Metab Res Suppl* **1981**, *11*, 108-112.

(16) Allen, B. W.; Piantadosi, C. A. *Am J Physiol-Heart C* **2006**, *291*, H1507-H1512.

(17) Ellsworth, M. L. *Med Sci Sport Exer* **2004**, *36*, 35-41.

(18) Chen, C. *3D-PRINTED IN VITRO ANALYTICAL DEVICES FOR DIABETES THERAPEUTICS AND BLOOD BANKING STUDIES*. Michigan State University2015.

(19) Subasinghe, W.; Spence, D. M. *Anal Chim Acta* **2008**, *618*, 227-233.

(20) Wang, Y.; Giebink, A.; Spence, D. M. *Integr Biol (Camb)* **2014**, *6*, 65-75.

(21) Shoji, N.; Nakagawa, K.; Asai, A.; Fujita, I.; Hashiura, A.; Nakajima, Y.; Oikawa, S.; Miyazawa, T. *J Lipid Res* **2010**, *51*, 2445-2453.

(22) Rubin, O.; Crettaz, D.; Canellini, G.; Tissot, J. D.; Lion, N. *Vox Sang* **2008**, *95*, 288-297.

(23) Rho, J.; Chung, J.; Im, H.; Liong, M.; Shao, H.; Castro, C. M.; Weissleder, R.; Lee, H. *ACS Nano* **2013**, *7*, 11227-11233.

(24) Bosman, G. J.; Lasonder, E.; Luten, M.; Roerdinkholder-Stoelwinder, B.; Novotny, V. M.; Bos, H.; De Grip, W. J. *Transfusion* **2008**, *48*, 827-835.

(25) Delobel, J.; Barelli, S.; Canellini, G.; Prudent, M.; Lion, N.; Tissot, J.-D. *ISBT Science Series* **2016**, *11*, 171 - 177.

(26) Connor, J.; Pak, C. C.; Schroit, A. J. *J Biol Chem* **1994**, *269*, 2399-2404.

(27) Koshkaryev, A.; Zelig, O.; Manny, N.; Yedgar, S.; Barshtein, G. *Transfusion* **2009**, *49*, 2136-2143.

(28) Singh, R.; Barden, A.; Mori, T.; Beilin, L. *Diabetologia* **2011**, *44*, 129 - 146.

(29) Administration, U. F. a. D., Ed., 2013.

(30) Cancelas, J. A.; Dumont, L. J.; Maes, L. A.; Rugg, N.; Herschel, L.; Whitley, P. H.; Szczepiokowski, Z. M.; Siegel, A. H.; Hess, J. R.; Zia, M. *Transfusion* **2015**, *55*, 491-498.